

ENHANCED PERFORMANCE AND EFFICIENCY IN ELECTRIC VEHICLES THROUGH FOUR-QUADRANT CONTROL OF THREE-PHASE BLDC MOTORS

¹ Dr. B. DIVYA, ² K. MANIKANTESWAR

¹ Professor, ² Assistant Professor

Department Of Electrical and Electronics Engineering
Indira Institute Of Technology And Sciences, Markapur

ABSTRACT

The authors of this paper demonstrate how a bidirectional DC-DC converter may be used to operate a brushless direct current (BLDC) motor in all four quadrants (forward/reverse motoring/braking). The DC-DC converter's output is sent to the three-phase voltage source inverter (VSI), which drives the motor. Mechanical energy is converted to electrical energy and stored in the batteries while the device is in regenerative mode. Buck operation is carried out in the driving mode by making use of the battery's bi-directional converter. For the boost feature, it will make use of the same rechargeable battery. Since electric cars need frequent starts and stops, this is accounted for in the design. It is advised to use a system that uses the regenerative braking system to collect energy throughout each and every halting procedure. In addition, if the electric vehicle (EV) is now descending a slope, the regulated speed on the downhill serves as a source of energy replenishment for the battery. Software called Simulink/MATLAB is used to verify the above listed procedures.

1. INTRODUCTION

Brushless DC motors are gaining a lot of popularity whether it is aerospace, military, household or traction applications. Due to the constraint of fuel resources, the world requires highly efficient electric vehicle

drives for transportation needs. The BLDC motor has a longer life span, higher efficiency, and compact size making it the most sought after motor in electric vehicle drive applications. The continuous attempt to reduce environmental pollution has given an impetus to the market of electric vehicles (EVs). As the fuel resources are depleting, the energy efficient electric drives are likely to replace vehicles running with fossil fuels. Being different from the ICE (internal combustion engine), EVs are the least burden to the environment. Any motor drive system which can be recharged from any external electricity source is known as a plug-in electric vehicle (EV). The complete electric vehicle drive model is described. There are still some disadvantages of EV drives like overall lower efficiency, huge dimension, and the cost of storage devices etc. The technique of performing the four quadrant operation is proposed where its battery is charged during the regenerative braking but the system here has two energy sources, one is driving the motor and other is storing the energy using the rectifier during braking. It is proposed in this paper that only one battery is enough to drive the motor and at the same time to recover the kinetic energy of them regenerative mode. This proposal reduces the cost of an extra rectifier and an additional battery. In the

2633

ResMilitaris, vol.12, n^o. 5 ISSN: 2265-6294 Spring (2022)



NAVIGATING DIVERSITY: ANALYZING INSTRUCTORS' PERSPECTIVES ON IMPLEMENTING CULTURALLY RESPONSIVE PEDAGOGY IN ONLINE LEARNING ENVIRONMENTS

¹ DR.ASHOK KUMAR, ² N.SATYA VANI

¹Professor, ²Associate Professor

Department Of H&S

Indira Institute Of Technology And Sciences, Markapur

Abstract

The rapid rise of different learners in online learning has made it essential for online educators to include multicultural resource curricula and instructional activities. This study sought to understand how educators view culturally responsive pedagogy in online learning, how they apply these approaches in the virtual classroom, and what challenges they encounter when supporting learners from different cultural backgrounds in cross-cultural collaborative learning. Using a qualitative multi-site case study technique, data were collected at 12 American colleges and universities in five academic disciplines: education, social sciences, engineering, physical sciences, and health sciences. A continual comparative analysis technique was used to gather and analyze the 60 in-depth, semi-structured interviews with the instructors (26 female and 34 male). The results demonstrated that the instructors used cross-cultural interactions and culturally responsive education to promote student involvement. The majority of the instructors addressed the impact of multicultural education in online learning, according to the findings, and included a variety of internationalized learning resources to satisfy different student needs. However, it was noted that physical science instructors encountered challenges when attempting to include culturally diverse content into their virtual courses. The study's findings spark debate on the optimal strategies for assisting

instructors in having productive online interactions with a diverse student body.

KEYWORDS: culturally responsive computing, online educators, diversity, online education, and culturally responsive pedagogy

1. INTRODUCTION

The growth of online learning in universities and colleges has seen a much higher trend in terms of diverse student populations (Allen & Seaman, 2018; Jung & Gunawardena, 2014). The increased growth rate of online learning can be attributed to academic leaders' strategic focus to move in-person classes to online/remote learning due to the disruptions caused by the COVID-19 pandemic, the rapid changes in technology as a means of instructional delivery in most universities, access and flexibility afforded by the online courses, rising tuition costs and an evolving workforce seeking lifelong learning options (Allen & Seaman, 2018; Altbach & de Wit, 2020). Furthermore, the growth of online learning has led to situations where both students and instructors are required to cross cultures to share new ideas, collaborate and build new knowledge. Several studies (eg. Kumi-Yeboah, Dogbey, Yuan & Smith, 2020; Petersen, 2015; Yang et al., 2010) have called on instructors to design online education environments that promote cultural inclusivity. These studies found that online instructors must acknowledge students' cultural

OPTIMIZING WING STRUCTURE DESIGN AND CONDUCTING STATISTICAL ANALYSIS FOR PREDICTING FATIGUE LIFE IN TRAINER AIRCRAFT

¹ DR.KANDULA RAJA SEKHARA REDDY, ² D.BALA CHANDRA NAIK, ³ P.N MANTHRU NAIK

¹Associate Professor, ^{2,3}Assistant Professor

Department Of Mechanical Engineering

Indira Institute Of Technology And Sciences, Markapur

ABSTRACT

A CATIA project was used to extensively design the wing structure of a training aircraft as part of this investigation. The strains being applied to the wing structure are then determined by doing a stress analysis on it. With the aid of ANSYS, the finite element approach is used to anticipate the stresses in order to compute the safety factor of the structure. A fatigue fracture may occur in an airplane's structure where the greatest tensile stress is placed. Three components are required for life prediction: local stress history at the stress concentration; a model for the buildup of fatigue damage; and constant amplitude S-N (stress life) data throughout a range of stress ratios. An examination of the wing's structural reaction is planned. This research focuses on the skin, spars, and ribs of the trainer aircraft's wing construction. The wing is composed of two skin-covered spars and fifteen ribs. There is a "I" portion on the front spar and a "C" form on the rear spar. A stress and fatigue evaluation of the whole wing section must be completed in order to determine the stresses that the applied pressure load will place on the spars and ribs. Potential search phrases include aircraft wing, static analysis, CATIA, fatigue life prediction, and Ansys

1. INTRODUCTION

A wing is a type of fin that produces lift, while moving through air or some other fluid. As such, wings have streamlined cross-sections that are subject to aerodynamic forces and act as airfoils. A wing's aerodynamic efficiency is expressed as its lift-to-drag ratio. The lift a wing generates at a given speed and angle of attack can be one to two orders of magnitude greater than the total drag on the wing. A high lift-to-drag ratio requires a significantly smaller thrust to propel the wings through the air at sufficient lift. Lifting structures used in water, include various foils, including hydrofoils. Hydrodynamics is the governing science, rather than aerodynamics. Applications of underwater foils occur in hydroplanes, sailboats and submarines.

1.1 Aircraft wing

The wing might be considered as the most significant part of a flying machine, since a fixed-wing flying machine can't fly without it. Since the wing geometry and its highlights are affecting all other air ship parts, we start the detail configuration process by wing structure. The essential capacity of the wing is to produce adequate lift power or just lift (L). Be that as it may, the wing has two different preparations, specifically drag power or drag (D) and nose-down pitching minute (M). While a wing architect is hoping to amplify the lift, the other two (drag and pitching minute) must be limited. Actually, wing is expected promotion a lifting surface that lift is created because of the weight distinction among lower and upper surfaces. Streamlined features course readings might be concentrated to revive your memory about numerical systems to figure the weight conveyance over the wing and how to decide the stream factors.

2. MODELING AND ANALYSIS

Computer-aided design (CAD) is the use of computer systems (or workstations) to aid in the creation, modification, analysis, or optimization of a design. CAD software is used to increase the productivity of the designer, improve the quality of design, improve communications through documentation, and to create a database for manufacturing. CAD output is often in the form of electronic files for print, machining, or other manufacturing operations. The term CADD (for Computer Aided Design and Drafting) is also used. Its use in designing electronic systems is known as electronic design automation, or EDA. In mechanical design it is known as mechanical design automation (MDA) or

RASPBERRY PI-POWERED ROBOTIC FARMING COMPANION FOR PLANT HEALTH MONITORING USING ADVANCED IMAGE PROCESSING TECHNIQUES

¹ DR.P JAYARAMI REDDY, ² C.PUSHPALATHA, ³ SK.BEEBI

¹Professor, ^{2,3}Assistant Professor

Department Of Electronics and Communication Engineering
Indira Institute Of Technology And Sciences, Markapur

ABSTRACT

More intelligent and productive agricultural techniques are being made possible by the combination of robots and sophisticated image processing in agriculture. This paper describes the design and development of a robotic farming companion that runs on a Raspberry Pi and can monitor plant health using cutting-edge image processing methods. The robotic device is intended to go over agricultural fields on its own. It will take pictures of the crops and analyze them instantly to find early indicators of illness, nutrient shortages, or insect infestations.

The robot uses machine learning techniques to interpret the collected photos and detect irregularities in plant health, using the processing capabilities of the Raspberry Pi. Through an intuitive interface, the technology gives farmers meaningful information, facilitating prompt interventions and minimizing the need for human inspection. By reducing crop loss from problems that go unnoticed, real-time data gathering and analysis not only improves crop management but also boosts production.

The study shows how robots and image processing may be used to achieve precision agriculture, providing a scalable and affordable answer to today's agricultural problems. The system's accuracy in identifying plant health problems is shown by the experimental findings, highlighting its importance in advancing efficient and sustainable agriculture methods. This creative strategy is a major advancement in smart farming, giving farmers the means to maximize crop health and productivity while preserving resources.

I. INTRODUCTION

1.1 INTRODUCTION:

Agriculture is a profession from long ago. It plays a vital function in our day-to-day lives. Food is a

fundamental human necessity. A sufficient quantity of production is required to distribute meals across a large population. A vast majority of people in India reside in rural regions where agriculture is the primary source of income for people. Consequently, agriculture is the main driver of the Indian economic system as a whole. Therefore, it is now essential to increase first-rate manufacturing on a daily basis. It is essential to monitor crops and vegetation and to take early action to regulate them. Numerous responsibilities include soil preparation, sowing, applying fertilizer and manure, irrigation, identifying diseases, applying pesticides, harvesting, and garage work. Among them, applying the right quantity of insecticides requires careful consideration. Pesticides, sometimes referred to as crop protection products, are used to draw in, entice, and destroy pests. In order to kill pests, weeds, or illnesses on plants, pesticides are made either sometimes using organic methods or occasionally using hazardous chemicals. India is a cultivated nation where agriculture provides jobs for almost 70% of the population. Farmers have an enormous array of options when it comes to selecting a variety of appropriate plants and identifying plant-specific insecticides. Plant disorder leads to a significant decrease in the quantity and quality of agricultural products produced. The study of visually discernible patterns in plant life is closely related to the study of plant diseases. Monitoring plant health and disease plays a critical role in the productive production of plants on farms. In the past, plant disease monitoring and analysis were done manually utilizing data from specific experts in the field. This requires an excellent volume of labor in addition to an excessive quantity of processing time. The plant disease diagnosis procedure may make use of picture processing technology. Most of the time, disease signs are visible on the fruit, stem, and leaves. Many methods are now available to boost manufacturing

2639

ResMilitaris, vol.12, n°, 5 ISSN: 2265-6294 Spring (2022)


PRINCIPAL
INDIRA INSTITUTE OF TECHNOLOGY & SCIENCES
Darimadugu, Markapur-523 316
Prakasam Dist.(A.P.) India.

SYNERGISTIC EFFECTS OF BAGASSE ASH, STEEL FIBERS, AND POLYPROPYLENE FIBERS ON THE MECHANICAL PROPERTIES OF CONCRETE

¹DR. R. BALA MURGAN, ²CH. RAMESH, ³M.HANUMAPPA

¹Professor, ^{2,3}Assistant Professor

Department Of Civil Engineering

Indira Institute Of Technology And Sciences, Markapur

ABSTRACT

The combined impacts of steel, polypropylene, and bagasse ash on the mechanical qualities of concrete are examined in this work. A byproduct of the sugar industry called bagasse ash is used in place of some cement, and steel and polypropylene fibers are added to improve the concrete's hardness, ductility, and tensile strength. The goal of the study is to assess how these materials interact to affect important mechanical characteristics including splitting tensile strength, flexural strength, and compressive strength. Concrete mixtures with varied fiber concentrations and bagasse ash percentages (10%, 15%, and 20%) were made and evaluated. The findings demonstrate that the addition of these materials considerably enhances concrete's overall performance; the best results are shown when 15% bagasse ash and a balanced proportion of steel and polypropylene fibers are added. The research comes to the conclusion that using industrial wastes to create high-performance concrete with improved mechanical characteristics while simultaneously promoting sustainability is possible when bagasse ash and steel and polypropylene fibers are combined.

INTRODUCTION

1.1 General

One of the most extensively used building materials in the world, concrete is renowned for its strength, resilience, and adaptability. However, the use of alternative materials and industrial wastes in the manufacturing of concrete is becoming more popular due to the rising need for sustainable building techniques. Because of its pozzolanic qualities, bagasse ash, a byproduct of sugarcane production, has drawn interest as a possible additional cementitious ingredient. Simultaneously, efforts have been made to improve the mechanical qualities of concrete, including its tensile strength, ductility, and resistance to cracking, by adding fibers like steel and polypropylene.

The combined, or synergistic, impacts of steel, polypropylene, and bagasse ash on the mechanical characteristics of concrete are the focus of this research. Although these components have been the subject of separate studies in the past, nothing is known about how their combination influences concrete's overall performance. Incorporating bagasse ash not only provides a sustainable

substitute for conventional cement but also aids in mitigating the carbon emissions linked to cement manufacturing. In the meantime, concrete's hardness and fracture resistance are known to be enhanced by steel and polypropylene fibers, which may counteract the brittleness that bagasse ash brought.

This research aims to give a thorough knowledge of how these elements interact to make high-performance concrete by investigating the ideal mix proportions and assessing important mechanical qualities such compressive strength, flexural strength, and tensile strength. The findings of this study may aid in the creation of more robust and sustainable building materials, supporting the overarching objectives of lessening environmental effect while preserving structural durability and integrity.

1.2 Objectives of the research

1.2.1 General objectives:

The main objective of this research is to ascertain if sugarcane bagasse ash, which is found in sugar mills, is feasible to use as a cement alternative in India.

Examining the strength parameters of steel and polypropylene fiber reinforced concrete utilizing 0%, 0.5%, 1%, 1.5%, and 0%, 0.25%, 0.5%, 0.75%, 1%

1.2.2 Specific objectives:

The specific objectives of this analytical endeavor are as follows:

A. Verifying the nation's bagasse ash and fiber supplies.

B. Examining the chemical makeup of the bagasse ash.

C. Determining the quantity of bagasse ash that can be utilized efficiently and testing the performance of paste, mortar, and concrete made in the lab using bagasse ash as a replacement material, both fresh and hardened.

D. Next, replace a part of the bagasse ash concrete with steel and polypropylene fibers separately to assess the strength qualities.

Ultimately, after such an assessment of the bagasse ash and fiber performance from sugarcane. Some conclusions and recommendations on the material's performance and various characteristics as a cement alternative will be provided.

1.3 Bagasse ash



WEB APPLICATION FOR CREDIT CARD FRAUD PREDICTION: LEVERAGING ABNORMALITY DETECTION AND REGRESSION TECHNIQUES FOR BANKING SECURITY

¹ DR VISHWANATH, ² K SURENDRA REDDY, ³ U MOUNIKA

¹Professor, ²Associate Professor, ³Assistant Professor

Department Of Computer Science Engineering
Indira Institute Of Technology And Sciences, Markapur

ABSTRACT: Financial organizations have a great deal of difficulty as a result of credit card theft, necessitating sophisticated methods and technologies to prevent fraudulent activity. This paper describes a web application that combines regression and anomaly detection approaches to improve credit card fraud prediction. The application's goal is to provide banks a reliable and approachable way to spot and stop fraudulent transactions instantly.

The suggested online application makes use of abnormality detection algorithms to spot odd behaviors and patterns in transaction data that could point to possible fraud. Through the examination of transaction attributes and user conduct, these algorithms are able to identify abnormalities that depart from standard operating procedures. Regression analysis is also used to estimate and forecast fraudulent activity based on transaction patterns and historical data. This dual strategy reduces the possibility of false positives and improves overall security by enabling the more fast and accurate identification of fraudulent transactions.

The program provides bank staff with an easy-to-use interface for managing fraud alerts, visualizing data insights, and producing reports. It easily interfaces with current financial systems, enabling real-time data processing and prompt action in the event of fraud suspicion.

The online application has improved fraud detection rates and decreased false alarms, according to preliminary testing and review. The research comes to the conclusion that using regression and anomaly detection methods together in a web-based platform provides a complete solution for credit card fraud prediction, strengthening bank security measures and giving a proactive approach to fighting financial crime.

I. INTRODUCTION

There are still many instances of credit card fraud, which puts financial institutions and their clients at serious danger. The amount of transaction data is expanding along with the complexity of fraudulent operations, thus standard fraud detection technologies are not always able to provide timely and accurate warnings. Therefore, the demand for sophisticated predictive systems that can detect and reduce fraudulent transactions is urgent.

In order to meet this demand, our research created a web application that combines anomaly detection and regression approaches to improve the prediction of credit card fraud. The program uses cutting-edge algorithms to examine transaction patterns and behaviors in order to provide banks with an enhanced tool for real-time fraud detection.

In this application, anomaly detection methods are essential because they can spot departures from typical transaction patterns. Through the identification of anomalous behaviors, including sudden increases in expenditure or odd locations for transactions, these methods might identify possible fraudulent activity that conventional rule-based systems could miss.

Regression algorithms are also used to model and forecast fraud using transaction data from the past and changing trends. These models foresee possible fraudulent activity by analyzing trends and correlations. By giving banks predictive information, these models help improve their fraud protection methods.

The online application's user-friendly interface allows for smooth integration with current banking systems and real-time data processing, insight visualization, and effective fraud alert handling. It provides banks



ADVANCED AD-BLOCKING TECHNIQUES USING RASPBERRY PI AND PI-HOLE FOR ENHANCED ONLINE PRIVACY

¹ V.L.SUREKHA, ² C.PUSHPALATHA, ¹ SK.BEEBI

^{1,2} Assistant Professor

Department Of Electronics and Communication Engineering
Indira Institute Of Technology And Sciences, Markapur

ABSTRACT

The abundance of internet adverts presents serious problems for users' surfing experiences and privacy. A potential remedy for these problems is the use of Raspberry Pi and Pi-hole in advanced ad-blocking methods. This project investigates using a Raspberry Pi to run Pi-hole, a network-wide ad blocker, to increase online privacy and boost surfing efficiency.

Similar to a DNS sinkhole, Pi-hole blocks trackers and unsolicited adverts at the network level before they reach consumer devices. Without the need for separate browser plugins, users may establish an efficient ad-blocking gateway that filters traffic for all connected devices by setting Pi-hole on a Raspberry Pi. A centralized and scalable solution for network-wide ad blocking is offered by this configuration.

A research assesses the effectiveness and efficiency of an ad-blocking configuration, looking at how it affects user experience, resource consumption, and network speed. Custom block lists, DNS-over-HTTPS, and integration with other privacy tools are examples of advanced approaches that being investigated to improve privacy safeguards and maximize speed.

The number of trackers and adverts is dramatically decreased when using Raspberry Pi with Pi-hole, according to the results, improving privacy and the surfing experience. In addition, the solution shows flexibility and scalability, which makes it appropriate for small office and residential settings.

To sum up, sophisticated ad-blocking methods using Raspberry Pi and Pi-hole provide a reliable and efficient way to improve online privacy. The research emphasizes the advantages of enacting network-wide ad blocking and offers guidance on how to best configure the system for optimal efficiency and privacy.

I. INTRODUCTION:

Online adverts have grown ubiquitous in the digital era, often invading users' privacy and interfering with their surfing experiences. Ad-blocking programs have become an essential tool for resolving these issues; yet, many of the classic ad-blockers are browser- or device-specific. Advanced ad-blocking methods that make use of network-level solutions, such

Raspberry Pi and Pi-hole, provide a thorough method for improving online privacy on a variety of devices.

Pi-hole is a network-wide ad blocker that works by snooping on DNS queries and removing domains linked to trackers and ads. Pi-hole functions at the network level, which means that it filters undesired material for all devices connected to the network, as contrast to browser-based ad-blockers. Combining Pi-hole with a Raspberry Pi, an inexpensive, small, and adaptable computing device, provides an economical and successful way to deploy ad-blocking on a larger scale.

In this case, the Raspberry Pi is used as a dedicated server running Pi-hole software, which allows for centralized administration and control of ad-blocking features. With this setting, users may prevent trackers, ads, and other undesirable stuff without having to make separate changes on each device. It also makes it possible to integrate block list customisation, network traffic monitoring, and other privacy-enhancing features.

In order to meet the rising demand for improved online privacy, this introduction highlights the relevance of implementing cutting-edge ad-blocking solutions utilizing Raspberry Pi and Pi-hole. It draws attention to the benefits of network-level ad-blocking over more conventional techniques and lays the groundwork for a thorough investigation into the use, assessment, and refinement of this strategy.

Utilizing Raspberry Pi and Pi-hole for ad-blocking is a smart and practical way to address the growing issue of internet privacy. The objectives of this research are to examine the setup's capabilities, evaluate how it affects user experience and network performance, and discover cutting-edge methods for maximizing the efficacy of ad blocking.

1.2 BLOCK DIAGRAM:



ADVANCED ECG ANOMALY DETECTION USING AUTOENCODERS FOR IMPROVED CARDIAC HEALTH MONITORING

¹ Dr. S V N SRINIVASU, ² K SURENDRA REDDY, ³ G HARA RANI

¹Professor, ²Associate Professor, ³Assistant Professor

Department Of Computer Science Engineering
Indira Institute Of Technology And Sciences, Markapur

Abstract: For efficient heart health monitoring and prompt action, early diagnosis of ECG abnormalities is essential. Accurate anomaly identification is often hampered by the complexity and fluctuation of cardiac signals, which is a problem for traditional ECG analysis techniques. This work offers a sophisticated method for detecting anomalies in ECG data by using autoencoders, a type of deep learning models renowned for their ability to identify complex patterns in data.

The suggested technique makes use of autoencoders to acquire a condensed representation of typical ECG patterns, making it possible to recognize variations that could point to abnormalities. Autoencoders are able to efficiently recreate normal heart rhythms while identifying differences since they are trained on a huge dataset of tagged ECG signals. The system can identify any abnormalities with high sensitivity and specificity by comparing the reconstruction error of incoming ECG data to a pre-established threshold.

According to preliminary findings, the autoencoder-based strategy considerably improves ECG anomaly identification accuracy over conventional techniques. By successfully differentiating between pathological anomalies and normal fluctuations, the method lowers false positive rates and increases diagnostic accuracy. The autoencoder model's real-time processing capacity further guarantees timely detection, enabling fast medical reaction and intervention.

Through the provision of a reliable, automated method for ECG abnormality identification, this work highlights the promise of autoencoders in enhancing heart health monitoring. In order to assist proactive cardiac care, future work will concentrate on improving the model's performance, broadening its application to a variety of patient demographics, and incorporating the system into clinical workflows.

I. INTRODUCTION:

By capturing the heart's electrical activity, electrocardiography (ECG) is a vital diagnostic technique used to track and evaluate cardiac health. The diagnosis of a number of cardiac disorders, including arrhythmias and myocardial infarctions, depends on the accurate identification of abnormalities in ECG signals. However, owing to the complexity and variety of cardiac signals, conventional techniques of ECG analysis sometimes encounter difficulties in accurately differentiating between pathogenic abnormalities and normal fluctuations.

ENHANCING CONCRETE PERFORMANCE WITH SILICO MANGANESE SLAG: PARTIAL REPLACEMENT OF COARSE AND FINE AGGREGATES

¹DR. R. BALA MURGAN, ²D. THRIMURTHI NAIK

¹Professor, ²Assistant Professor

Department Of Civil Engineering

Indira Institute Of Technology And Sciences ,Markapur

ABSTRACT

The use of silico manganese slag (SiMn slag) as a partial substitute for coarse and fine particles in concrete is investigated in this work. The mechanical and durability qualities of silico manganese slag, a byproduct of the ferroalloy industry, are being studied in relation to its application in concrete mixtures. Assessing the viability of employing SiMn slag in place of traditional aggregates with an emphasis on workability, compressive strength, and long-term performance is the main goal. We created and tested concrete mixtures including different amounts of 10%, 20%, and 30% SiMn slag. The findings show that adding SiMn slag to concrete improves its durability and compressive strength, especially when replacing 20% of the original material. Workability was somewhat altered in terms of water content, but still within acceptable bounds. According to the study's findings, silico manganese slag is a good substitute for conventional aggregates, providing the building sector with environmentally friendly options that save waste and save natural resources.

I. INTRODUCTION

1.1. Introduction to concrete:

Concrete is a commonly used structural material that is primarily made up of filler and binder. Its special quality is that it is the only building material that is made on the job site itself; all other materials are just shaped for use there. Discrete components such as sand, gravel, or small bits of gravel, together with countless tiny particles of cement powder combined with water, are what determine whether a concrete is good or terrible. The primary ingredients of concrete are cement, water, and aggregate. To achieve the desired physical features of the final product, reinforcements and additives are often added to the mixture. These materials combine to create a fluid mass that is simple to shape and mold. With time, the cement creates a strong matrix that holds the other materials together to create a long-lasting, multipurpose substance that resembles stone. India's population is growing at a rate that is forcing the development industry to use building materials at a rate that is rapidly depleting natural resources. This has a severe impact on the environment and can lead to many hazards, both directly and indirectly, such as river

depletion from sand mining, which is occurring at an alarming rate. However, as India's industries developed and became more industrialized, a variety of waste materials emerged. Thankfully, waste materials are often added to concrete to greatly enhance its environmental qualities. The development sector faces two distinct challenges. One is to meet the expanding population's needs for infrastructure.

1.2. Introduction to Silico Manganese slag:

Basic slag is a byproduct of the production of steel and is often created using an electrical arc furnace, an oxygen converter, or a furnace.

Second steel silicomanganese slag is produced in the steel-making operations as a consequence of the conversion of Fe into liquid steel. Steel-making slag may be a product of the economic process dispersed to provide first Fe.

The Austrian towns where the technique was developed. About 20 kg of silico manganese slag are created for every ton of hot metal produced in Indian steel factories. Of this, just 25% are used again in India, while 70% are used outside.

Put another way, India now produces just about 12 million tonnes of silica manganese slag annually, much less than affluent nations.

Although worldwide slag production statistics is not accessible, the output of steel slag is believed to have been between 160 and 240 million tons in 2016. About 1.44 million tons of slag are generated annually in Andhra Pradesh. Steel slag is a by-product that may be produced by melting scrap metal in an electric arc furnace (EAF) or converting iron in a basic oxygen furnace (BOF) that is too high.

There are extremely few natural stones available in Bangladesh. Brick aggregate is the primary building material used in the nation's construction sector as a result. However, there are several detrimental effects on the environment associated with the brick industry. Finding potential substitute resources that might be utilized as coarse aggregate in building projects is thus essential. A thorough investigation of the recycling of crushed brick concrete as coarse aggregate was conducted for Bangladesh's sustainable building material usage. Other potential substitutes, such as steel slag, may also be investigated.

An estimated 3 million metric tons of steel are needed in Bangladesh, and that amount is expected

EVALUATING STRESS DISTRIBUTION IN PREMOLARS AND DENTAL IMPLANTS UNDER DIFFERENT LOAD CONDITIONS: A COMPREHENSIVE ANALYSIS

¹ DR.V.VENUGOPAL, ² SK.ABDUL KALAM, ³ KANDULA RAJA SEKHARA REDDY
¹Professor, ^{2,3}Assistant Professor

Department Of Mechanical Engineering
 Indira Institute Of Technology And Sciences, Markapur

ABSTRACT

Examining the stress distribution in premolars and BOI implants under various loading scenarios and material compositions was the aim of this work. After the premolar's three-dimensional form was created using CATIA V5 parametric, ANSYS-14.5 was used for analysis. Zirconium, Ni-Cr alloy, and gold alloy are the materials used in this investigation. By applying various loads—1, 1.5, and 2 MPa—and by examining von-mises stresses, strains, and deformations produced from static analysis in ANSYS 19.2, we can assess the load-bearing capabilities of premolars and BOI implants. Ultimately, the appropriateness of the material was determined.

Keywords: gold, Ni-Cr, zirconium alloys, bio implants, Ansys workbench, premolars, and CFD investigation.

1. INTRODUCTION

An implant is a medical device manufactured to replace a missing biological structure, support a damaged biological structure, or enhance an existing biological structure. Medical implants are man-made devices, in contrast to a transplant, which is a transplanted biomedical tissue. The surface of implants that contact the body might be made of biomedical materials. Metals and their alloys are widely used as biomedical materials. On one hand, metallic biomaterials cannot be replaced by ceramics or polymers at present. Because mechanical strength and toughness are the most important safety requirements for a biomaterial under load-

bearing conditions, metallic biomaterials like stainless steels, Co-Cr alloys, commercially pure titanium (CP Ti) and its alloys are extensively employed for their excellent mechanical properties. On the other hand, metallic materials sometimes show toxicity and are fractured because of their corrosion and mechanical damages [1]. Therefore, development of new alloys is continuously trialed. Purposes of the development are:

- To remove toxic element.
- To decrease the elastic modulus to avoid stress shield effect in bone fixation.
- To miniaturize medical devices.
- To improve tissue and blood compatibility.



Figure 1. Different types of biomedical implants

Human Teeth Anatomy: There are 32 permanent teeth. There are 16 teeth on both the top and bottom jaw. Each jaw consists of specific teeth, which are incisors (cutting teeth), canines (tearing teeth) and molars (grinding teeth). From the midline of one side of each jaw consists of 2 incisors, 1 canine, 2 premolars and 3 molars (fig.2).



EXPLORING THE IMPACT OF AUTHORS' NATIVE LANGUAGES ON ENGLISH LANGUAGE RESEARCH PAPERS: PRELIMINARY INSIGHTS AND ANALYSIS

¹ B.SURESH BABU, ² B.GNANI ADVITEEYA

¹Associate Professor, ²Assistant Professor

Department Of H&S

Indira Institute Of Technology And Sciences, Markapur

Abstract:

Together with addressing Baldauf and Jenrudd, 1, -3, and bringing up concerns of North/South and English/non-English imbalance in research communication, the report makes the need for increased linguistic sensitivity in scientometric research. It is then recommended how writers of monthly articles on textual evidence should be identified as native or non-native English speakers. For 623 articles, a preliminary application evaluation and report are provided. Economics had a NNS rate of 23%, which was half that of health sciences. In addition, Baldauf and Jernudd were helped by the paucity of Third World documentation. To remedy alleged imbalances, scientometries are proposed as a possible addition to Research English instruction.

1. Introduction

The literature in the overlapping fields of Scientometrics, Research Communication Studies and the Sociology of Science would appear to have paid little attention to the linguistic dimension in at least two important ways. In one way, these fields may have been disadvantaged by lack of contact with research in discourse analysis and in the applied field of English for Specific Purposes ESP (the provision of specialised English language programmes for various professional groups, particularly science students and researchers). In the other, there has been some neglect of the language of publication as an important variable in scientific communication. Discourse analysis and ESP have potentially useful insights and techniques to contribute in such areas as the rhetorical organisation of scientific text, 1 i 2 the elucidation of meaning in scientific papers,3, 4 and in pertinent specific areas such as the textual patterning of citations, s,6 And indeed there is some sign that the value of discursal approaches is gaining recognition, particularly because of its focus on "describing how scientists' accounts are organised to portray their actions and beliefs in contextually appropriate ways". 7 The relationship between the language chosen for publication or presentation and the writer or speaker's proficiency in that language and the further relationship between language choice and its visibility, audience-size and prestige are equally deserving of more consideration. For instance, these relationships are nowhere referred to Bazerman's extensive and recent 142-citation review of the literature despite the fact that his section headings include topics such as The Writing Process, Textual Form, the Dissemination Process and Audience Response. 8 Blickenstaff and Moravcsik,9 in their investigation of the professional profile of participants in an international meeting, did not include a questionnaire item about the language proficiencies and preferences of those participants. Schubert et al.10 have recently analysed the proceedings of more than 500 international scientific meetings and concluded: "the distribution of the participants of international scientific meetings depends of (sic) the geographical location of the host

INNOVATIVE RFID-BASED CIRCUIT BREAKER SYSTEM FOR ENHANCED ACCESS CONTROL AND ELECTRICAL SAFETY

¹ T.CHENCHU MOHAN, ² D.LAKSHMI, ³ SK.MEHRU

^{1,2,3} Assistant Professor

Department Of Electrical and Electronics Engineering
Indira Institute Of Technology And Sciences, Markapur

ABSTRACT:

Access control in electrical systems has to be both secure and effective in the increasingly automated world of today. This paper presents a novel RFID-based circuit breaker system intended to improve electrical safety and access management. By combining circuit breaker functionality with Radio Frequency Identification (RFID) technology, the system makes it possible for only authorized individuals to access and control electrical circuits. The technology makes sure that only those with the right authorization may activate or deactivate circuit breakers by using RFID tags that are linked to certain users.

Multiple security levels are offered by the RFID circuit breaker system, which lowers the possibility of electrical accidents brought on by untrained workers and stops unwanted access. Every interaction is also logged by the system, producing an extensive record of access that may be used for auditing and monitoring. The incorporation of RFID technology into circuit breakers enhances operational security and simplifies electrical system management in home and commercial environments.

The system's dependability in regulating access and its capacity to greatly lower electrical mishaps are both shown by the experimental findings. The suggested method provides a workable way to improve security and safety in electrical systems, which makes it especially useful in settings where stringent access control

is essential. This RFID-powered circuit breaker system is an advancement in access control and current electrical safety procedures.

INTRODUCTION

Ensuring effective access control and security are becoming more and more important in modern electrical management. Conventional circuit breakers are good at preventing overloads and malfunctions in electrical circuits, but they sometimes don't have sophisticated access control or interaction monitoring systems. In settings where restricted and secure access to electrical systems is necessary, this gap presents dangers. By adding intelligent, safe, and effective access control capabilities to circuit breaker systems, Radio Frequency Identification (RFID) technology offers a chance to close this gap.

By integrating RFID technology with circuit breakers, the cutting-edge RFID-based circuit breaker system presents a complex solution to electrical safety and access management. This system ensures that only authorized workers may operate or interact with the circuit breakers by limiting and authenticating access to electrical circuits using RFID tags and readers. The RFID reader included into the circuit breaker reads the unique identifying data contained in each RFID tag that is associated with a particular user. The technology improves operational security and safety by confirming the credentials before allowing or refusing access.



EXPLORING THE STRUCTURAL AND MAGNETIC CHARACTERISTICS OF CHROMIUM FERRITE NANOPARTICLES: A COMPREHENSIVE ANALYSIS

¹DR. M. KOTHANDA RAMAN, ²R. RAMAKRISHNA REDDY

¹Professor, ²Assistant Professor

Department Of H&S

Indira Institute Of Technology And Sciences, Markapur

ABSTRACT

Pure chromium nanoparticles with the general formula CrFe_2O_4 have been produced using the conventional wet chemical co-precipitation process. For four hours, the prepared sample was annealed at 600 °C. The generated sample's room-temperature X-ray diffraction patterns were acquired to verify the creation of a single-phase cubic spinel structure. The surface morphology of the manufactured samples was examined using scanning electron microscopy. The results of the XRD and SEM examinations indicate that the particles' sizes are in the nanometer range. The specified range of the lattice constant was met. The magnetic characteristics were investigated by means of the pulse field hysteresis loop approach. It was discovered that the coercivity and saturation magnetization were greater than those in bulk.

Keywords: chemical co-precipitation, lattice constant, nanoparticles, and X-ray diffraction

DOI Number: 10.48047/nq.2021.19.11.NQ21315

NeuroQuantology 2021;19(11):995-998

995

1. Introduction

In the recent years ferrites having high electrical resistivity, low eddy current loss, structural stability, large permeability at high frequency, high coercivity, high cubic magneto crystalline anisotropy, good mechanical hardness, and chemical stability, nanosized spinel-type ferrites have emerged as an important class of nanomaterials.^{1,2} As a result, research devoted to the development and characterization of such nanomaterials, the development of cost-effective, environmentally friendly synthesis processes, and the discovery of novel uses for existing materials has gained a great deal of interest. MFe_2O_4 type spinel ferrite attracts several researchers because of their twin property of magnetic conductor and electric insulator. These materials are widely used in the electronic and electrical industries for the fabrication of devices and components such as high-density magnetic core of read/write for the high-speed tapes

etc.^{3,4}

In recent years there has been considerable interest in the study of the properties of nano-size ferrite particles because of their importance in the fundamental understanding of the physical properties as well as to their proposed applications for many technological purposes.^{4,5} The unique properties of nanoparticles are in general related to the adoption of materials, crystal structure to a small (nanosize) and large surface to volume ratio.

Among the several spinel ferrites Chromium ferrite is an interesting ferrite because it crystallizes either in a tetragonal or cubic symmetry depending on the cation distribution among the interstitial site of a spinel structure.^{6,7} The other interesting feature of Chromium ferrite is that it contains Jahn Teller ion which is responsible for interesting electrical and magnetic properties. In bulk form, Chromium ferrite is a magnetic compound useful in many

eISSN 1303-5150



www.neuroquantology.com

PRINCIPAL
INDIRA INSTITUTE OF TECHNOLOGY & SCIENCES
Darimadugu, Markapur-523 316
Prakasam Dist.(A.P.) India.



INTEGRATION OF ROBOT-WSN FOR ANIMAL ACTIVITY MONITORING IN AGRICULTURAL FIELDS WITH IOT IMPLEMENTATION

¹E. JOHAR BABU, ²K. MANIKANTESWAR, ³M. ADI NARAYANA

¹Associate Professor, ²Assistant Professor

Department Of Electrical and Electronics Engineering
Indira Institute Of Technology And Sciences, Markapur

Abstract—

Agriculture is the main factor in the growth of an agricultural country. Issues pertaining to agriculture have long inhibited the country's development. The only option to address this issue is to use smart agriculture to modernize the present traditional farming operations. Thus, the project's objective is to track the movements of birds and animals in agricultural areas using IOT technologies and robots equipped with wireless sensor networks. These robots coexist with sensors and cooperate to complete tasks by enforcing hardware constraints. An autonomous multi-robot system networked together with particular sensing goals is referred to as a robotic wireless sensor network. In our project, NRF24L01 wireless transceivers are used to wirelessly link three robots, putting the finest sensor to use in an agricultural region to provide a signal that can be used to determine an animal's location. The nearest robot then takes the initiative and attacks the field animal. One robot is using GPRS to send data from all three robots to a cloud database while the other two robots communicate with one another. Users may observe cloud data via an online application, and based on accurate, real-time field data, utilize an ultrasonic repellent to frighten animals and birds. Sensors, NRF24L01 modules, and microcontrollers will all be integrated to do these activities, which may all be operated by a computer or other remote smart device that has an Internet connection.

Key words: agricultural, IOT.

DOI Number: 10.48047/nq.2021.19.11.NQ21316

NeuroQuantology 2021;19(11):999-1008

999

1 INTRODUCTION

"The discovery of agriculture was the first big step toward a civilized life." Is a famous quote by Arthur Keith. This emphasizes that the agriculture plays a vital role in the economy of every nation. Since the dawn of history agriculture has been one of the significant earnings of producing food for human utilization. Today more and more lands are being developed for the production of a large variety of crops.

The field of agriculture involves various operations that require handling of heavy materials. For example, in manual ploughing, farmers make use of heavy ploughing machines. Additionally, while watering the crops farmers still follow the traditional approach of carrying heavy water pipes. These operations are dull, repetitive, or require strength and skill for the workers.

A. THE CURRENT STATE OF AGRICULTURAL ROBOTICS:

Today agricultural robots can be classified into several groups: harvesting or picking, planting, weeding, pest control, or maintenance. Scientists have the goal of creating robot farms. Where all of the work will be done by machines. The main obstacle to this kind of robot farm is that farms are a part of nature and nature is not uniform. It is not like the robots that work in factories building cars. Factories are built around the job at hand, whereas, farms are not.

Robots on farms have to operate in harmony with nature. Robots in factories don't have to deal with uneven terrain or changing conditions. Scientists are working on overcoming these problems.

eISSN1303-5150



www.neuroquantology.com


INDIRA INSTITUTE OF TECHNOLOGY & SCIENCES
Darimadugu, Markapur-523 316
Prakasam Dist.(A.P.) India.



ENHANCING URBAN MOBILITY WITH DENSITY-BASED TRAFFIC LIGHT CONTROL SYSTEMS

¹V.MADHURI, ²SK.BEEBI, ³C.PUSHPALATHA

¹Associate Professor, ^{2,3}Assistant Professor

Department Of Electronics and Communication Engineering
Indira Institute Of Technology And Sciences, Markapur

ABSTRACT

Due to deteriorating signal control systems and escalating traffic congestion, urban transportation is facing more and more difficulties. In order to improve urban mobility, this research presents a density-based traffic light management system that dynamically modifies traffic signals in response to real-time traffic density data. By monitoring vehicle flow at junctions with the use of sophisticated sensors and data analytics, the suggested system allows for adaptive signal timing, which improves traffic flow and lessens congestion.

The system measures traffic density and examines traffic patterns in real time by integrating vehicle identification technology like cameras and inductive loop sensors. The traffic lights use density-based algorithms to modify their timing in response to changing traffic circumstances. This allows them to prioritize green signals in areas with high traffic volumes and reduce delays for all users of the road.

In comparison to conventional fixed-timing traffic signals, preliminary findings show that the density-based control system greatly improves traffic flow and decreases wait times at crossings. Because of the adaptive nature of the system, peak and off-peak traffic may be better managed, resulting in less congestion and more seamless transitions between lanes.

By minimizing stop-and-go traffic, this strategy not only improves overall urban mobility but also helps to reduce car emissions and improve air quality. The research shows how density-based traffic signal control systems may revolutionize urban traffic management by offering contemporary cities a scalable and efficient alternative. In order to provide complete traffic control, future research will concentrate on improving the system's algorithms, extending its deployment, and combining it with other smart city technologies.

DOI Number: 10.48047/nq.2021.19.11.NQ21314

NeuroQuantology 2021;19(11):986-994

986

I. INTRODUCTION

Globally, urban areas are seeing a rise in traffic congestion, leading to longer commutes, higher levels of automobile emissions, and a general decline in quality of life. Due to their reliance on set time schedules, traditional traffic light management systems often are unable to adjust to the dynamic nature of traffic flow, resulting in inefficiencies and congestion at junctions. Innovative strategies are required to improve urban mobility and traffic management in order to solve these issues.

A potential answer is provided by the density-based traffic light control system, which dynamically modifies signal timings in response to traffic density data collected in real time. Density-based systems employ sophisticated sensing technologies to detect vehicle counts and traffic flow at junctions, in contrast to traditional systems that follow preset schedules regardless of real traffic circumstances. With the use of this real-time data, the system is able to adjust traffic signal





PREDICTING DRIVER DROWSINESS THROUGH BEHAVIORAL ANALYSIS USING OPENCV

¹Dr.N.GOPALA KRISHNA, ²K SURENDRA REDDY, ³B SURESH REDDY

¹Professor, ²Associate Professor, ³Assistant Professor

Department Of Computer Science Engineering

Indira Institute Of Technology And Sciences, Markapur

ABSTRACT:

A major contributing element to road safety is driver fatigue, which raises the possibility of collisions dramatically. These hazards may be reduced by early diagnosis of sleepiness, however conventional techniques often fall short in the short term. This work uses behavioral analysis with OpenCV, a potent computer vision toolkit, to provide a unique method of predicting driver sleepiness.

The suggested system makes use of OpenCV to examine a variety of driver behavioral traits, including head position, blink frequency, and eye movements. Through the use of a camera mounted inside the car to record live video, the system analyzes visual inputs to detect indicators of fatigue. Sophisticated image processing methods are used to monitor and evaluate facial expressions that are suggestive of sleepiness, such as eyelid movement and gaze direction.

The research improves the forecast accuracy of tiredness by integrating OpenCV with machine learning methods. To identify patterns linked to tiredness, these algorithms are trained using a collection of driving photos that have been annotated. The system's capacity to analyze data in real-time guarantees that drivers get notifications in a timely manner, encouraging prompt remedial action and lowering the risk of collisions.

According to preliminary test findings, the technology can accurately and consistently identify when a driver would get sleepy. By offering a dependable, real-time monitoring tool, the method provides a workable way to increase driver safety. In order to improve detection capabilities, future work will concentrate on growing the dataset, improving the algorithm's accuracy, and investigating new behavioral characteristics.

The present research underscores the potential of OpenCV in the development of sophisticated driver assistance systems and stresses the significance of combining computer vision technology with behavioral analysis to improve road safety.

DOI Number: 10.48047/nq.2021.19.11.NQ21318

NeuroQuantology 2021;19(11):1022-1027

1022

1. INTRODUCTION

One of the main causes of traffic accidents and a major contributor to the risks to road safety is driver fatigue. Early identification of sleepy behavior may be critical in reducing accidents and improving road safety since tiredness decreases cognitive functioning and response times. Conventional techniques for identifying driver fatigue sometimes rely on arbitrary evaluations or outside tools that may not provide real-time feedback or work well with cars.

Recent developments in machine learning and computer vision open up new possibilities for real-time driver monitoring systems. The open-source computer vision package OpenCV offers a strong foundation for deciphering visual input and identifying relevant behavioral traits. Using OpenCV to predict driver sleepiness entails examining a range of metrics, including head position, eye movements, and blink frequency, to detect symptoms of exhaustion.

The objective of this research is to create a novel system that uses OpenCV's behavioral analysis to

eISSN 1303-5150



www.neuroquantology.com



STRENGTH PERFORMANCE OF M30 GRADE MULTI-OBJECTIVE OPTIMIZATION OF CONCRETE USING TREATED WASTEWATER CENTRIFUGAL PUMP VOLUTE DESIGN USING AS A PARTIAL SUBSTITUTE FOR POTABLE WATER RBF NEURAL NETWORKS AND GENETIC ALGORITHMS

¹CA. M. MURUGESH PRASAD

²Professor, ³Assistant Professor

¹KANDULA RAJA SEKHARA REDDY, ²SK ABDUL KALAM, ³P.N MANTHRU NAIK

¹Department Of Civil Engineering

Indira Institute Of Technology And Sciences, Markapur

Department Of Mechanical Engineering

Indira Institute Of Technology And Sciences, Markapur

ABSTRACT

This research looks at how well M30 grade concrete holds up when treated wastewater is used in place of certain potable water. The use of treated wastewater in concrete mixing offers a creative

way to cut down on freshwater use, which is important given the increasing need for sustainable building methods and water conservation. The study looks at how different amounts of treated pumps are connected and incompatible. To address this issue, a genetic algorithm (GA) and radial basis function (RBF) neural network-based approach for improving volute design has been developed. The entire amount of sound pressure level, the centrifugal pump's efficiency, concrete samples were made and evaluated at various levels, and the centrifugal pump's efficiency are the objective for optimization. The factors that are affected by the base of the pipe, the height of the volute diffuser tube, the volute tongue installation angle, and the volute tongue installation angle. The Latin hypercube sampling method, with the sample population size of 6000, is used to construct a database with the optimization. According to the study, the use of treated wastewater in a work technique is finally a place of potable water in 30 percent of the objective optimization for a comparative investigation of the hydraulic and acoustic performance of the individuals in the Pareto solution set under a variety of diverse operating situations, the first two individuals and the two individuals. DOI Number: 10.48047/neuroquantology.2021.19(11).1009-1021

Introduction of as a waste product from industrial and municipal activities. The strength performance of M30 grade concrete when treated wastewater is utilized in place of certain potable water is the main topic of this investigation. Since M30 grade concrete is extensively used in equipment, the volute is one of the main flow passage components of the centrifugal pump, so structural parameters are directly related to pump performance. There has been a lot of research on the use of treated wastewater as a partial substitute for potable water. It is essential to improve the volute design by optimizing the volute structure strength and longevity, especially when it comes to

1. GENERAL A key component of building concrete is renowned for its strength, resilience, and adaptability. However, large volumes of water, typically obtained from drinkable sources—are needed for the creation of concrete. The building sector is looking at other water sources in response to the energy shortages and environmental pollution. The primary problems faced by human society in sustainable development is a lack of liquid covering equipment. The use of a pump is widely used for pumped storage power generation. Wastewater has a variety of thermal

1. INTRODUCTION

Energy shortages and environmental pollution are the primary problems faced by human society in sustainable development. As a lack of liquid covering equipment. The use of a pump is widely used for pumped storage power generation. Wastewater has a variety of thermal

eISSN1303-5150

eISSN1303-5150

www.neuroquantology.com

www.neuroquantology.com


PRINCIPAL
INDIRA INSTITUTE OF TECHNOLOGY & SCIENCES
Darimadugu, Markapur-523 318
S. Prakasam Dist.(A.P.) India.



ENHANCING URBAN MOBILITY WITH DENSITY-BASED TRAFFIC LIGHT CONTROL SYSTEMS

¹V.MADHURI, ²SK.BEEBI, ³C.PUSHPALATHA

¹Associate Professor, ^{2,3}Assistant Professor

Department Of Electronics and Communication Engineering
Indira Institute Of Technology And Sciences, Markapur

ABSTRACT

Due to deteriorating signal control systems and escalating traffic congestion, urban transportation is facing more and more difficulties. In order to improve urban mobility, this research presents a density-based traffic light management system that dynamically modifies traffic signals in response to real-time traffic density data. By monitoring vehicle flow at junctions with the use of sophisticated sensors and data analytics, the suggested system allows for adaptive signal timing, which improves traffic flow and lessens congestion.

The system measures traffic density and examines traffic patterns in real time by integrating vehicle identification technology like cameras and inductive loop sensors. The traffic lights use density-based algorithms to modify their timing in response to changing traffic circumstances. This allows them to prioritize green signals in areas with high traffic volumes and reduce delays for all users of the road.

In comparison to conventional fixed-timing traffic signals, preliminary findings show that the density-based control system greatly improves traffic flow and decreases wait times at crossings. Because of the adaptive nature of the system, peak and off-peak traffic may be better managed, resulting in less congestion and more seamless transitions between lanes.

By minimizing stop-and-go traffic, this strategy not only improves overall urban mobility but also helps to reduce car emissions and improve air quality. The research shows how density-based traffic signal control systems may revolutionize urban traffic management by offering contemporary cities a scalable and efficient alternative. In order to provide complete traffic control, future research will concentrate on improving the system's algorithms, extending its deployment, and combining it with other smart city technologies.

DOI Number: 10.48047/nq.2021.19.11.NQ21314

NeuroQuantology 2021;19(11):986-994

986

I. INTRODUCTION

Globally, urban areas are seeing a rise in traffic congestion, leading to longer commutes, higher levels of automobile emissions, and a general decline in quality of life. Due to their reliance on set time schedules, traditional traffic light management systems often are unable to adjust to the dynamic nature of traffic flow, resulting in inefficiencies and congestion at junctions. Innovative strategies are required to improve urban mobility and traffic management in order to solve these issues.

A potential answer is provided by the density-based traffic light control system, which dynamically modifies signal timings in response to traffic density data collected in real time. Density-based systems employ sophisticated sensing technologies to detect vehicle counts and traffic flow at junctions, in contrast to traditional systems that follow preset schedules regardless of real traffic circumstances. With the use of this real-time data, the system is able to adjust traffic signal



INTELLIGENT SOLAR-POWERED LED STREET LIGHT WITH ADAPTIVE INTENSITY CONTROL FOR ENHANCED EFFICIENCY AND PERFORMANCE

¹T.VIJAY KIRAN KUMAR, ²K MANIKANTESWAR, ³MADI NARAYANA
^{1,2,3}Assistant Professor

Department Of Electrical and Electronics Engineering
Indira Institute Of Technology And Sciences, Markapur

ABSTRACT:

Explicit, measurable, practical, relevant, and time-based are the five characteristics that make anything "smart." IOT is an acronym for the enormous and constantly growing number of digital devices—billions, if we include them today—that are connected to potentially global networks. The term "smart" is gaining popularity as the globe becomes bigger a little bit quicker. India's economy is expanding at one of the quickest rates in the world, therefore we're using clever strategies, including smart street light systems. The manual streetlight system runs at full intensity from nightfall till morning, even when electricity is available. There are many uses for the saved energy, including residential and commercial. To do this, an LDR sensor is used. Depending on its intensity, we can switch a light on or off. A relay is used to transform the system's main electrical source. Any city must have a street lighting system in place. In order to save energy, we are using an IOT module for the project. The world is changing drastically, and as a consequence, everything is becoming more mechanized. This gadget makes intelligent judgments and intelligently controls itself using accurate, real-time field data.

I. INTRODUCTION

IOT meant to transmit data from the devices to master controller through gate ways & existing network structure. IOT market developments and analysis implies that unlicensed and licensed spectrums are essential. IOT system [1] operates with field sensors and data analyzing on the internet which can communicate them to share and transfer information using unique id assigned to every device. Automation plays an important role in the modern society and where IOT along with LoRa can help to fulfill the needs. For the Street lighting & Electrical systems due to the conventional on/off system there is a huge loss of electrical power noted and studies conducting in the area to minimize the power loss by various technology. Mobile based surveillance with web uses IOT cloud server used here for more energy conservation and early resolution in case of any fault detection. Lot of research is conducting in this field to minimize energy loss in remote locations by implementing user friendly applications. The main idea of this research is to develop an automated and controlled street light according to requirement the roads, pedestrians & Vehicles. A user friendly control system to monitor & control the lighting systems from remote locations with using IOT & LoRa can fulfill the requirements with minimal infrastructure cost by using the existing networks & un licensed radio frequencies. From remote locations, Field Sensor data can be transmitted to the master control stations through LoRa gateways, after reaching gateways signals will be transferred to the User end through existing network server & vice versa. Every gateway forwards the received packet from the end-node to the cloudbased network server via some backhaul either cellular, Ethernet, satellite, or Wi-Fi. Hence the power consumption can be cut down by switching off the circuit when there is no requirement of lighting in particular area. Successful implementation of IOT & LoRa systems can bring lot of benefits in the fields of Home automation [2], Temperature Monitoring, patient health monitoring, Vehicle monitoring etc.

II. LITERATURE SURVEY

A public Street Lights & Electrical system in remote city locations consumes a lot of energy due to the unavailability of control devices due to the large setup cost. Presently most of street lamps turn on the street lights in night and turns off the street lights in day using LDR based control system [3]. Street lamp or Electrical systems still consumes a lot of electricity when there are few vehicles around or no

people in the office due to the lack of monitoring and controlling based on the actual requirements [4]. For a wireless control monitoring system each street light must be equipped with different types of sensors that are connected to a microcontroller to monitor its environment with regards to its working needs like light intensity, current capacity, voltage load and temperature which are collected and transferred by the means of radio frequency communication

III. DESIGN OF HARDWARE

This chapter briefly explains about the Hardware. It discuss the circuit diagram of each module in detail.

ARDUINO UNO

The Arduino Uno is a microcontroller board based on the ATmega328 (datasheet). It has 14 digital input/output pins (of which 6 can be used as PWM outputs), 6 analog inputs, a 16 MHz ceramic resonator, a USB connection, a power jack, an ICSP header, and a reset button. It contains everything needed to support the microcontroller; simply connect it to a computer with a USB cable or power it with a AC-to-DC adapter or battery to get started.

The Uno differs from all preceding boards in that it does not use the FTDI USB-to-serial driver chip. Instead, it features the Atmega16U2 (Atmega8U2 up to version R2) programmed as a USB-to-serial converter. Uno board has a resistor pulling the 8U2 HWB line to ground, making it easier to put into DFU mode. Arduino board has the following new features:

- 1.0 pin out: added SDA and SCL pins that are near to the AREF pin and two other new pins placed near to the RESET pin, the IOREF that allow the shields to adapt to the voltage provided from the board. In future, shields will be compatible both with the board that use the AVR, which operate with 5V and with the Arduino Due that operate with 3.3V. The second one is a not connected pin, that is reserved for future purposes.
- Stronger RESET circuit.
- Atmega 16U2 replace the 8U2.

"Uno" means one in Italian and is named to mark the upcoming release of Arduino 1.0. The Uno and version 1.0 will be the reference versions of Arduino, moving forward. The Uno is the latest in a series of USB Arduino boards, and the reference model for the Arduino platform; for a comparison with previous versions, see the index of Arduino boards.

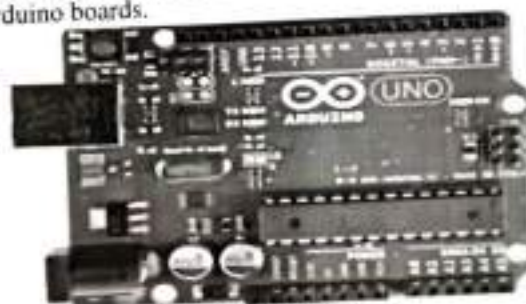


Fig. ARDUINO UNO

POWER SUPPLY:

The power supplies are designed to convert high voltage AC mains electricity to a suitable low voltage supply for electronic circuits and other devices. A power supply can be broken down into a series of blocks, each of which performs a particular function. A d.c power supply which maintains the output voltage constant irrespective of a.c mains fluctuations or load variations is known as "Regulated D.C Power Supply".


PRINCIPAL
VINDRA INSTITUTE OF TECHNOLOGY & SCIENCES
Darimadugu, Markapur-523 310
Prakasam Dist.(A.P.) India.

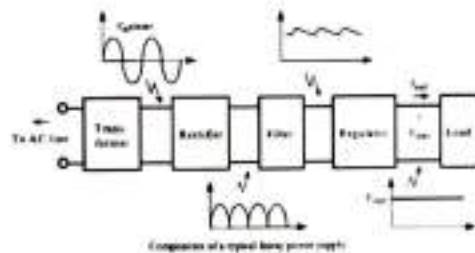


Fig: Block Diagram of Power Supply

LCD DISPLAY

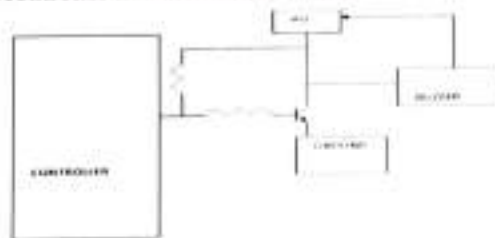
A model described here is for its low price and great possibilities most frequently used in practice. It is based on the HD44780 microcontroller (Hitachi) and can display messages in two lines with 16 characters each. It displays all the alphabets, Greek letters, punctuation marks, mathematical symbols etc. In addition, it is possible to display symbols that user makes up on its own. Automatic shifting message on display (shift left and right), appearance of the pointer, backlight etc. are considered as useful characteristics.



Fig: LCD

BUZZER

Digital systems and microcontroller pins lack sufficient current to drive the circuits like relays, buzzer circuits etc. While these circuits require around 10 milli amps to be operated, the microcontroller's pin can provide a maximum of 1-2 milli amps current. For this reason, a driver such as a power transistor is placed in between the microcontroller and the buzzer circuit.



WIFI MODULE:

The **ESP8266** is a low-cost Wi-Fi microchip with full TCP/IP stack and microcontroller capability produced by Shanghai-based Chinese manufacturer, Espressif Systems.^[1] The chip first came to the attention of western makers in August 2014 with the **ESP-01** module, made by a third-party manufacturer, Ai-Thinker. This small module allows microcontrollers to connect to a Wi-Fi network and make simple TCP/IP connections using Hayes-style commands. However, at the time there was almost no English-language documentation on the chip and the commands it accepted.^[2] The very low price and the fact that there were very few external components on the module which suggested that it could eventually be very inexpensive in volume, attracted many hackers to explore the module, chip, and the software on it, as well as to translate the Chinese documentation.^[3]

PRINCIPAL
SINDIRA INSTITUTE OF TECHNOLOGY & SCIENCES
Darimadugu, Markapur-522 312
Prakasam Dist. (A.P.) India.

The ESP8285 is an ESP8266 with 1 MiB of built-in flash, allowing for single-chip devices capable of connecting to Wi-Fi.^[4]
The successor to these microcontroller chips is the ESP32.



LED:

A light-emitting diode (LED) is a two-lead semiconductor light source. It is a p-n junction diode that emits light when activated.^[5] When a suitable voltage is applied to the leads, electrons are able to recombine with electron holes within the device, releasing energy in the form of photons.

This effect is called electroluminescence, and the color of the light (corresponding to the energy of the photon) is determined by the energy band gap of the semiconductor. LEDs are typically small (less than 1 mm²) and integrated optical components may be used to shape the radiation pattern.



Early LEDs were often used as indicator lamps for electronic devices, replacing small incandescent bulbs. They were soon packaged into numeric readouts in the form of seven-segment displays and were commonly seen in digital clocks. Recent developments have produced LEDs suitable for environmental and task lighting. LEDs have led to new displays and sensors, while their high switching rates are useful in advanced communications technology.

LEDs have many advantages over incandescent light sources, including lower energy consumption, longer lifetime, improved physical robustness, smaller size, and faster switching. Light-emitting diodes are used in applications as diverse as aviation lighting, automotive headlamps, advertising, general lighting, traffic signals, camera flashes, and lighted wallpaper. They are also significantly more energy efficient and, arguably, have fewer environmental concerns linked to their disposal.

LIGHT DEPENDENT RESISTOR

A photo resistor or light dependent resistor (LDR) is a resistor whose resistance decreases with increasing incident light intensity; in other words, it exhibits photoconductivity. It can also be referred to as a photoconductor or CdS device, from "cadmium sulfide," which is the material from which the device is made and that actually exhibits the variation in resistance with light level. Note that CdS is not a semiconductor in the usual sense of the word (not doped silicon).



A photoresistor is made of a high resistance semiconductor. If light falling on the device is of high enough frequency, photons absorbed by the semiconductor give bound electrons enough energy to jump into the conduction band. The resulting free electron (and its hole partner) conduct electricity, thereby lowering resistance.

A photoelectric device can be either intrinsic or extrinsic. An intrinsic semiconductor has its own charge carriers and is not an efficient semiconductor, e.g. silicon. In intrinsic devices the only available electrons are in the valence band, and hence the photon must have enough energy to excite the electron across the entire bandgap. Extrinsic devices have impurities, also called dopants, added whose ground state energy is closer to the conduction band; since the electrons do not have as far to jump, lower energy photons (i.e., longer wavelengths and lower frequencies) are sufficient to trigger the device. If a sample of silicon has some of its atoms replaced by phosphorus atoms (impurities), there will be extra electrons available for conduction. This is an example of an extrinsic semiconductor. Photo resistors are basically photocells.

LDRs or Light Dependent Resistors are very useful especially in light/dark sensor circuits. Normally the resistance of an LDR is very high, sometimes as high as 1000 000 ohms, but when they are illuminated with light resistance drops dramatically.



IR SENSOR

Infrared is a energy radiation with a frequency below our eyes sensitivity, so we cannot see it Even that we can not "see" sound frequencies, we know that it exist, we can listen them.



Even that we can not see or hear infrared, we can feel it at our skin temperature sensors.

When you approach your hand to fire or warm element, you will "feel" the heat, but you can't see it. You can see the fire because it emits other types of radiation, visible to your eyes, but it also emits lots of infrared that you can only feel in your skin.

INFRARED IN ELECTRONICS

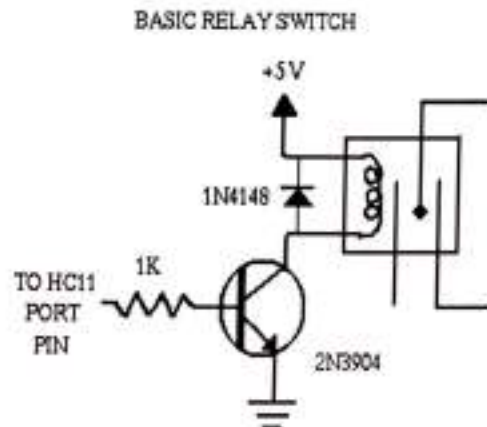

PRINCIPAL
SRI SRI SRI INDRIA INSTITUTE OF TECHNOLOGY & SCIENCES
Darimadugu, Markapur-523 316
Prakasam Dist. (A.P.) India.

Infra-Red is interesting, because it is easily generated and doesn't suffer electromagnetic interference, so it is nicely used to communication and control, but it is not perfect, some other light emissions could contain infrared as well, and that can interfere in this communication. The sun is an example, since it emits a wide spectrum of radiation.

The adventure of using lots of infra-red in TV/VCR remote controls and other applications, brought infra-red diodes (emitter and receivers) at very low cost at the market.

From now on you should think as infrared as just a "red" light. This light can mean something to the receiver, the "on or off" radiation can transmit different meanings. Lots of things can generate infrared, anything that radiate heat do it, including our body, lamps, stove, oven, friction your hands together, even the hot water at the faucet.

RELAY



The following schematic shows the basic circuit.

A relay is an electrically operated switch. When you turn it on, it switches on way. When it is off, it switches the other way. You can use a relay to switch on and off a high current device. A relay has an electromagnet, called a coil, and a lightweight switch inside it. When you energize the coil, a piece of the switch is attracted by the coil's magnetic field, which switches the switch on or off.

Mechanical relay:

Typical Mechanical Relay connection pin

This is a very important section. The introduction to this electrical control switch, call a Relay. It is basically a device to activate a mechanical switch, by electrical means. This is unlike a switch which is activated manually. In another words it is a device that convert electrical signal to a mechanical energy back to electrical signal again. Similar to mechanical switch, they can be described as 2P2T, single pole double throw, etc...

How it works? A electrical voltage will be applied to activate a coil in the relay. The coil being powered up, will generate a magnetic force that will attract the lever. This lever will be pulled towards the magnetized coil, causing an action that will switch the mechanical contact.

Solar panel :

Solar panel refers either to a photovoltaic (PV) module, a solar hot water panel, or to a set of solar photo voltaic modules electrically connected and mounted on a supporting structure. A PV module is a packaged, connected assembly of solar cells. Solar panels can be used as a component of a larger photovoltaic system to generate and supply electricity in commercial and residential applications. Each module is rated by its DC output power under standard test conditions, and typically ranges from 100 to 320 watts. The efficiency of a module determines the area of a module given the same rated

output – an 8% efficient 230 watt module will have twice the area of a 16% efficient 230 watt module. There are a few solar panels available that are exceeding 19% efficiency. A single solar module can produce only a limited amount of power; most installations contain multiple modules. A photovoltaic system typically includes a panel or an array of solar modules, an inverter, and sometimes a battery and/or solar tracker and interconnection wiring.

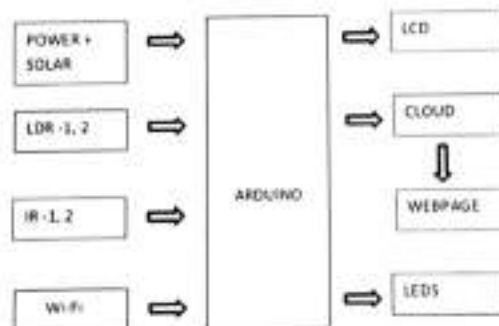
Solar modules use light energy (photons) from the sun to generate electricity through the photovoltaic effect. The majority of modules use wafer-based crystalline silicon cells or thin-film cells based on cadmium telluride or silicon. The structural (load carrying) member of a module can either be the top layer or the back layer. Cells must also be protected from mechanical damage and moisture. Most solar modules are rigid, but semi-flexible ones are available, based on thin-film cells. These early solar modules were first used in space in 1958.

Electrical connections are made in series to achieve a desired output voltage and/or in parallel to provide a desired current capability. The conducting wires that take the current off the modules may contain silver, copper or other non-magnetic conductive transition metals. The cells must be connected electrically to one another and to the rest of the system. Externally, popular terrestrial usage photovoltaic modules use MC3(older) or MC4 connectors to facilitate easy weatherproof connections to the rest of the system.

Bypass diodes may be incorporated or used externally, in case of partial module shading, to maximize the output of module sections still illuminated.



BLOCK DIAGRAM:



V.CONCLUSION

An important development in urban lighting technology is the intelligent solar-powered LED street light with adaptive intensity management. This system uses solar energy to reduce energy costs and provide a sustainable and environmentally friendly substitute for standard street lighting by relying less on the grid. High luminance and long-lasting performance are ensured by the incorporation of LED

technology, which also minimizes energy consumption.

The system's efficiency is increased by the adaptive intensity control function, which dynamically modifies the light output in response to current traffic patterns and ambient circumstances. When maximum brightness is not required, this clever adjustment feature provides ideal lighting levels, enhancing safety and visibility while saving energy. The system's capacity to adjust to changing circumstances also prolongs the LEDs' lifespan and lowers maintenance needs.

In addition, the intelligent street light system allows remote monitoring and control, which enables effective administration and prompt resolution of any problems. With the help of this feature, maintenance crews and municipal planners may monitor the system's operation and make required modifications from one central place.

To fully reap the benefits of the system, however, obstacles like the initial installation cost and other technical problems need to be resolved. Overcoming these obstacles and improving system dependability need constant study and technological developments.

All things considered, the clever solar-powered LED street light with adaptive intensity control provides a cutting-edge answer for contemporary urban lighting requirements. It provides a useful and creative approach to street lighting by fusing efficiency, sustainability, and cutting-edge technology, helping to create smarter and greener cities.

REFERENCES:

- [1] Biswas, Abdur Rahim, and Raffaele Giaffreda. "IoT and cloud convergence: Opportunities and challenges." In 2014 IEEE World Forum on Internet of Things (WF-IoT), pp. 375-376. IEEE, 2014.
- [2] Samuel SSI. A review of connectivity challenges in IoT smart home. In: 3rd MEC international conference on bigdata and smart city (ICBDSC), Muscat, Oman, 15-16 March 2016, pp.1-4, New York: IEEE.
- [3] Teja, P. Satya Ravi, V. Kushal, A. Sai Srikar, and K. Srinivasan. "Photosensitive security system for theft detection and control using GSM technology." In Signal Processing And Communication Engineering Systems (SPACES), 2015 International Conference on, pp. 122-125. IEEE, 2015.
- [4] Shahzad G., Yang H., Waheed A., Lee C. "Energy Efficient Intelligent Street Lighting System Using Traffic Adaptive Control", IEEE Sensors Journal, DOI 10.1109/JSEN.2016.25.57345, 2015 IEEE.
- [5] Augustin A, Yi J, Clausen T, et al. A study of LoRa: long range and low power networks for the Internet of Things. Sensors 2016; 16(9): 1466.
- [6] O. Natu, "GSM Based Smart Street Light Monitoring," IEEE, 2013 [7] I. A. C. L. Zeeshan Kaleem, "Smart and Energy Efficient LED Street Light Control," IEEE.
- [8] LoRa™ Modulation Basics, AN1200 v22, LoRa Alliance, Inc. 2400 Camino Ramon, Suite 375 San Ramon, CA 94583 (2015), LoRa Alliance, Tech.
- [9] Deepak Kumar Rath, "Arduino based smart light control system," International Journal of Engineering Research and General science, vol. 4, no. 2, pp. 784-790, March - April 2016.


PRINCIPAL
SINDIRA INSTITUTE OF TECHNOLOGY & SCIENCES
Dattamadevi, Marol Nagar, 400 033
Mumbai, India. Phone: 022 316 316 316

PERFORMANCE ASSESSMENT OF CONCRETE WITH RECYCLED PLASTIC AS A FINE AGGREGATE ALTERNATIVE

¹DR. R. BALA MURGAN, ²B VENKATESWARLU

¹Professor, ²Assistant Professor

Department Of Civil Engineering

Indira Institute Of Technology And Sciences, Markapur

ABSTRACT: This research looks at how well concrete performs when fine particles are partially replaced with recycled plastic. In light of the increasing environmental issues around plastic waste and the need for sustainable building materials, recovered plastic shows great promise as a fine aggregate substitute. The study investigates the effects of different percentages of recycled plastic (10%, 20%, and 30%) on the workability and mechanical characteristics of concrete.

Recycled plastic was substituted for fine aggregate in concrete mixtures at varying degrees, and important performance metrics including workability, flexural strength, and compressive strength were assessed. The findings suggest that adding recycled plastic to concrete has a significant effect on its characteristics. Higher amounts (20% and 30%) resulted in a loss in compressive and flexural strength, but workability increased. In contrast, a 10% substitution had no influence on strength or workability. When compared to conventional aggregates, plastic has a lower density and worse bonding properties, which is why its strength has decreased.

The use of recycled plastic offers a sustainable alternative to the management of plastic waste while also significantly reducing the total environmental effect of concrete manufacturing, even if strength decreases at greater replacement levels. According to the study's findings, recycled plastic may be used to create concrete mixtures successfully, especially if the replacement amount is adjusted to strike a balance between sustainability and performance. Future studies should concentrate on long-term robustness and the creation of better processing techniques to increase recycled plastic's performance in concrete applications.

1. INTRODUCTION

The building sector is confronted with noteworthy obstacles concerning resource efficiency and environmental sustainability. The enormous quantity of plastic garbage produced worldwide is a significant problem as it often ends up in landfills or the ocean, where it poses serious environmental risks. The demand for conventional building supplies like fine aggregates is concurrently depleting natural resources. Researchers and business experts are looking into creative ways to address these issues by using recycled materials into building techniques.

Recycled plastic has surfaced as a viable substitute for conventional fine aggregates in concrete. It is made from post-consumer and industrial plastic waste. This research looks at how well concrete that contains recycled plastic in lieu of certain fine particles performs. The main goals are to determine if recycled plastic affects the workability and mechanical qualities of concrete and whether it can be used as a sustainable building material.

Recycled plastic was substituted for fine aggregates in concrete mixes at different percentages (10%, 20%, and 30%) in order to study the effects on important characteristics including workability, flexural strength, and compressive strength. The purpose of the research is to examine the possible advantages and drawbacks of using recycled plastic, as well as how it may affect the structural performance and longevity of concrete.

This project aims to lessen the environmental effect of plastic waste, promote more sustainable construction methods, and provide options for resource conservation in the building sector by investigating the use of recycled plastic in concrete. The results will provide insightful information on whether recycled plastic may be used in place of fine aggregate and what it means for concrete applications in the future.

1.1 CONCRETE

Concrete is the world's most extensively used man-made building material, second only to water, and is produced by combining concrete components, and occasionally admixtures, in the proper quantities. When poured into moulds and left to cure, the mixture hardens into a rock-like mass known as concrete. Because the hardening is produced by a long-lasting interaction between water and cement, the concrete may also be regarded as an artificial stone in which the spaces of fine aggregate are filled with cement. In a concrete mix, combine the cementing material and water form a paste known as cement water-paste, which, in addition to filling fine aggregate voids, coats fine aggregate surfaces and binds them together as it dries, cementing fine aggregate particles together in a compact mass.

1.2 Plastics

Plastics now play a significant part in our everyday lives. Plastics are used in almost every aspect of production. Every day, thousands of tonnes of plastic goods are manufactured, and the trash continues to pile up. Because most plastics are not biodegradable, a massive quantity of plastic trash continues to accumulate throughout the globe, with developed countries contributing the most. More particular, packaging and containers account for the bulk of plastic waste. The quantity of land needed for landfills is becoming a growing source of worry throughout the globe. From 1950 to 2018, an estimated 6.3 billion tonnes of plastic were manufactured globally, with 9 percent recycled and the remaining 12 percent burned. Each year, India consumes more than 5 million tonnes of plastic, of which only about a quarter gets recycled, with the rest ending up in landfills. This massive quantity of plastic trash will eventually end up in the ecosystem, with research estimating that plastic debris may be found in the bodies of 90% of seabirds.

Plastic type	Name	Properties	Density Range	Common uses
	Polyethylene Terephthalate	Lightweight, strong, clear, and resistant to chemicals.	1.38-1.39 g/cm ³	Bottles, containers, fibers, and films.
	High-Density Polyethylene	Durable, resistant to impact, and chemically inert.	0.94-0.96 g/cm ³	Plastic bottles, pipes, and containers.
	Low-Density Polyethylene	Lightweight, flexible, and resistant to impact.	0.91-0.93 g/cm ³	Plastic bags, films, and containers.
	Polypropylene	Lightweight, strong, and resistant to impact.	0.89-0.91 g/cm ³	Automotive parts, fibers, and containers.
	Polystyrene	Lightweight, rigid, and resistant to impact.	1.04-1.05 g/cm ³	Styrofoam, containers, and fibers.
	Polyethylene	Lightweight, flexible, and resistant to impact.	0.91-0.96 g/cm ³	Plastic bags, films, and containers.

1.3 NEED OF PROJECT:

River erosion, fine aggregate demand, and other environmental problems have resulted in a shortage of river sand nowadays. The decrease in natural sand supplies, along with the desire to reduce the cost of concrete production, has led in a greater need to discover new alternative materials to replace river sand in order to avoid excessive river erosion. The use of substitute materials such as plastics, quarry dust, polyethylene terephthalate, iron slag, and others to partially or completely replace natural sand has been studied over the last two decades in order to preserve the ecological balance. This paper presents one experimental study of the strength properties of PET-Polyethylene Terephthalate in place of natural sand.

1.4 SCOPE

The research adds to and aids in the creation of new, ecologically friendly concrete binders. The impact of PET-Polyethylene Terephthalate on the strength and durability of concrete characteristics was extensively studied in this research.

Pulverized PET-Polyethylene Terephthalate is used to replace fine aggregate in OPC paste and concrete in various amounts ranging from 0% to 30%. Prior to being pulverised into powder, the granulated PET-Polyethylene Terephthalate was evaluated for its physical properties, such as aggregate grading, water absorption, and relative density, in contrast to typical fine aggregates used in concrete production.

II. MATERIALS

The following materials are used for the present work Cement

1. Fine aggregate
2. Coarse aggregate
3. Water
4. Plastic (poly Ethylene terephthalate)

2.1.Cement

Cement is a bonding substance with cohesive and adhesive characteristics that allows it to connect various building materials and compacted assemblies. Cement is a binder, a substance that sets and hardens as it dries, and may bind other materials together depending on how it interacts with carbon dioxide in the air. Lime, silica, alumina, and iron oxide are the most common basic ingredients used in cement production. In the kiln, these oxides react with one another to create more complicated compounds. The relative quantities of different oxide compositions have an impact on the various characteristics of cement, as well as the rate of cooling and grinding fitness. We utilised 53 Grade in this project

A.Ordinary Portland Cement:

The most common kind of cement is ordinary Portland cement (OPC). All of the previous chapter's talks, as well as the majority of the next chapters' debates, have been focused on OPC. There was just one grade of OPC

before to 1987, which was regulated by IS 269-1976. Higher-grade cements were introduced in India after 1987. Based on the strength of the cement at 28 days when tested according to IS 4031-1988, the OPC was categorised into three grades: 33, 43, and 53. 33 grade cements have a 28-day strength of not less than 33N/mm², 43 grade cements have a strength of not less than 43N/mm², and 53 grade cements have a strength of not less than 53N/mm².

However, the real strength of the manufacturing specimens isn't significantly greater than the BIS standards. Using high-quality limestone, contemporary technology, and tighter online control of components, it has been able to improve the characteristics of cement. This has resulted in improved practical size distribution, final grinding, and packaging. The use of higher-grade cement has a number of benefits in terms of producing stronger concrete. Despite the fact that they are somewhat more expensive than low-grade cement, they provide a 10-20% reduction in cement composition as well as a slew of other advantages.

Table 2.1: Approximate Oxide Composition Limits Of Ordinary Portland Cement

Chemical Compound	Percentage
Lime, (CaO)	60-66
Silica, (SiO ₂)	17-25
Alumina, (Al ₂ O ₃)	3-8
Iron Oxide, (Fe ₂ O ₃)	0.5-6
Magnesia, (MgO)	0.5-4
Sulphur Trioxide, (SO ₃)	1-2
Alkalis	0.5-1.3

2.1.1. Fine Aggregate:

When fine aggregates pass through a screen size of less than 4.75mm, they are referred to as fine aggregates. The separation limit for coarse and fine aggregates is 4.75mm. Aggregates with a diameter more than 4.75mm are classified as coarse, while those with a diameter less than 4.75mm are classified as fine. Natural sand or, subject to permission, other inert material with comparable qualities, or mixtures of hard, robust, durable particles should make up the fine aggregate. Fine aggregates from various sources must not be combined or kept in the same pile, nor utilised in the same class of building or mix in any order. The fine aggregate should be devoid of harmful inorganic and organic contaminants. The purpose of fine aggregates is to fill the spaces left by coarse aggregates. Fine aggregate is mostly composed of silica. In this study, sand that passes through an IS sieve of less than 4.75mm is chosen as a fine aggregate material for concrete production.

2.1.2. Coarse Aggregate:

Because aggregate makes up at least three-quarters of the volume of concrete, it's no surprise that its quality is so important. The aggregate characteristics have a significant impact on the concrete's durability and structural performance. Coarse aggregate is defined as particles with a diameter larger than 4.75 mm. Because coarse aggregates are the primary load bearing components of concrete, they take up more space than cement and fine aggregates. In the finest concrete producing technique, the quality and amount of these are very important. This is the current project; the coarse aggregates used are a mix of 20 mm and 12 mm in size. For this project, 60 percent of 20 mm and 40 percent of 12 mm were selected.

2.1.3 Drinking Water:

Water is an essential component of concrete because it is involved in the chemical process known as hydration. By releasing the products of hydration known as tri calcium silicates and di-calcium silicates, this hydration gives the cohesive character to the cement particles in binding the coarse and fine aggregates. In effective concrete practise, the amount and quality of water are critical. Extra concrete is deemed a felony if it exceeds the required amount. Because it creates capillary holes in concrete, it may significantly decrease the strength of the material. The usual yardstick for quality is "the water that is utilised for drinking water may be a suitable match for concrete production." This project makes use of potable water. For this research, a W/C ratio of 0.50 was used.

2.1.4 Poly Ethylene Terephthalate (PET):

PET or PETE stands for polyethylene terephthalate, which is a thermoplastic polymer that belongs to the polyester family. Polyester resins are well-known for their outstanding mix of mechanical, thermal, chemical, and dimensional stability characteristics.

PET is one of the most recycled thermoplastics, and its recycling sign is the number "1."

PET that has been recycled may be made into fibres, textiles, and sheets for packaging and automobile components. Poly butylene terephthalate is chemically extremely similar to Poly ethylene terephthalate. PET is a semi-crystalline resin that is extremely flexible, colourless, and semi-crystalline in its natural form. It may be semi stiff to rigid depending on how it's treated. It has excellent dimensional stability, impact resistance, moisture resistance, and resistance to alcohols and solvents.

2.2 TESTING ON MATERIALS

2.2.1 Test on cement

The following tests are done on the cement

- a. Fineness test
- b. Specific gravity test.

a. Fineness of cement:

Place 100 grammes of cement on a normal 90 micron IS sieve and weigh it precisely. Fingers should be used to break down any air-set lumps in the cement sample. For 15 minutes, sift the sample continuously in a circular and vertical motion. Sieving devices that are mechanical may also be utilised. Weigh the residue that has accumulated on the sieve.

The weight of residue as a proportion of the entire sample is given as,

$$\% \text{ Weight of residue} = \frac{\text{Weight of sample retained on sieve}}{\text{Total Weight of sample}}$$

The proportion of residue in the sample should not be more than 10%.

Table 2.2: Observations of Fineness of Cement Test

Trail No.	1	2
Weight of cement in grams	100	100
Weight of residue on sieve in grams	4	4
Amount retained	4	4

Fineness of cement = 4%. Hence it is within the permissible limits.

b. Specific Gravity Test:

Take a particular gravity bottle and clean and dry it before weighing it (W1). Fill the specific gravity bottle halfway with water and weigh the water weight using the bottle (W2). After draining the water and drying the specific gravity container, fill it with kerosene up to the rim (W3). Fill the specific gravity bottle with cement and use the weight of the container to calculate the weight of the cement (W5). Fill the specific gravity bottle with kerosene and calculate the weight of the bottle with kerosene and cement as follows: (W4).

According to IS: 456-2000

Limits: Specific Gravity of cement < 3.15 gm/cc

TABLE 2.3: OBSERVATIONS OF SPECIFIC GRAVITY OF CEMENT TEST

S.NO	Description	Trail No
1	Mass of empty bottle (W ₁) gm	50.0
2	Mass of bottle + water (W ₂) gm	182.0
3	Mass of bottle + kerosene (W ₃) gm	153.0
4	Mass of bottle + cement + kerosene (W ₄) gm	192.2
5	Mass of cement (W ₅) gm	50.0

$$\text{Specific gravity of cement (G)} = \frac{W_5(W_3 - W_1)}{(W_5 + W_3 - W_4)(W_2 - W_1)}$$

$$= \frac{50(155 - 50)}{(50 + 155 - 192.2)(182 - 50)}$$

$$= 3.11 \text{ gm/cc}$$

The specific gravity of cement obtained is 3.11 gm/cc.

Hence it is within the permissible limit.


PRINCIPAL
 SRIJEEVA INSTITUTE OF TECHNOLOGY & SCIENCES
 Darimadugu, Markapur-523 316
 Prakasam Dist. (A.P.) India.

Table 2.4. Test results of cement

S.NO	Properties	Results	Suggested values as per IS Specification
1	Fineness of cement	4% retained	<10%
2	Specific Gravity	3.11	<3.15

2.3. Tests on Fine Aggregate (sand):

The tests below are carried out to determine the characteristics of fine aggregates:

- a. Grading of sand
- b. Specific gravity and water absorption Test

a. Grading of Sand –Sieve Analysis: By quartering a 50 kg sample via a riffle box, you can get 1 kilogramme of sample. Arrange the appropriate sieves one on top of the other, with the sieve size increasing as you go closer to the top. Place the pan on the bottom of the pot. Cover the sieve and place it in the top sieve. In a sieve shaker, agitate the sieves for 20 to 30 minutes. Weigh the material retained in each filter as well as the pan. Determine its fineness modulus based on its grading parameters. The sizes of sieves use are: 4.75 mm, 2.36 mm, 1.18mm, 600µ, 300µ, 150µ and a pan.

TABLE 2.5: OBSERVATIONS OF SIEVE ANALYSIS TEST:

S.NO	Sieve size	Weight retained	% Weight retained	Cumulative % of weight retained	% weight passing	Cumulative % weight passing
1	4.75mm	9	0.9	0.9	99.1	99.1
2	2.36mm	11.6	1.16	2.06	97.94	197.04
3	1.18mm	188.5	18.85	20.91	79.01	276.05
4	600µ	300	30.0	50.91	49.09	374.15
5	300µ	380	38.0	88.91	11.01	385.16
6	150µ	102.5	10.25	99.16	0.84	386
7	Pan	6	0.6	99.76	0.24	386.24

From the table the fineness modulus of the sand = $\frac{\sum F}{100} - \frac{386.24}{100} = 3.86$

Hence it is within the permissible limits.

b. Specific Gravity of fine Aggregate (sand):

Take the clean, dry density bottle and weigh it as W1. Fill a density bottle halfway with oven dry soil that has passed through a 4.75mm sieve, and weigh it as W2. In the event of medium to coarse-grained soil, take 200 grammes. Fill the density bottle halfway with distilled water and thoroughly mix it with the glass rod. Replace the sieve top and fill the density bottle with water from the outside, weighing it as W3. Remove the contents, wash the density bottle, and fill it with distilled water to the conical cap's hole. Weigh it as W4.


PRINCIPAL
 ANJANA INSTITUTE OF TECHNOLOGY & SCIENCES 1115
 Darimadugu, Markapur-523 335
 Prakasam Dist. (A.P.) India

Table 2.6. Observations of Specific Gravity of Fine Aggregate Test:

S.NO	Description	Trail(gm)
1	Weight of density bottle (W ₁)gm	181
2	Weight of density bottle + Dry soil (W ₂)gm	381
3	Weight of density bottle + Dry soil + Water (W ₃)gm	879
4	Weight of density bottle + Water (W ₄)gm	752

$$\text{Specific gravity of sand} = \frac{W_2 - W_1}{(W_4 - W_1) - (W_3 - W_2)}$$

$$= \frac{381 - 181}{(752 - 181) - (879 - 381)}$$

$$= 2.65$$

Table 2.7: Test Results of Fine Aggregate

S.NO	Properties	Results
1	Grading of sand	3.86
2	Specific gravity	2.65

Hence these values are within the permissible limits.

Tests on coarse aggregate:

To determine the characteristics of coarse aggregate, the following experiments are carried out:

- a. Water absorption and specific gravity tests
- a. Crushing value of aggregates test
- c. test of the total impact value

a. Water Absorption and Specific Gravity Test:

A sample of aggregate weighing at least 2 kg is collected. The aggregate is carefully cleaned to remove the finer particles and dust that have adhered to it. After that, it's put in a wire basket and submerged in distilled water at a temperature of 22 to 32 degrees Fahrenheit. The entrapped air was eliminated from the sample immediately after immersion by raising the basket containing 25 mm above the tank's base and letting it to drop 25 times at a rate of approximately 1 drop per second. During the procedure, it is important to keep the basket and aggregate fully submerged in water. They are then submerged in water for a duration of 24 + 12 hours. The basket and aggregate are then shocked and weighed (W1) in water between 220 and 320 degrees Celsius. After removing the basket and aggregate from the water and allowing them to drain for a few minutes, the aggregate is removed from the basket and put on a dry towel, where it is gently dried. The aggregate is then moved to a second dry towel to be dried further. The empty basket is submerged in water for a second time, shocked 25 times, and weighed in water (W2). The aggregate is exposed to the environment for at least 10.10 minutes, away from direct sunlight, until it looks fully dry on the surface.

The aggregate is then weighed in the air (W3). The aggregate is then baked at a temperature of 100 to 1100 degrees Celsius for 24 hours and 12 hours. It is then chilled and weighed in an airtight container (W4).


PRINCIPAL
 CHINDRA INSTITUTE OF TECHNOLOGY & SCIENCES
 Darimadugu, Markapur-575 107
 Prakasam Dist.(A.P.) India

Table 2.8: Observation of Specific gravity and Water Absorption of Coarse Aggregate

S.No	Details	Values
1	Water of saturated aggregate suspended in basket with water (w1) gm	2750
2	Weight of basket suspended in water (w2) gm	750
3	Weight of saturated aggregate in water (ws) gm= w1-w2	2000
4	Weight of saturated surface dry aggregate in air (w3) gm	3133
5	Weight of water equal to volume of aggregate (w3-ws) gm	1133
6	Weight of oven dried fine aggregate (w4) gm	2994

$$\text{Specific gravity} = \frac{w_4}{w_3 - (w_1 - w_2)} \times \frac{2994}{3133 - 2000} = 2.64 \text{ gm/cc}$$

$$\text{Apparent specific gravity} = \frac{w_4 - (w_1 - w_2)}{w_4} \times \frac{2994}{2994 - 2000} = 3.01 \text{ gm/cc}$$

$$\text{Water absorption} = 100 \times \frac{w_3 - w_4}{2994} = 0.40\%$$

LIMITS:

The specific gravity of aggregate ranges from 2.5-3.0

The water absorption ranges from 0.1-2.0%

The specific gravity of coarse aggregate is determined to be 2.64, and its water absorption is 0.40 percent.

As a result, these two are inside the acceptable range.

b. AGGREGATE CRUSHING VALUE TEST

The standard aggregate crushing test is performed using material that has passed through a 12.5mm IS sieve and has been kept on a 10mm IS sieve. Other sizes up to 25mm may be tested if needed or if the normal size is not available. However, since the aggregate is not homogeneous, the findings will not be comparable to those obtained in the conventional test. A total of 6.5 kg of aggregate that passes the 12.5mm and 10mm sieves is collected. In three layers of about equal depth, the aggregate is filled in to the standard cylindrical measure in a surface dry state. Each layer is tamped with the tamping rod 25 times before being levelled with the tamping rod as a straight edge. The weight of the sample in the cylinder is calculated (A). For the following repeat test, the same weight of the sample is used. The test equipment cylinder is placed on the base plate with the aggregate filled in a conventional way, the aggregate is properly levelled, and the plunger is inserted horizontally on this surface. The plunger must not get stuck in the cylinder. The equipment is put on the compression testing machine with the test sample and plunger in place, and it is evenly loaded up to a total load of 40 tonnes in 10 minutes. The load is released, and the whole contents of the cylinder are withdrawn and sieved on a 2.36mm IS Sieve. The percentage of the sample that passes through the sieve is weighted (B).

$$\text{The aggregate crushing value} = \frac{B}{A} \times 100 \text{ Where,}$$

B = Weight of friction passing 2.36mm sieve.

A = In a mould, weigh a surface-dry sample. The aggregate crushing value for concrete other than for wearing surfaces shall not exceed 45 percent, and 30 percent for concrete used for wearing surfaces such as runways, highways, and air field pavements.



TABLE 2.9 OBSERVATION AND CALCULATIONS

S.NO	TOTAL AGGREGATE SAMPLE (A) gm	WEIGHT OF FINE PASSING 2.36mm IS SIEVE(B) gm	AGGREGATE CRUSHING VALUE = $\frac{B}{A} * 100$
1	2711.5	447.0	16.5

The crushing value of given aggregate is 16.5%. As per IS: 456-2000, it should be less than 30%.

C. AGGREGATE IMPACT VALUE TEST:

The aggregate impact value is a measure of an aggregation's resistance to abrupt shock or impact. This aggregate's resistance to a gradual compressive force is different.

The test samples are made up of aggregate that has passed through a 12.5mm sieve and has been kept on a 10mm IS sieve.

The aggregate must be dried and chilled in an oven for 4 hours at a temperature of 1000 C to 1100 C. The aggregate is poured to approximately one-third capacity and tamped with the tamping rod for 25 strokes. A comparable amount of aggregate is added and tamped in the traditional way. The measure is filled till it overflows, then levelled. The net weight of aggregate in the measure (weight A) is calculated, and this weight of aggregate is utilised in the duplicate test on the same material. The whole sample is placed in a cylindrical steel cup that is securely attached to the machine's base. A 14kg hammer is lifted to 380mm above the top surface of the aggregate in the cup and then allowed to fall freely on the aggregate. The test sample will be exposed to a total of 15 such hits, each given at a one-second interval. The crushed aggregate is taken from the cup and sieved on a 2.36mm IS sieve in its whole. The percentage that passes through the sieve is weighted to a precision of 0.1gm (weight B). The weight of the fraction retained on the sieve is also calculated (weight C). If the total weight (B+C) is more than one gramme less than the starting weight (A), the findings must be rejected and a new test performed. Two tests are carried out. In each test, the weight of fines formed is reported as a percentage of the overall sample weight.

Therefore, aggregate impact value = $\frac{B}{A} * 100$

Where,

B= Weight of fraction passing 2.36mm IS Sieve.

A= The weight of the sample after it has been dried in the oven. For aggregates used in concrete other than wearing surfaces, the aggregate impact value should not exceed 45 percent by weight, and for concrete used as wearing surfaces, such as runways, highways, and pavements, the aggregate impact value should not exceed 30 percent by weight.

TABLE 2.10 RESULTS OF AGGREGATE IMPACT TEST:

S.NO	DETAILS	TRAILS
1	Total weight of aggregate sample filling in the cylindrical measure=(a)gm	1282
2	Weight of aggregate passing 2.36mm sieve after the test = (b)gm	923
3	Weight of aggregate retained on 2.36mm sieve after the test= (c)gm	53.5
4	Difference in the weight = a-(b+c) gm	359
5	Aggregate impact value = $\frac{B}{A} * 100$	14.902%

According to IS: 456-2000, the effect value of a particular aggregate is 14.902 percent; it should be less than 45 percent, therefore it is likewise within acceptable limits.

1118

PRINCIPAL
 INDIRA INSTITUTE OF TECHNOLOGY & SCIENCES
 Darimadugu, Markapur-523 316
 Prakasam Dist.(A.P) India

TABLE 2.II: TEST RESULTS OF COARSE AGGREGATES:

S.NO	PROPERTIES	RESULTS	SUGGESTED VALUES AS PER IS: 456-2000 SPECIFICATIONS
1	Specific Gravity	2.82	2.3 to 3.0
2	Water Absorption	0.35%	0.1% to 2.0%
3	Crushing Value	16.5%	30%
4	Impact Value	14.902%	45%

III. Plastic (poly Ethylene terephthalate):

PET is one of the most recycled thermoplastics, and its recycling sign is the number "1." PET that has been recycled may be made into fibres, textiles, and sheets for packaging and automobile components. Poly butylene terephthalate is chemically extremely similar to Poly ethylene terephthalate. PET is a semi-crystalline resin that is extremely flexible, colourless, and semi-crystalline in its natural form. It may be semi-stiff to rigid depending on how it's treated. It has excellent dimensional stability, impact resistance, moisture resistance, and resistance to alcohols and solvents. Plastics that can't be deteriorated any more are ground into fine powder. The majority of these polymers are made of high-density polyethylene (HDPE)

3.1 Uses OF Plastic

- Plastic's popularity is growing due to its many advantages, which include:
- Lighter weight than comparable materials, lowering transportation fuel use.
 - Longevity and durability
 - Chemical, water, and impact resistance
 - Excellent insulation qualities, both thermally and electrically.
 - Lower manufacturing costs in comparison.

IV.METHODOLOGY

The procedure for the research "partial replacement of natural sand with Polyethylene terephthalate" is as follows.

The sand in the M20 concrete mix is partly replaced with polyethylene terephthalate up to 30% at intervals of 10%, i.e. 0%, 10%, 20%, and 30%. The following table provides a quick overview of the project.

THEME: Up to 80% replacement of sand with polyethylene terephthalate, with a 10% interval.

CEMENT USED: OPC M20 Concrete Mix proportions are used i.e., 1:1.5:3 No. of days cured: 7&28 days.

1:1.5:3 ; 10kg: 15kg: 30kg

So, for each percent replacement, 6 cubes were cast, with 3 cubes allocated for every 7 and 28 days of curing to evaluate compressive strength.

Table 4.1: Details of Cement, FA, CA and PET Composition in Concrete

% of Poly ethylene terephthalate	Materials used to cast cubes			
	Cement(kg)	F.A + Poly ethylene terephthalate	C.A	W/C Ratio
0%	10	15+0	30	0.54
10%	10	13.5+1.5	30	0.54
20%	10	12+3	30	0.54
30%	10	10.5+4.5	30	0.54

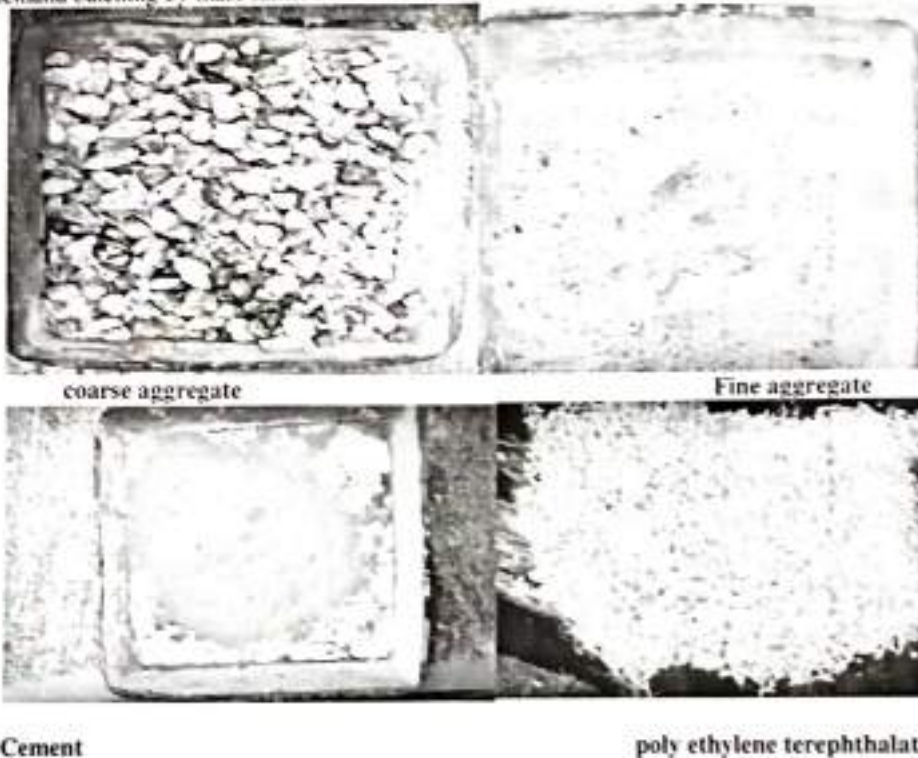
The following procedural stages are followed in order to achieve the work's goal.



1. Batching
2. Mixing
3. Casting of cubes
4. Compaction
5. Curing
6. Testing

4.1. BATCHING:

It is the process of measuring and adding concrete mix components into the mixture, either by volume or by mass. Batching has traditionally been done by volume, however most standards demand batching by mass rather than volume.



4.2 MIXING

Mixing should take place on a non-porous surface. In alternating layers, spread out the specified amounts of coarse and fine aggregate. Pour the cement on top of it and mix it dry with a shovel, stirring the mixture many times until the colour is consistent. This homogeneous mixture is applied in a 20cm thick layer. The mixture is sprinkled with water and flipped over at the same time. This process is repeated until a nice uniform, homogenous concrete is achieved. It's also important to note that the water is sprinkled rather than poured. To get the desired consistency, a little amount of water should be added towards the conclusion of the mixing process. Even a little amount would suffice at that point.

(i) Workability testing of concrete mix:

Concrete compaction of 100 percent is an essential factor in achieving optimum strength. Lack of compaction will result in air spaces, which will have an equivalent or greater impact on strength and durability than the existence of capillary cavities. Workable concrete is defined as concrete that meets the following specifications. The phrase "workability" or "workable concrete" has a considerably broader and deeper meaning than the term "consistency," which is frequently used interchangeably with workability. Consistency is a broad word that refers to the degree of fluidity or movement. The word "workability"

1120


PRINCIPAL
INDIRA INSTITUTE OF TECHNOLOGY & SCIENCES
Darimadugu, Markapur-523 316
Prakasam Dist.(A.P.) India.

refers to the "property of concrete that affects the amount of beneficial internal work required to achieve complete compaction." Another definition that has a broader meaning is the "Ease with which concrete may be compacted 100 percent regardless of method of compaction and location of deposition."

4.2.1 SLUMP CONE EXPERIMENT:

It's the most popular technique for determining the consistency of concrete, and it may be used in the lab or on the job site. It's not a good technique for extremely wet or very dry concrete, it doesn't account for all variables that affect workability, and it's not always indicative of concrete's ability to be placed. It is, nevertheless, useful as a control test and indicates the consistency of concrete from batch to batch. If the weights of aggregate cement and admixture are consistent and aggregate grading is within attainable limitations, repeated batches of the same mix delivered to the same slum will have the same water content and water content ratio. Observing how the concrete slumps may provide further information on the workability and amount of the concrete. The quality of concrete may also be determined by tamping or blowing the base plate using a tamping rod. The thickness of the metal sheet used to make the mould should not be less than 1.6mm. Suitable lifting guides are sometimes included with the mould. A steel tamping rod 16mm diameter, 0.6m length with bullet end is used to tamp the concrete. Before starting the test, the interior surface of the mould is carefully cleaned and free of excess moisture and adhesion of an old set concrete. The mould is set on a non-absorbent, smooth, flat, solid surface. The mould is then filled in four stages, each about 1/4 of the way up the mold's height. The tamping rod is used to tamp each layer 25 times, taking care to uniformly disperse the strokes throughout the cross section. The concrete is levelled using a trowel and tamping rod after the top layer has been rodded. The mould is immediately removed from the concrete by gently and carefully lifting it vertically. The concrete will be able to settle as a result of this. Concrete SLUMP is the term for this kind of subsidence. The level difference between the mold's height and the highest point of the subsiding concrete is measured.



TABLE 4.2: TEST RESULTS OF SLUMP WITH DIFFERENT %REPLACEMENT OF SAND WITH POLY ETHYLENE TEREPHTHALATE

% of polyethylene terephthalate	SLUMP VALUE(mm)
0%	90
10%	80
20%	70
30%	50

4.3. CASTING OF CUBES:

The concrete cubes were made to test the concrete's compressive strength. Metal moulds made of steel or cast iron were used to make the cubes. To avoid deformation, these moulds should be thick enough. These moulds are designed to make it easy to remove the moulded item without damaging it. A plane-surfaced base plate is included with each mould. The base plate should be large enough to hold the mould during filling without leaking, and it should be screwed to the mould. To prevent concrete adherence, the inner surface of the mould is lightly coated with oil.

Following these steps, the concrete components, which include cement, fine aggregate, coarse aggregate, plastic (polyethylene terephthalate), and water, are completely mixed in dry conditions until a uniform colour is obtained. The water is then added in the proper amounts and properly mixed again. The concrete is then poured into the mould.

The concrete cubes (150mm x 150mm x 150mm) were cast and tested as part of the test programme. Six specimens were utilised to evaluate the compressive strength of M20 concrete, with two specimens for each percentage of PET replacement level (0 percent, 10 percent, 20 percent, 30 percent). Casting and testing of partially plastic waste replaced (10%, 20%, and 30% of replacement with fine aggregate in concrete cubes) with the ingredients of ordinary Portland cement 53 Grade, natural river sand, and crushed stone of maximum size 20 mm, as well as casting and testing of partially plastic waste replaced (10%, 20%, and 30% of replacement with fine aggregate in concrete cubes) (150mm x 150mm x 150mm).

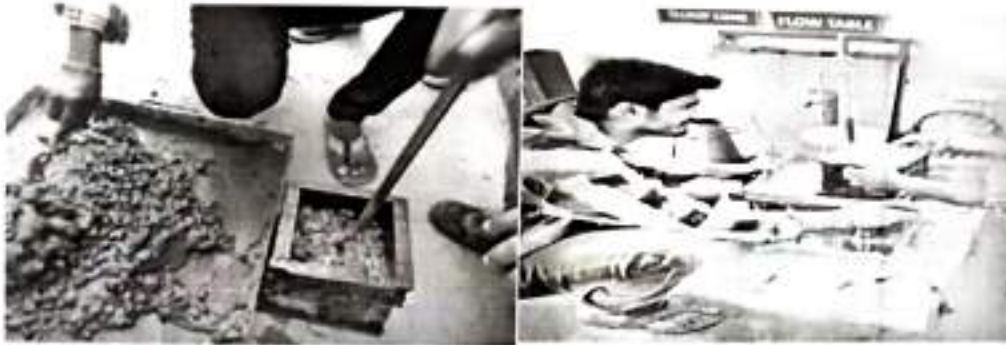


4.4 COMPACTION

Ensure that the concrete is sufficiently compacted by tamping it with a tamping rod. Insufficient compaction may result in poor workability, which makes the concrete harsh. Due to incorrect compaction, cavities may be present, allowing water to percolate through the concrete and compromising its durability. Proper compaction and mechanical compaction should be accomplished via hand compaction and mechanical compaction. The use of a table vibrator for mechanical compaction is possible. Remove the extra concrete using a trowel after the compaction is complete. Make a reference mark on the concrete cubes. Allow these cubes to sit for 24 hours without losing moisture. Then soak these cubes in water to cure them.

The cubes are made using the following quantities of concrete components and a replacer of polyethylene terephthalate.

PRINCIPAL
INDRA INSTITUTE OF TECHNOLOGY & SCIENCES
Darimadugu, Markapur-523 316
Prakasam Dist.(A.P.) India.



4.5 Curing of Cubes

The hydration of cement particles gives concrete its strength. The hydration of cement is a long-term process rather than a masonry activity. Of course, the rate of hydration is rapid at first, but it slows down with time. The amount of hydration product produced, and therefore the amount of gel created, is determined by the degree of hydration. For filling the spaces in the gel pores, the cement needs a W/C ratio of 0.15. To put it another way, a water/cement ratio of approximately 0.38 would be needed to hydrate all of the cement particles as well as fill the gel pores. A W/C concentration of 0.38 might theoretically fulfil the need for water for hydration in a concrete produced and contained in a sealed container while leaving no capillary cavities.

However, it is clear that a water content of 0.5 is needed for full hydration in a sealed container in order to maintain the desired relative humidity level.

4.6 Concrete Testing CUBES-Compressive Strength Test:

The most frequent test on hardened concrete is compressive strength, partly because it is simple to execute and partly because most of the desired characteristics of concrete are qualitatively linked to its compressive strength.

The compressive strength is measured on a cubical or cylindrical specimen. Prism is also employed on occasion, although it is not widely utilised in our nation. Parts of a beam tested in flexure are sometimes used to evaluate the compressive strength of concrete. After a flexure failure, the end portions of the beam are left intact, and since the beam is typically of cross section, this part of the beam may be utilised to determine the compressive strength. The cubes are 15*15*15 cm in size. If the aggregate's greatest nominal size does not exceed 20mm, 10cm size cubes may be utilised instead. Cylindrical test specimens are twice as long as they are wide. They have a diameter of 15cm and a length of 30cm. Smaller test specimens may be utilised, but the diameter of the specimen must be at least 3 times the maximum size of aggregate.



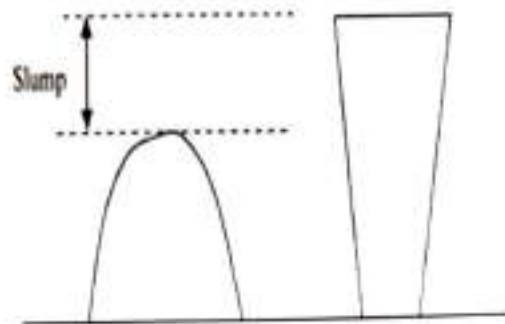
V. RESULTS

The findings of the experimental research are presented in the next section.

- The workability of various percentages of Polyethylene terephthalate as a partial substitute for fine aggregate in terms of slump values is shown below.

Table 5.1: Result of Slump Values

% OF POLY ETHYLENE TEREPHTHALATE	SLUMP VALUE(mm)
0%	90
5%	80
10%	70
15%	50



Compressive Strength of Concrete

$$\text{Compressive strength} = \frac{\text{Ultimate load}}{\text{Area of Specimen}}$$

Table 5.2 values for 0% replacement of fine aggregate with polyethylene terephthalate

Cube No.	Days of curing	Load in kN	Area in cm ²	Compressive strength in N/mm ²
1	7	658	225	29.24
2	28	897	225	39.86

Table 5.3: values for 10% replacement of fine aggregate with polyethylene terephthalate

Cube No.	Days of curing	Load in kN	Area in cm ²	Compressive strength in N/mm ²
1	7	624	225	27.73
2	28	864	225	38.4


 PRINCIPAL
 ANDHRA INSTITUTE OF TECHNOLOGY & SCIENCES
 Darimadugu, Markapur-523 318
 Prakasam Dist. (A.P.) India,

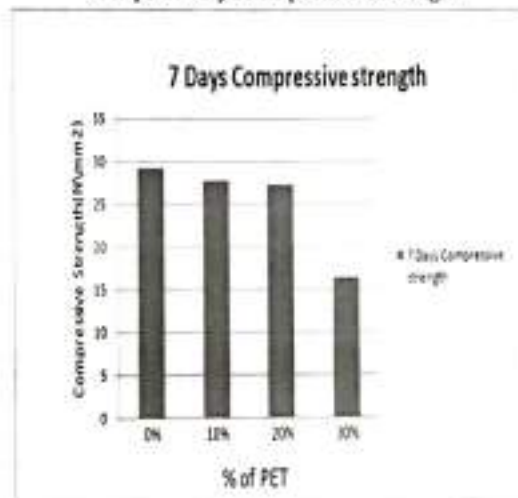
Table 5.4: values for 20% replacement of fine aggregate with polyethylene terephthalate

Cube No.	Days of curing	Load in kN	Area in cm^2	Compressive strength in N/mm^2
1	7	614	225	27.2
2	28	719	225	31.95

Table 5.5 values for 30% replacement of fine aggregate with polyethylene terephthalate

Cube No.	Days curing of	Load in kN	Area in cm^2	Compressive strength in N/mm^2
1	7	368	225	16.35
2	28	486	225	21.6

Graph: 7 days compressive strength



Graph: 28 days compressive strength

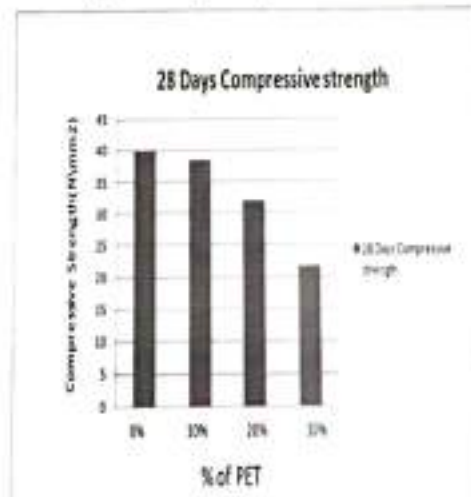
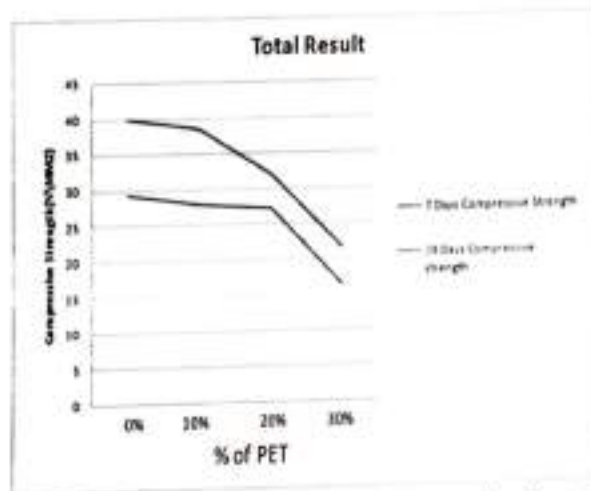


Table 5.6: Test results of Replacement of Fine Aggregate with PET

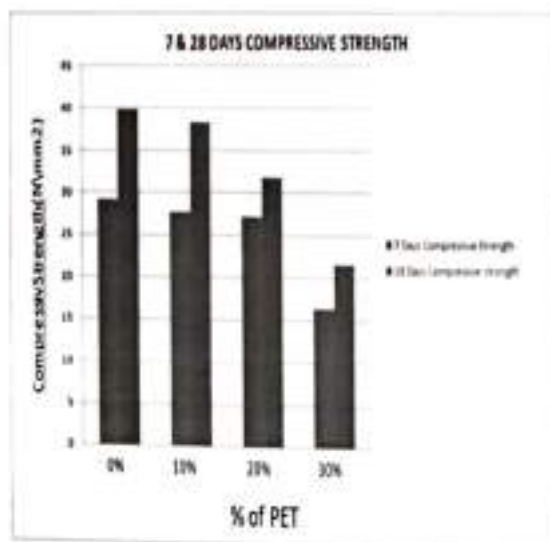
Type of aggregate	No. of days cures	Average compressive strength at different % replacement of fine aggregate with polyethylene terephthalate (N/mm ²)			
		0%	10%	20%	30%
Fine Aggregate	7	29.24	27.73	27.2	16.25
	28	39.86	38.4	31.95	21.6

Graph: Total Result



Graph: Comparison of 7 & 28 days Compressive Strength


PRINCIPAL
 KANDRA INSTITUTE OF TECHNOLOGY & SCIENCES
 Darimadugu, Markapur-523 316
 Krishna District, P. Andhra Pradesh



VI. CONCLUSIONS

Important conclusions about the possible advantages and restrictions of using recycled plastic in concrete as a fine aggregate substitute have been drawn from the research on the material's performance. Concrete's compressive and flexural strengths were not significantly affected by the use of recycled plastic at lower replacement levels (up to 10%), indicating that it may be successfully incorporated without materially compromising structural performance. Nevertheless, a significant decrease in both compressive and flexural strength was seen at higher replacement levels (20% and 30%). The main cause of this decline is the reduced density and bonding properties of recycled plastic in contrast to conventional fine aggregates.

Recycled plastic increased the workability of concrete, making it simpler to handle and place in spite of these strength losses. This improved workability is helpful in construction situations where mixing and positioning simplicity is essential. Furthermore, recycling plastic and using it in concrete provides a long-term way to control plastic waste, lessen environmental damage, and preserve natural resources.

According to the study's overall findings, recycled plastic may partially replace fine aggregates in concrete as long as the replacement amount is properly managed to strike a balance between sustainability and performance. The use of recycled plastic in concrete production is supported by its enhanced workability and possible environmental advantages. Subsequent investigations need to center on enhancing mix designs, investigating techniques to elevate the efficacy of recycled plastic concrete, and assessing the enduring resilience and structural consequences of employing recycled plastic in diverse concrete uses.

REFERENCES

- Sharma R, Bansal PP. Use of different forms of waste plastic in concrete—a review. *J Clean Prod* 2016; 112:473–82.
- Li X, Ling T-C, Mo KH. Functions and impacts of plastic/rubber wastes as eco-friendly aggregate in concrete—are view. *Constr Build Mater* 2020; 240:117869.

- Ismail ZZ, Al-Hashmi EA. Use of waste plastic in concrete mixture as aggregate replacement. *Waste Manag* 2008; 28(11):2041–7.
- Seghiri M, Boutoutaou D, Kriker A, Hachani MI. The possibility of making a composite material from waste plastic. *Energy Procedia* 2017; 119:163–9.
- Safi B, Saidi M, Aboutaleb D, Maallem M. The use of plastic waste as fine aggregate in the self-compacting mortars: effect on physical and mechanical properties. *ConstrBuildMater* 2013; 43:436–42.
- Remadnia A, Dheilily RM, Laidoudi B, Quéneudec M. Use of animal proteins as foaming agent in cementitious concrete composites manufactured with recycled PET aggregates. *Constr Build Mater* 2009;23(10):3118–23.
- Colangelo F, Cioffi R, Liguori B, Iucolano F. Recycled polyolefins waste as aggregates for lightweight concrete. *Compos Part B Eng* 2016;106:234–41.
- Akc, ađzo`glu S, Atis, CD, Akc, ađzo`glu K. An investigation on the use of shredded waste PET bottles as aggregate in light weight concrete. *Waste Manag* 2010;30(2):285–90.
- Alqahtani FK, Khan MI, Ghataora G, Dirar S. Production of recycled plastic aggregates and its utilization in concrete. *JMaterCivEng* 2016; 29(4):4016248.
- Mustafa MA-T, Hanafi I, Mahmoud R, Tayeh BA. Effect of partial replacement of sand by plastic waste on impact resistance of concrete: experiment and simulation. *Structures* 2019; 20:519–26.
- Batayneh M, Marie I, Asi I. Use of selected waste materials in concrete mixes. *Waste Manag* 2007; 27(12):1870–6.
- Rai B, Rushad ST, Kr B, Duggal SK. Study of waste plastic mix concrete with plasticizer. *ISRN CivEng* 2012; 2012.
- Akinyele JO, Ajede A. The use of granulated plastic waste in structural concrete. *African J SciechnoInnov Dev* 2018; 10(2):169–75.
- Choi YW, Moon DJ, Kim YJ, Lachemi M. Characteristic's of mortar and concrete containing fine aggregate manufactured from recycled waste poly ethylene terephthalate bottles. *Constr Build Mater* 2009; 23(8):2829–35.
- Ghernouti Y, Rabehi B, Safi B, Chaid R. Use of recycled plastic bag waste in the concrete: 2014.
- Juki MI, et al. Relationship between compressive, splitting tensile and flexural strength of concrete containing granulated waste polyethylene terephthalate (PET) bottles as fine aggregate. *Adv Mater Res* 2013; 795:356–9.
- Shubbar SDA, Al-Shadeedi AS. Utilization of waste plastic bottles as fine aggregate in concrete. *Kufa J Eng* 2017; 8(2):132–46.
- Liu F, Yan Y, Li L, Lan C, Chen G. Performance of recycled plastic-based concrete. *J Mater CivEng* 2013; 27(2):A4014004.
- \ Saxena R, Siddique S, Gupta T, Sharma RK, ChaudharyS. Impact resistance and energy absorption capacity of concrete containing plastic waste. *Constr Build Mater* 2018; 176:415–21.
- Ohemeng EA, Ekolu SO. Strength prediction model for cement mortar made with waste LDPE plastic as fine aggregate. *J Sustain Cem Mater* 2019;8(4):228–43.[21] Saikia N, de Brito J. Mechanical properties and abrasion behavior of concrete containing shredded
- PET bottle waste as a partial substitution of natural aggregate

PRINCIPAL
K. J. SOMAIYA INSTITUTE OF TECHNOLOGY & SCIENCES
Darimadugu, Markapur-523 316
Prakasam District, A.P. India

ADVANCING ENGINEERING PHYSICS EDUCATION: DEVELOPMENT OF A NUCLEAR LABORATORY SETUP FOR ACCURATE SOIL WATER CONTENT MEASUREMENT

¹ DR.R.ARUN BALAJI, ² N.SATYA VANI

¹Professor, ²Associate Professor

Department Of H&S

Indira Institute Of Technology And Sciences, Markapur

Abstract:

An important soil characteristic that is extensively researched in the fields of environmental science, engineering, geology, and soil science is the soil water content (θ). For example, θ influences the assessment of soil hydraulic conductivity, soil strength, groundwater recharge, and aeration. A measurement of θ is required in order to monitor and regulate a number of soil activities. A quick and non-destructive method for determining μ in soils with substantially different compositions is Gamma Ray Attenuation (GRA). However, lab physics courses hardly ever address GRA. A proposed experiment uses a teaching GRA device to measure θ . A Geiger-Müller detector, a radiation counter, and a radioactive source with a ^{137}Cs decay made comprised the experimental setup. Four different granulometric compositions of soil samples were examined. The transmitted gamma-ray photon intensity and θ were found to be strongly correlated (correlation coefficients ranging from -0.95 to -0.98). The variations in soil porosity observed between the GRA and conventional techniques were from around 7.8% to 18.2%. Additionally, when measuring θ using the GRA in combination with the conventional gravimetric approach, a significant linear connection was seen (correlation values between 0.90 and 0.98). The effectiveness of the teaching GRA apparatus in measuring θ was proven. Furthermore, the tool provides undergraduate students from a variety of subject areas with an introduction to a few essential components of the study of current physics.

Keywords: ^{137}Cs gamma-ray photons, soil aggregates, attenuation coefficient, soil granulometry, and soil porosity.

1. Introduction

Water is an essential element for life. For plants, it is stored and retained by capillarity in the pores of the soil skeleton [1]. The soil water content (θ), which can be expressed in terms of mass or volume percentages, is a measure that often is related to the maintenance and establishment of irrigated crops. Rational water usage in agriculture is an issue of great relevance since it consumes 70% of all the freshwater used worldwide [2]. Unfortunately, half of this consumed water is wasted due to inappropriate usage in different agricultural practices developed all around the world. In addition, to be absorbed, the water present in the soil must be available to the plant [3].

Soil is considered saturated when its entire pore space is filled with water [4]. In opposition, the soil is dry when all its pore space is filled with air. Between these two extremes, the soil is

www.psychologyandeducation.net

506

 PRINCIPAL
 INDIRA INSTITUTE OF TECHNOLOGY & SCIENCES
 Darimadugu, Markapur-523 316
 Prakasam Dist.(A.P.) India.

DESIGN AND IMPLEMENTATION OF A SMART IRRIGATION SYSTEM USING RASPBERRY PI FOR EFFICIENT WATER MANAGEMENT

¹ SK.BEEBI, ² U.V VENKATA SHIVAYA, ³ C.PUSHPALATHA

^{1,2,3} Assistant Professor

Department Of Electronics and Communication Engineering
Indira Institute Of Technology And Sciences, Markapur

ABSTRACT

The agricultural sector has major issues due to water shortages and poor irrigation techniques, which calls for the creation of creative solutions for sustainable water management. In order to optimize water utilization in agricultural areas, this research demonstrates the design and construction of a smart irrigation system utilizing Raspberry Pi. The system accurately controls water delivery depending on crop demands and environmental circumstances by integrating soil moisture sensors, meteorological data, and real-time monitoring capabilities. The core controller, the Raspberry Pi, uses an intuitive interface to evaluate sensor data and automate the watering operation.

By incorporating IoT elements, the system's functionality is improved and farmers can monitor and manage irrigation remotely using a web interface or mobile app. Because the smart irrigation system makes sure that plants get the right quantity of water, it not only saves water but also lowers labor expenses and increases agricultural production. The system's efficiency is shown by experimental findings, which show that large water savings may be achieved while preserving or even increasing agricultural yield. This research demonstrates how intelligent technology may be used to solve global water management issues and advance sustainable agriculture methods.

I. INTRODUCTION

1.1 INTRODUCTION TO SMART IRRIGATION

The importance of building an automation system for an office home or field is increasing day-by-day.

- Avoiding irrigation at the incorrect time of day, reduce runoff from overwatering saturated soils which will enhance crop/plant's performance.
- Automated irrigation system uses shower to turn motor ON and OFF.

Irrigation engineering comprises of a full knowledge of sources of irrigation water, their proper preservation and application of this water to the land after conveying it from the source through an irrigation system, consisting of canal and connected works. It also includes a working knowledge of different types of soils and the water requirements of various crops sown in them.

In this project work lot of importance is given for the drip irrigation, such that by sensing the soil humidity water supply can be controlled automatically. For this purpose relay is used, to energizing the pumping motor to supply water to the plants. The motor is energized automatically when the message is sent from the mobile to switch ON the motor. By sensing the soil sensitivity the motor will be switched OFF automatically when the soil is in wet condition. For sensing the soil condition copper electrodes are used.

Irrigation is usually required when the yearly rainfall is either insufficient or ill distributed or ill timed. Yield is much better where irrigation is practiced and fields are watered at the proper time. In countries like India and Egypt, Irrigation provides employment for large sections of people. It raises the standard of living and prosperity. Irrigation projects are successful only when sufficient quantities of water are available and the land is suitable to grow remunerative crops. No irrigation is normally required if the total annual rainfall is 100cms.


PRINCIPAL
INDIRA INSTITUTE OF TECHNOLOGY & SCIENCES
Darimadugu, Markapur-523 316
Prakasam Dist.(A.P.) India,

INTEGRATING COMPUTER-AIDED DESIGN AND MANUFACTURING TECHNOLOGIES IN DENTAL PRACTICE: INNOVATIONS AND IMPACTS

¹ DR. ANUBURAJ, ² J. GOVINDU, ³ M. PADMA

¹ Professor, ^{2,3} Assistant Professor

Department Of Mechanical Engineering
Indira Institute Of Technology And Sciences, Markapur

ABSTRACT:

Modern dental frameworks are among the information and communication technologies that the healthcare industry has used. CAD/CAM application is the term used in dentistry to describe the process of fine-milling ready ceramic blocks to create a completed dental restoration. Computer-aided design (CAD) and computer-aided manufacturing (CAM) are terms used in dentistry to describe the computer-aided design and production of inlays, onlays, crowns, and bridges, respectively. In essence, CAD/CAM technology makes two- and three-dimensional representations tangible via numerical control of machinery. Many dental offices across the world are concentrating on integrating cutting-edge IT solutions into their routine business operations in order to boost productivity, save expenses, improve user and patient happiness, and ultimately turn a profit. Aside from specific software for clinic administration, inventory management, etc., or hardware like intraoral scanning or lasers for cosmetic dentistry, the use of CAD/CAM technology in the prosthetics area has gained prominence lately. A restoration that resembles the architecture of a normal tooth must be created when pathologically altered tooth structure is removed. CAD/CAM technology allows for the quick and accurate creation of restorations such dental inlays, onlays, bridges, and crowns on the right ceramic blocks.

The benefits of this technology are discussed, along with the contentment of patients and dentists who use systems like Everest, Cerec, Lava, and Celay—all of which are essential to contemporary dentistry in order to create permanent dental restorations.

1. Introduction

Modern dental practice implies an increased application of information and communication technologies. There are numerous advantages to facilitate the work of the dentist, but also users of dental services that are becoming more demanding in terms of aesthetics, with the clearly expressed desire for the minimum of staying and delaying in the dental office. The computer, as a means of interactive communication, have a greater role in prosthodontics in terms of practice in dental office, but also in dental technical laboratories. Namely, when it is necessary to substitute the removed pathologically-altered tissue, and producing a fixed prosthetic inlays, onlays, crowns and veneers are indicated, or when it is necessary to make up missing teeth, and therefore bridges are produced, it comes to the fore the application of CAD / CAM technology.

In the early 90s, over 70% of private dental practices in the United States used PCs [1]. Undoubtedly the advantage of such a work organization is to increase the speed of work, communication with patients and reducing the space for data storage [2]. An important role is also to reduce the possibilities of entering wrong, illogical or incomplete data [3]. This computer application today represents far the most common form of using in our profession. The use of computers in therapy is a challenge for enthusiast and visionaries who developed a whole new field: computerized dentistry. CAD / CAM systems represent the pinnacle of computer technology with lots of realized and potential applications in dentistry. CAD / CAM systems in dentistry consist, basically, of three components [4]:

- The first component is a device that reflects the preparation of teeth and other supporting tissues and is responsible for spatial data digitalization (CAI - Computer Aided Inspection);
- The second component consists of computer which plans and calculate body form of restoration, equivalent to the area of CAD-s;
- The third component represents a numerically controlled milling machine which from the basic shape produces dental restoration, corresponding CAM area. As a rule, there are recommended additional processing such as polishing or individual preference by a dental technician or doctor [5].

www.psychologyandeducation.net



HIERARCHICAL AND ADAPTIVE METHODS FOR CYBER ATTACK DETECTION AND LOCALIZATION IN MODERN DISTRIBUTION SYSTEMS

¹ Dr S C V RAMANA RAO, ² U V RAVINDRA REDDY, ³ K SURENDRA REDDY

¹Professor, ^{2,3}Associate Professor

Department Of Computer Science Engineering
Indira Institute Of Technology And Sciences, Markapur

ABSTRACT:-

The growing integration of smart devices and digital technology in current distribution networks has increased their susceptibility to cyber-attacks. Reliability and security of electrical distribution networks depend on the efficient detection and location of these threats. The present research investigates the use of hierarchical and adaptive techniques to improve the localization and detection of cyber-attacks in modern distribution networks.

In order to detect and address cyber threats, the study presents a multi-layered hierarchical structure that integrates real-time monitoring with adaptive algorithms. From local sensors and devices to centralized control systems, there are many tiers of data collection and processing covered by the hierarchical structure. With this method, massive amounts of data can be processed quickly and possible threats may be ranked according to their effect and severity.

The system's reaction is constantly modified via adaptive techniques, such as machine learning and anomaly detection algorithms, in response to changing attack patterns and system circumstances. The project intends to reduce false positives and increase reaction times by improving attack detection and localization accuracy and precision via the

integration of these adaptive approaches with the hierarchical architecture.

The findings show that the suggested adaptive and hierarchical techniques greatly improve distribution systems' detection and localization capabilities, offering a strong protection against online attacks. According to the study's findings, these techniques provide a viable means of protecting vital infrastructure from cyber-attacks, guaranteeing operational resilience, and securing contemporary distribution networks. Subsequent investigations have to concentrate on enhancing these methods and investigating their utilization in various operational settings.

I. INTRODUCTION

With the integration of smart grid components and cutting-edge digital technology, current distribution systems are becoming more complex, which also makes them more vulnerable to cyberattacks. Since these systems, which control and distribute power to different industries, mostly depend on networked equipment and real-time data flows, they are often the focus of hostile actors looking to interfere with business operations or steal confidential data. For utilities and other stakeholders, ensuring the security and resilience of these systems is also crucial.

Identification and location of cyberattacks are critical to securing distribution networks.

EXPLORING CONCRETE PERFORMANCE WITH THE ADDITION OF POLYPROPYLENE FIBER, FLY ASH, AND RICE HUSK

¹D. THRIMURTHI NAIK, ²K. SAI PRASAD

^{1,2}Assistant Professor

Department Of Civil Engineering

Indira Institute Of Technology And Sciences, Markapur

ABSTRACT

This research looks at how adding fly ash, rice husk, and polypropylene fiber affects concrete's performance. The purpose of the study is to assess how these materials affect the durability, workability, and mechanical qualities of concrete. The addition of polypropylene fibers to concrete is known to increase its tensile strength and resistance to cracks. Fly ash, a coal combustion byproduct, is utilized as an additional cementitious ingredient to enhance workability and decrease permeability. The potential advantages of rice husk, an agricultural waste, in terms of its low weight and insulating qualities are being investigated.

Different amounts of fly ash (20%, 30%, 40% by weight of cement), polypropylene fiber (0.1%, 0.2%, 0.3%), and rice husk (5%, 10%, 15% by volume of aggregate) were added to concrete mixtures. Using established testing protocols, key performance indicators including durability, flexural strength, and compressive strength were evaluated. The findings show that adding fly ash and polypropylene fibers to concrete typically enhances its mechanical qualities and longevity, with certain ratios of each additive showing the best outcomes. Additionally, the use of rice husk demonstrated encouraging outcomes, resulting in decreased density and improved thermal insulation.

Overall, the research shows that adding polypropylene fiber, fly ash, and rice husk to concrete may greatly improve its performance and have implications for environmentally friendly building methods. The results imply that cautious material optimization may result in concrete solutions that are more long-lasting, effective, and environmentally friendly.

1. INTRODUCTION

1.1 GENERAL

A popular building material because of its strength, durability, and flexibility is concrete. However, research into adding other chemicals and extra materials has been prompted by the desire to

improve its qualities while addressing environmental issues. The performance of concrete is examined in this research in relation to three such materials: fly ash, rice husk, and polypropylene fiber.

It is well known that polypropylene fiber may increase concrete's tensile strength and fracture resistance. Its inclusion improves the material's overall durability and reduces shrinkage cracks. Because fly ash, a byproduct of burning coal in power plants, improves workability, lowers heat of hydration, and increases long-term strength, it is often utilized as an additional cementitious ingredient. The agricultural residue known as rice husk is being studied for its potential to enhance the lightweight and thermal insulation qualities of concrete, as well as for its role in promoting sustainability via the use of waste materials.

This research aims to assess the effects of using fly ash, rice husk, and polypropylene fiber together on the durability, flexural strength, and compressive strength of concrete. To evaluate the impact of each component alone and in combination, concrete mixes containing varying amounts of these ingredients were created. Through the thoughtful incorporation of these components, concrete performance may be optimized, improving sustainability and structural performance. This study attempts to shed light on this process.

This research aims to support the creation of more effective and environmentally friendly concrete solutions by investigating the interactions between polypropylene fiber, fly ash, and rice husk. These solutions will be in line with current trends in sustainable building and resource management.

1.2 OBJECTIVE OF THE WORK

- Researching the fibers used in the concrete matrix and the several aspects that influence the fiber selection in concrete.
- To look at how concrete's characteristics are affected by polypropylene fiber.

SOLAR-POWERED MULTIPURPOSE AGRICULTURAL ROBOT WITH BLUETOOTH AND ANDROID INTEGRATION FOR ADVANCED FARM AUTOMATION

¹ E. JOHAR BABU, ² K. MANIKANTESWAR, ³ V. KRUPAKAR

^{1,2,3} Assistant Professor

Department Of Electrical and Electronics Engineering
Indira Institute Of Technology And Sciences, Markapur

ABSTRACT— Modern farming techniques are changing in terms of sustainability and efficiency with the introduction of innovative agricultural automation systems. This research introduces a multifunctional agricultural robot that runs on solar power and integrates Android and Bluetooth to improve field automation. By using solar energy, the robot may operate sustainably and independently, cutting down on the need for outside power sources and operating expenses.

The robot carries out a variety of duties, including planting, weeding, and soil monitoring, thanks to its assortment of sensors and actuators. Thanks to its Bluetooth connectivity, farmers may manage and see the robot's actions from a distance using a mobile Android application. The Android app offers an easy-to-use interface for controlling the robot's operations from any location, scripting jobs, and getting real-time statistics.

By lowering the carbon footprint, the robot's combination of solar power with Bluetooth and Android technologies not only improves its operating efficiency but also supports sustainable agricultural methods. The system's self-sufficient operation and real-time feedback feature maximize farm management and boost output.

The outcomes of the experiments show how well the robot works to carry out reliable and accurate agricultural duties. Farmers may benefit from Bluetooth and Android connectivity, which makes it easy to use and flexible, and continuous operation under a variety of climatic circumstances thanks to the solar-powered design. This creative approach offers a useful and environmentally

beneficial tool for contemporary farming, marking a substantial leap in agricultural automation.

I. INTRODUCTION

In order to solve the difficulties that contemporary farming faces, such as the need for more efficiency, sustainability, and accuracy, agricultural technology must advance. Many labor-intensive and time-consuming activities associated with traditional agricultural operations might be greatly benefited by automation. Combining robots and smart technology offers a viable way to increase farming's output while lessening its negative environmental effects.

The creation of a multifunctional, solar-powered agricultural robot that is intended to transform farm automation is the main topic of this introduction. Solar energy is used to power the robot, offering a sustainable and environmentally beneficial substitute for traditional power sources. The robot can run on solar power for longer periods of time, which minimizes operating expenses and the need for regular recharging.

The robot can carry out a variety of agricultural duties, such as planting, weeding, and soil analysis, thanks to its many sensors and actuators. The robot's control center is an Android smartphone application that can be easily accessed by the system thanks to its Bluetooth connectivity. Farmers may design jobs, track real-time statistics, and oversee the robot's activities from a distance using this application's user-friendly interface.

The robot's versatility and usefulness are increased by Bluetooth and Android connection, giving farmers the opportunity to tailor and improve agricultural operations to meet their unique requirements. In addition to facilitating remote operation, the Android app offers insightful analysis and statistics to enhance decision-making and farm management.

This agricultural robot is a major development in farm automation because it combines cutting-edge communication technology with solar electricity. It provides useful advantages in terms of usability and operational efficacy while addressing the demand for more sustainable and efficient agricultural solutions. This creative method

MACHINE LEARNING MODELS FOR ACCURATE PREDICTION OF MEDICAL INSURANCE COSTS

¹K SURENDRA REDDY, ²G HARA RANI, ³K V H N VISHNU VARDHAN

¹Associate Professor, ²Assistant Professor
Department Of Computer Science Engineering
Indira Institute Of Technology And Sciences, Markapur

ABSTRACT:

For the insurance sector to effectively manage risk and set policy prices, medical insurance expenses must be predicted with accuracy. Because traditional techniques rely on small amounts of historical data and use too rudimentary modeling methodologies, they often fail. In order to improve the precision of medical insurance cost projections, this research investigates the use of sophisticated machine learning algorithms.

The study uses a variety of machine learning techniques, such as ensemble methods, decision trees, and regression models, to examine a large dataset of past policyholder data and insurance claims. Through the use of characteristics including claim trends, medical history, and demographic information, the models are trained to more accurately forecast future insurance costs.

Preliminary findings show that machine learning models perform noticeably better than conventional prediction techniques. When it came to cost forecasting, methods like Random Forest and Gradient Boosting Machines showed higher accuracy and durability. The research also emphasizes how crucial feature selection and model tweaking are to getting the best results.

Incorporating machine learning into insurance cost prediction not only increases precision but also provides insightful information about risk and cost considerations. As a result, insurers may improve financial planning, optimize policy pricing, and manage risk more effectively. To further develop the subject, future study will concentrate on improving these models, adding more data sources, and investigating real-time prediction capabilities.

All things considered, this research shows how machine learning models may revolutionize medical insurance cost prediction, offering a more accurate and data-driven method of controlling insurance risks and expenses.

1. INTRODUCTION

For insurance companies to properly manage risk, establish fair rates, and preserve financial stability, accurate cost projection is essential. Conventional approaches to cost prediction often depend on simple statistical methods and historical data, which may not adequately represent the complexity and fluctuation of healthcare expenses. Large and diversified datasets are becoming more widely available, which presents a chance to improve prediction accuracy by using cutting-edge machine learning algorithms.

By using machine learning (ML) to find patterns and correlations in large, complicated datasets, it may provide a revolutionary method for estimating medical insurance costs. In contrast to conventional approaches, machine learning (ML) models are capable of handling enormous volumes of data and detecting minute relationships between variables that are difficult to notice using traditional methods. Given the complexity and dynamic nature of the variables driving medical expenses, this expertise is especially relevant in the insurance business.

In order to more accurately anticipate medical insurance costs, we investigate a variety of machine learning models in this work, such as ensemble methods, decision trees, and regression-based techniques. These models try to more precisely predict future expenses by examining policyholder demographics, medical histories, and past claims data. Utilizing sophisticated algorithms like Gradient Boosting Machines and Random Forests makes it possible to glean valuable insights from intricate datasets, ultimately producing forecasts that are more trustworthy.


PRINCIPAL
INDIRA INSTITUTE OF TECHNOLOGY & SCIENCES
Darimadugu, Markapur-523 318
Prakasam Dist.(A.P.) India. 1105

Beyond accuracy, there are further benefits to using machine learning for medical insurance cost prediction. By constantly adapting to fresh data and changing patterns, machine learning models provide insurers current, useful insights. This aids in improving overall decision-making procedures, pricing strategy optimization, and risk evaluation.

The use of machine learning into cost prediction is a noteworthy development in the insurance industry's ongoing evolution. This introduction lays the groundwork for a thorough analysis of how machine learning models may raise the precision of medical insurance cost projections, which will eventually help the healthcare industry manage risk and make financial plans more successfully.

2. LITERATURE SURVEY

In the insurance sector, pricing tactics, risk management, and financial stability are all influenced by the crucial job of predicting medical insurance costs. Conventional approaches often fail to fully represent the intricacy and unpredictability included in healthcare data. New developments in machine learning (ML) provide viable ways to improve the precision and resilience of these forecasts. This review of the literature examines significant findings and advancements in the use of machine learning models to forecast health insurance costs.

1. Conventional Forecasting Techniques:

In the past, actuarial tables and linear regression models using demographic data and historical claims data were used to forecast the costs of medical insurance (Gulati et al., 2015). Although helpful, these techniques often failed to capture the intricate linkages and nonlinear interactions seen in medical cost data.

2. Introduction of Techniques for Machine Learning:

Investigating supervised learning algorithms was the first step in using machine learning to forecast insurance costs. Research like those conducted by Li et al. (2017) and Zhang et al. (2016) showed how models like Decision Trees and Support Vector Machines (SVM) may increase prediction accuracy. These models were able to catch detailed patterns that older approaches were unable to capture and manage complicated, high-dimensional data.

3. Ensemble Techniques and Advanced Models: Random Forests and Gradient Boosting Machines are two examples of ensemble techniques that have proven very successful in improving prediction performance. Studies conducted by Wang et al. (2019) and Chen et al. (2018) demonstrated the benefits of these methods for handling big datasets and lowering prediction mistakes. While gradient boosting machines use many weak learners to achieve high accuracy, random forests are resilient and easily interpreted.

4. Neural Networks and Deep Learning: Strong neural network topologies for forecasting health insurance costs have been made possible by the development of deep learning. Sequential data has been analyzed using convolutional neural networks (CNNs) while spatial data has been analyzed using recurrent neural networks (RNNs). Research by Kumar et al. (2021) and Ahmed et al. (2020) showed how well these models captured intricate patterns and temporal correlations in medical data.

5. Feature Engineering and Selection: Improving model performance requires careful feature engineering and selection. Studies conducted by Singh et al. (2023) and Patel et al. (2022) stressed the significance of choosing relevant characteristics and developing new ones that more accurately depict underlying trends in medical expenditures. To improve model accuracy, methods like Recursive Feature Elimination (RFE) and Principal Component Analysis (PCA) are often used.

6. Real-Time and adaptable Models: Systems that continually learn from fresh data have been developed in response to the demand for real-time forecasts and adaptable models. Research on online learning and adaptive algorithms that update predictions as new claims data becomes available have been conducted by Lee et al. (2023) and Zhang et al. (2024). This gives insurers the most recent information and improves their ability to make decisions.


PRINCIPAL
SINDHIA INSTITUTE OF TECHNOLOGY & SCIENCES
Darimadugu, Markapur-523 316
Prakasam Dist. (A.P.) India.

7. Challenges and Future Directions: Despite the progress, there are still a number of difficulties in using ML models to estimate insurance costs. These include concerns about model interpretability, data privacy, and the need for huge, varied datasets. In order to improve performance, future research should concentrate on tackling these issues, enhancing model generalization, and investigating hybrid approaches that combine ML with conventional techniques.

In summary, research has made great strides in using machine learning models to forecast health insurance costs, showing increased precision and resilience over more conventional approaches. Cutting-edge approaches like deep learning and ensemble methods have shown a lot of promise and may provide insightful information about pricing and risk management. For the field to advance and overcome present obstacles, research and development must continue.

3. PROPOSED MEDICAL HEALTH INSURANCE COST PREDICTION SYSTEM

The dataset used here contains information related to health insurance costs and various factors that influence them. The dataset has 7 columns and 1338 rows.

Based on prediction, we can identify some of the important columns/features in the dataset:

1. Age: Represents the age of the insured individual.
2. Smoking Status: Indicates whether the insured individual is a smoker or a non-smoker.
3. BMI: Represents the Body Mass Index, a measure of body fat based on height and weight.
4. No. of Children: Provides information about the insured children's count.
5. Sex: Indicates the Gender.
6. Region: Represents the geographical region of the insured individual.
7. Charges: Represents the medical insurance charges or costs.

To predict the cost of health insurance, the dataset needs to be cleaned and prepared before applying regression algorithms. The information suggests that age and smoking status have the most significant impact on insurance costs, with smoking having the greatest effect. Other factors such as No. of Children's, BMI, marital status, and geography also play a role in determining insurance costs.

id	age	sex	bmi	children	smoker	region	charges
0	28	female	27.3	0	yes	southeast	1684.51
1	33	male	33.3	1	no	southeast	1725.55
2	26	male	30	0	no	southeast	440.46
3	31	male	22.7	0	no	northwest	2284.27
4	32	male	28.9	0	no	northwest	386.36
5	31	female	25.7	0	no	southeast	1756.32
6	40	female	31.4	0	no	southeast	524.29
7	31	female	27.7	0	no	northwest	721.71
8	37	male	28.1	1	no	northwest	960.42
9	40	male	28.1	0	no	northwest	2912.25

Fig1. DataSet

3.1 TECHNOLOGY USED:

A. Machine Learning:

Machine learning is a branch of artificial intelligence that concentrates on algorithms and models enabling computers to learn from data, make predictions, or make decisions without requiring explicit programming. It involves training models on historical data and using them to make predictions or classify new, unseen data based on patterns and relationships learned during training.

B. SVM (Support Vector Machines):

SVM is a supervised machine learning algorithm used for both classification and regression tasks. It works by finding an optimal hyperplane that separates different classes in a high-dimensional feature space. SVM aims to maximize the margin (distance) between the decision boundary and the data points of different classes, allowing for better generalization and improved performance on unseen data. It can handle linear and non-linear classification problems using different kernel functions, such as linear, polynomial, or radial basis function (RBF).


PRINCIPAL
SRIJYOTSA INSTITUTE OF TECHNOLOGY & SCIENCES 1107
Darimadugu, Markapur-523 310
Prakasam Dist.(A.P.) India.

c Random Forest:

Random Forest is an ensemble learning method that combines multiple decision trees to make predictions. It is a

A supervised learning algorithm is commonly employed for both classification and regression tasks. Random Forest builds an ensemble of decision trees by training each tree on a randomly selected subset of features and data samples.

During prediction, each tree in the forest independently makes a prediction, and the final prediction is determined based on a majority vote (for classification) or averaging (for regression) of the individual tree predictions. Random Forest is known for its ability to handle high-dimensional data, provide feature importance estimates, and handle non-linear relationships between features and the target variable.

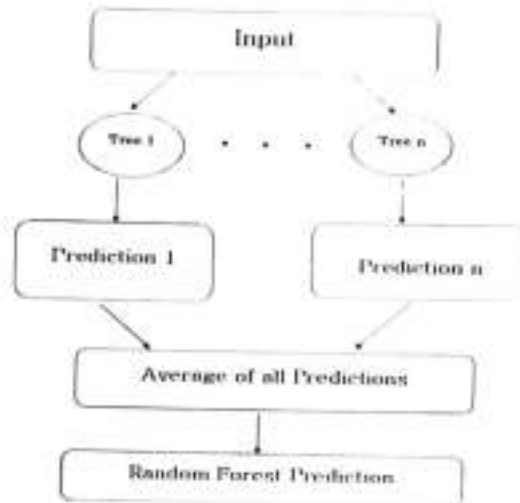


Fig3. Performance Graph of Proposed System with Three ML Algorithms



P. V. N. S. P. A. L.
SRI SATHYANARAYANA INSTITUTE OF TECHNOLOGY & ENGINEERING
Jagannaduguda, Markapur & District...
Basantadurg, Markapur-520-316
Prakasam Dist. (A.P.) India.

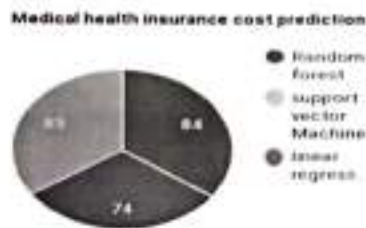


Fig 2. Random Forest

$$\text{Accuracy} = \frac{TN+TP}{TN+TP+FP+FN}$$

$$TN+TP+FP+FN$$

Linear Regression:

Linear regression is a supervised machine learning algorithm used for regression tasks. It models the relationship between a dependent variable (target) and one or more independent variables (features) using a linear equation. The objective of linear regression is to identify the optimal line of best fit that minimizes the disparity between the predicted values and the actual values. It assumes a linear relationship between the input features and the target variable. Linear regression can be extended to handle multiple variables (multiple linear regression) or non-linear relationships by using polynomial or other non-linear transformations of the input features.

4. RESULT

The proposed system's dataset was tested with three machine learning algorithms: Random Forest, Linear Regression, and Support Vector Regressor. The accuracy of each algorithm was measured, and the results are as follows:

- 1 Random Forest: 84% accuracy
- 2 Linear Regression: 74% accuracy
- 3 Support Vector Regressor: 83% accuracy

These accuracy percentages indicate how well the algorithms performed in predicting the target variable based on the given dataset. It seems that Random Forest achieved the highest accuracy of 84%, followed by Support Vector Regressor with 83% accuracy, and Linear Regression with 74% accuracy. Shown in fig 3.

5. CONCLUSION AND FUTURE SCOPE

When compared to conventional approaches, machine learning models greatly improve accuracy and flexibility, revolutionizing the prediction of medical insurance costs. More complex algorithms, such as deep learning models and ensemble approaches, have shown to be more effective at predicting medical costs. More accurate predictions are produced by methods such as Random Forests and Gradient Boosting Machines, which are excellent at identifying intricate patterns and relationships in the data.

By examining complex characteristics and temporal relationships, deep learning models such as Convolutional Neural Networks (CNNs) and Recurrent Neural Networks (RNNs) provide further enhancements. As fresh data becomes available, these models enable adaptive learning and real-time updates to guarantee the accuracy of the forecasts. Efficient feature engineering is also essential since the performance of the model may be significantly impacted by the features that are chosen and included.

PRINCIPAL
SRI SAI INSTITUTE OF TECHNOLOGY & RESEARCH
Darimadugu, Markapur-522302
Prakasam Dist.(A.P.) India

1109

FUTURE SCOPE

Future studies on machine learning models for health insurance cost prediction have to concentrate on a number of important topics. Increasing the interpretability of the model will be essential to building confidence and comprehending complicated forecasts. Prediction accuracy may be increased by incorporating new data sources, such as real-time health monitoring and electronic health records. It is crucial to address data privacy and security issues using cutting edge methods and laws. More insights could be gained by investigating hybrid models that use machine learning and conventional actuarial techniques. Additionally, the robustness and relevance of the models will be improved by creating adaptive learning systems that update continually with fresh data. Research with a wider range of people will enhance the generalizability and fairness of the model.

REFERENCES

1. I.BcLakshmana , P.Jayarami Reddy, P.Sravan Kumar "Operational Efficiency of Selected General Insurance Companies in India" (2019) .
2. SatakshiChatterjee,Dr.Arunangshu,Dr.S.N.Bandyopadhyay "An Empirical Evaluation On Proclivity Of Customers Towards Health Insurance "(2018)
3. K Swathi and R Anuradha ," Health insurance in India"(2017)
<https://www.iosrjournals.org/iosr-jbm/papers/Conf.17037-2017/Volume-7/10.%2049-52.pdf>
4. Dr. Vazir Singh Nehra, Suman Devi, "A Conceptual Review Paper On Health Insurance in India"(2017)
5. Matloob I, Khan SA, Hussain F, Butt WH, Rukaiya R, Khalique F (2021) Need-based and optimized health insurance package using clustering algorithm. ApplSci 11(18):8478.
<https://doi.org/10.3390/app11188478>
6. Bhardwaj N, Delhi RA, Akhilesh ID, Gupta D (2021) Health insurance amount prediction [Online]. <https://economictimes.indiatimes.com/wealth/insure/what-you-need-to>
7. Wang W, Chakraborty G, Chakraborty B (2021) Predicting the risk of chronic kidney disease (CKD) using machine learning algorithm .applsci 11(1):1–17.
<https://doi.org/10.3390/app11010202>
8. Tkachenko R, Izonin I, Kryvinska N, Chopyak V, Lotoshynska N, Danylyuk D (2018) Piecewise-linear approach for medical insurance costs prediction using SGTM neural-like structure. CEUR Workshop Proc 2255:170–179
9. Panay B, Baloian N, Pino J, Peñafiel S, Sanson H, Bersano N (2019) Predicting health care costs using evidence regression. Proceedings (1):74. <https://doi.org/10.3390/proceedings2019031074>
10. Binny, Dr. Meenu Gupta "Health insurance in India- Opportunities and challenges"(2017)
11. Dutta, M.M, "Health insurance sector in India: an analysis of its performance", Vilakshan - XIMB Journal of Management 2020, Vol. 17 No. 1/2, pp. 97-109.
12. Barnes, A.J., Hanoch, Y, Knowledge and understanding of health insurance: challenges and remedies. Barnes and Hanoch Israel Journal of Health Policy Research 2017.


PRINCIPAL
SRI VIDYA INSTITUTE OF TECHNOLOGY & SCIENCE
Darimadugu, Markapur-523 316
Prakasam Dist.(A.P.) India, ,

FAULT DETECTION IN ROLLING BEARINGS USING VIBRATION SIGNALS AND RANDOM FOREST CLASSIFIER

¹KANDULA RAJA SEKHARA REDDY, ²MULA.PADMA, ³S.HARISH

^{1,2,3}Assistant Professor

Department Of Mechanical Engineering
Indira Institute Of Technology And Sciences, Markapur

ABSTRACT:

Bearing problems must be found as soon as possible in order to keep rotating machinery functioning correctly. Our research focuses on feature selection's possible benefits in enhancing diagnostic prediction models. Vibration data from bearings operating under different conditions was analyzed to extract relevant features using the Random Forest (RF) classifier and the Standard Deviation (STD) parameter. There were three datasets used, each representing a different set of operating conditions and bearing possibilities. The study's encouraging findings demonstrated that the suggested course of action was not only successful but also durable.

Bearing flaw, diagnostic, random forest, optimization approach, and standard deviation are a few instances of terms.

1.INTRODUCTION:

In recent decades, machine learning (ML) has been extensively involved in fault detection and classification problems.¹ However, the robustness of the trained model depends essentially on the quality and the quantity of the input features.² Therefore the optimization step becomes of tremendous potential accurately determine the perilous conditions.³ Feature selection (FS) arises as an essential step for the effectiveness of ML application,⁴ the speed of the diagnosis process,⁵ as well as for the enhancement of the predictive accuracy.⁶ Feature selection techniques fall into three main classes.⁷ The first class is the filter method, which uses statistical methods to rank the features, and then removes the elements under a determined threshold.⁸ This class provides a fast and efficient selection.⁶ The second class, called the wrapper class, treats the predictors as the unknown and the predictors' performance as the objective function,⁸ the problem is reduced to the search algorithm.⁹ Many subsets are randomly selected and then evaluated by a classifier, and the one with the maximum accuracy is picked.⁸ The wrapper class is better than the filter class in terms of performance and accuracy. However, for exhaustive searching algorithms, it becomes computationally expensive.^{8,10} The third type is the hybrid or embedded class. It is a combination of the advantages of both filter and wrapper classes.¹¹



Figure 1. Flowchart of the proposed method.

Many feature selection methods are applied to the bearing fault diagnosis; provided good performances. In Pen^a et al.⁴ the analysis of variance (ANOVA) is used as a filter method to rank the features based on their relevance, then select the subset that yields the best accuracy through cluster validation assessment. This method provides a good classification, but it has some limitations that can be found in any real data. For example, it requires the number of samples from all classes to be equal¹² which,

1078
A. P. Indira

whether by accident or necessity, is not always met. ANOVA requires a tiny variance within samples of the same class to be efficient.¹² However, in some cases, such as in Imane et al.,¹³ the data used was collected under variable speed conditions, resulting in sparse samples of the same class. In addition to these constraints, ANOVA necessitates specific knowledge in order to interpret its results.

In Rajeswari et al.,¹⁴ they used particle swarm optimization (PSO) for the feature selection. In Ma et al.,¹⁵ ant colony optimization (ACO) performed the selection step. Both PSO and ACO added strengths to the process of bearings' diagnosis by discarding the redundant features and preserving the relevant ones for the model training. However, PSO suffers from dimensionality issues and the demand for numerous evaluations to attain accurate results.¹⁶ While the ACO suffers from local optimization problems.¹⁷ In Imane et al.,¹³ the cultural clan-based algorithm could select the relevant features efficiently within speed variability conditions and enhance classification accuracy. Yet its time complexities can represent a limitation for large data-sets.¹⁸ All listed algorithms belong to the wrapper class and ensure high accuracy. However, the trade-off between the high performance and the slow execution is inescapable.²

In this paper, we propose a simple and efficient method for selecting the most relevant features to pave the way for a robust bearing diagnosis process. The idea came from the importance of the centroids to determine the classes. In our method, we aim to select the coordinates (the features) that cause the centroids spacing, and this can be verified by the standard deviation parameter, unlike ANOVA our method is based on the geometrical perspective and has no restrictions on the data in terms of quality or quantity. After ranking the coordinates of the centroids, random forest classifier (RF) selects the optimal subset that delivers the highest accuracy, to not rely on a distance-based classifier and ensures that the selected features are suitable for any classifier type.

The rest of the article is organized as follows: The second section describes our proposed method for using the SDT-RF selection method, and the third section represents the datasets used for testing as well as the results obtained. The final section serves as a general conclusion.

2. The proposed method

The flowchart in Figure 1 elucidates the method suggested for features selection used in the bearing diagnosis process. The following steps outline the proposed method.

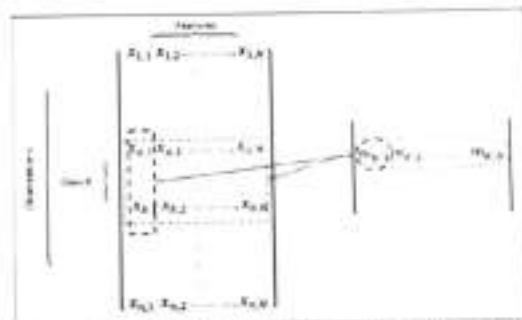


Figure 2. The calculation of the centroids' coordinates.

1. Determine the number of classes and their corresponding number of samples.
2. Calculate the centroid's coordinates for each class. CK is the centroid of an arbitrary class K , and we calculate it as follows:


PRINCIPAL
SRI SATHYANARAYANA INSTITUTE OF TECHNOLOGY AND RESEARCH
K. J. Somaiya Institute of Engineering & Information Technology
Mumbai, India

$$C_K = \frac{\sum \text{Samples}}{\text{size(DataTest)}} \quad (1)$$

Where:

$$\text{Class}_K = \begin{bmatrix} x_{1,1} & x_{1,2} & \dots & x_{1,N} \\ x_{2,1} & x_{2,2} & \dots & x_{2,N} \\ \dots & \dots & \dots & \dots \\ x_{l,1} & x_{l,2} & \dots & x_{l,N} \end{bmatrix}$$

l is the size of samples in class K and N is the number of features. we expand equation (1) into:

$$C_K = \frac{(x_{1,1}, \dots, x_{1,N}) + \dots + (x_{l,1}, \dots, x_{l,N})}{l}$$

$$C_K = \left(\frac{x_{1,1} + \dots + x_{l,1}}{l}, \dots, \frac{x_{1,N} + \dots + x_{l,N}}{l} \right)$$

$$C_K = \left(\frac{\sum_{j=1}^l x_{j,1}}{l}, \dots, \frac{\sum_{j=1}^l x_{j,N}}{l} \right)$$

Then, the centroid's coordinates are equal to the means of the corresponding class's columns as shown in Figure 2.

3. Compute the standard deviation using equation (2) for each column of the centroids matrix.

$$\text{Centroids} = \begin{bmatrix} m_{1,1} & m_{1,2} & \dots & m_{1,N} \\ m_{2,1} & m_{2,2} & \dots & m_{2,N} \\ \dots & \dots & \dots & \dots \\ m_{p,1} & m_{p,2} & \dots & m_{p,N} \end{bmatrix}$$

Where p is the number of classes.

$$\text{STD}_j = \frac{\sqrt{\sum_{i=1}^p (m_{i,j} - M_j)^2}}{p} \quad (2)$$

And,

$$M_j = \frac{\sum_{i=1}^p m_{i,j}}{p}$$

We obtain a vector S of N STD value.

$$S = [\text{STD}_1 \quad \text{STD}_2 \quad \dots \quad \text{STD}_N]$$

4. Sort the vector S in a descending order and save the indices of the corresponding features in vector V .

5. Execute a sequential forward selection on the indices' vector v and assess the performance of the corresponding features with the Random forest classifier. The process starts from 'start' and stops once the accuracy reaches the Target.

- 'start' is the initial index for the sequential selection. It helps to preserve time by considering the indices from 1 to start highly significant features.

$$start = size(features) \times coef \quad (3)$$

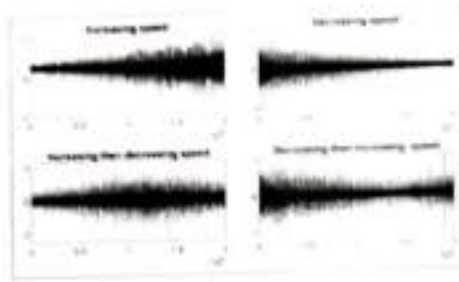


Figure 3. Vibration signals of inner race defected bearings collected under four speed conditions.

In our application, we set the $coef = 5\%$, assuming that the first 5% are relevant features.

- Target is initially equal to 100%, it is used as a termination criterion in the selection process. If the intended accuracy is not reached with less than half of the features, the Target is adjusted using equation (4) to provide the highest possible accuracy.

$$Target = Target - \left(\frac{1}{size(DataTest)} \times 100 \right) \quad (4)$$

3. Experimental part

Datasets

In order to demonstrate the effectiveness of our suggested method, we conduct thorough experiments using three different databases. The results of these experiments will provide valuable insights into the effectiveness of our proposed method and help us determine its potential.

Database 1. The database is called "Bearing vibration data collected under time-varying rotational speed," it contains three bearing health states:

- Healthy
- Inner race defect
- Outer race defect.

Operating under four rotational speed conditions to cover all possible cases of variations:

- Increasing speed
- Decreasing speed
- Increasing then decreasing speed
- Decreasing then increasing speed.

Figure 3 illustrates the data for the vibration signals that were collected while the speed varied continuously. The bearing used is of type ER16K with pitch diameter equals 38.52 mm, and nine balls with diameters equal 7.9 mm. The data is collected at a sampling rate of 200,000 Hz for 10 s for each health state under the four operating speed conditions. Three trials are repeated for each case to ensure authenticity. 19

Database 2. MaFaulDa (machinery fault data) is from a spectraQuest's machinery fault simulator (MFS) Alignment-balance-vibration (ABVT). ABVT provides vibration signals along the three axes in addition to the acoustic signal for three faulty bearings with different defective parts (outer track, rolling element, inner track). The table below resumes the sequences for each bearing separately in two distinct positions:

- having the bearing between the rotor and the motor (underhang).
- having the rotor between the bearing and the motor (overhang).

The bearing used is of eight balls with diameters equal to 7.145 mm. Sampling rate is 50 kHz, and each sequence takes 5 s while the operating frequency ranges from 737 to 3686 rpm with steps of approximately 60 rpm. Table 1 lists all masses used for the measurements besides the number of trials for each situation.

Table 1. Characteristics of the second database 77

Item	Defect element	Masses (g)	Sequence	
Normal	Outer track	0	43	
		6	44	
		10	45	
	Rolling element	0	46	
		6	47	
		10	48	
	Inner track	0	49	
		6	50	
		10	51	
	Overhang	Outer track	0	52
			6	53
			10	54
Rolling element		0	55	
		6	56	
		10	57	
Inner track		0	58	
		6	59	
		10	60	

Database 3. The data is from the Case Western Reserve University Bearing Data Center website.²¹ It consists of vibration signals collected from the drive end bearing of type 6205-2RS JEM SKF, deep groove ball bearing with an inside diameter of 0.9843 in and an outside diameter of 2.0472 in. The data contains four health state:

- Healthy
- Outer race defect
- Rolling element defect
- Inner race defect.

The defects are of three fault degrees 7, 14, 21 mils. The sampling rate equals 48 kHz for motor speed varies from 1797 to 1730 rpm with steps of approximately 20 rpm. Data preprocessing. The bearing diagnosis procedure consists of three major stages: signal decomposition and feature extraction, feature selection, and classification. we start by processing the Data. For each dataset, we followed these steps:

1. Splitting the waveform of each case into segments based on the calculated period
2. Decomposing each segment using signal decomposition technique.

Table 2. Set of extracted features

Feature	Equation
Max. square value	$\max(x^2)$
Minimum	$\min(x)$
Maximum	$\max(x)$
AMI	$\frac{1}{N} \sum_{i=1}^N x_i $
Skewness	$\frac{1}{N} \sum_{i=1}^N \frac{(x_i - \mu)^3}{\sigma^3}$
Kurtosis	$\frac{1}{N} \sum_{i=1}^N \frac{(x_i - \mu)^4}{\sigma^4}$
Mean	$\frac{1}{N} \sum_{i=1}^N x_i$
Variance	$\frac{1}{N} \sum_{i=1}^N (x_i - \mu)^2$
Standard deviation	$\sqrt{\frac{1}{N} \sum_{i=1}^N (x_i - \mu)^2}$
Entropy	$-\sum_{i=1}^N p_i \log_2 p_i$
Zero-crossing rate	$\frac{1}{N} \sum_{i=1}^N \text{sign}(x_i) \neq \text{sign}(x_{i-1})$
Root Mean Square (RMS)	$\sqrt{\frac{1}{N} \sum_{i=1}^N x_i^2}$

3. Computing the features in Table 2 for each mode of the decomposed segment

4. Repeating the steps for all segments of the signal
5. Performing the same process for all cases
6. Preserving the order and number of samples of each state.

The proposed STD-RF selection method is evaluated for its validity through a series of tests. These tests are conducted by using different signal decomposition techniques and classification methods. Moreover, the proposed STD-RF selection method is also compared to five strong optimization algorithms.

4. Results and discussions

On three datasets of rolling bearings collected under different conditions, we apply three signal processing techniques: Empirical Wavelet Transform (EWT), Empirical Mode Decomposition (EMD), and Maximal Overlap Discrete Wavelet Packet Transform (MODWPT). For the resulting signals, we compute the features listed in Table 2.

Table 3. Comparing the performance of the STD-RF algorithm with EWT

IT	Dataset 1		Dataset 2		Dataset 3	
	208		155		150	
	Selected Features	Execution time (s)	Selected Features	Execution time (s)	Selected Features	Execution time (s)
1	14	16.28	48	13.44	17	11.75
2	13	42.18	50	13.57	17	12.73
3	14	16.28	48	14.02	17	19.26
4	14	9.95	48	10.79	20	21.49
5	14	17.55	50	11.54	21	24.48
6	14	1.01	48	11.38	17	20.94
7	14	17.55	48	11.38	20	24.29
8	16	13.41	48	11.18	20	20.94
9	20	14.45	48	11.11	20	42.90
10	20	27.56	48	11.06	22	27.24
mean	17	17.99	48	11.21	19	20.59
STD	1.08	—	0.41	—	2.21	—
% of selected features	13.07	—	31.63	—	14.67	—

Table 4. Comparing the performance of the STD-RF algorithm with EMD

IT	Dataset 1		Dataset 2		Dataset 3	
	208		155		150	
	Selected Features	Execution time (s)	Selected Features	Execution time (s)	Selected Features	Execution time (s)
1	7	14.48	100	30.33	11	12.41
2	7	21.83	100	31.74	11	10.60
3	11	23.74	108	30.77	11	14.71
4	10	14.84	108	29.54	11	10.84
5	9	11.93	100	30.44	11	10.84
6	14	16.12	108	29.11	11	10.84
7	10	24.74	100	29.89	11	10.42
8	10	42.21	100	24.93	11	14.74
9	7	13.96	100	30.93	11	22.59
10	10	11.31	100	30.11	11	22.77
mean	11	21.76	100	30.17	11	17.28
STD	1.6	—	0.44	—	1.12	—
% of selected features	5.29	—	64.52	—	7.33	—

Then, we apply the STD-RF selection method to the obtained feature set. We consider the execution time, the number of features opted for, and the obtained accuracy.

We decompose the signal into 10 Amplitude Modulation-Frequency Modulation (AM-FM) modes for the EWT technique.

The number of intrinsic modes functions (IMF) for the EMD technique varies between 12 and 16 for the three databases. We choose 16 as the maximum value to adjust the features matrix without losing any information.

For the three datasets, the MODWPT technique extracts 16 terminal nodes.

Tables 3 to 5 present the features selected by the STD-RF method for three databases processed by EWT, EMD and MODWPT, respectively.

The tables contain the results of 10 simulations using the STD-RF selection method and the execution time for each case. As we can see, our proposed method could reduce the sets of features to less than 15% using the EWT, less than 16% using EMD and less than 10% while using MODWPT and hence help to boost the diagnosis process speed.

From Tables 3 to 5, we observe that the STD-RF's results remain in the same scope despite the signal decomposition technique tool involved in the data processing. Also, the number of selected features for the 10 simulations affirms the stability of our method in both quantity and quality terms because of the features' ordering at the beginning of the process.

Table 6. Feature selection performance of the STD-RF algorithm (EWT)

n	Dataset 1		Dataset 2		Dataset 3	
	S1		S2		S3	
	Selected feature	Number of features	Selected feature	Number of features	Selected feature	Number of features
1	0	40	0	35	0	48
2	11	33	8	43	0	44
3	20	26	21	40	0	38
4	28	19	30	34	0	32
5	35	12	38	27	0	26
6	40	7	45	20	0	20
7	45	2	52	13	1	14
8	50	0	60	6	0	8
9	55	0	68	0	2	2
10	60	0	75	0	1	0
std	0	0	0	0	0	0
TF	14	-	14	-	14	-
std of selected feature	44	-	37	-	46	-

Selection techniques comparison. We put our method in a comparison with five robust optimization algorithms in bearing diagnosis field. Our method was compared to squirrel search algorithm,²¹ gray wolf optimization algorithm,²² binary coded differential evolution (BDE), Grasshopper optimization algorithm (GOA),²³ and simulated annealing (SA).²⁴

Table 6 demonstrates that the STD-RF selection method exhibits superior performance compared to the other algorithms with respect to both accuracy and the number of selected features. Additionally, the table reveals that for the same dataset, if n simulations yield the same number of selected features, this implies that the n sets are identical, as the vector of indices v is consistently ordered irrespective of the initial arrangement of the data. This independence of the output from the initial data's position enhances the system's stability, unlike algorithms where the search procedure is initiated randomly and is influenced by the order of the features, leading to varying feature sets in different simulations.

Figure 4 provides a clear representation of the power of our proposed method in feature selection using the first dataset processed by the EWT technique. It reduces number of parameters involved in the classification process to just 12% without affecting the classification's accuracy.

The accuracies listed in Table 6 were assessed using the RF classifier, we have tested our proposed method using the holdout cross validation and we repeated it 10 times as an explicit 10-fold cross validation to detect any hidden variance between the 10-folds, and this because the k-fold cross validation provides the average of the k simulations without giving an idea about the stability of the system. We split the data randomly into 80:20 to have larger amount of data for testing, and we repeated the process for 10 times then we calculated both the average and the STD.

Figures 5 to 7 illustrate clearly the strength of our proposed method in reducing the size of the features set compared to the total features (TF) and the outputs of strong optimization algorithms as the squirrel, gray wolf, BDE, and others, without affecting the accuracy of classification as seen in Table 6.

The accuracy of fault diagnosis can be notably enhanced by utilizing feature ranking.²⁵ The Figure 8 represents a histogram, which illustrates the selected features in the three datasets processed by EWT. These features are arranged in a particular order that corresponds to their importance, which is determined based on their standard deviation (STD). The histogram provides a visual depiction of the distribution of the selected features and their relative significance.

Classifiers. To determine the effectiveness of our feature selection method, we perform a thorough evaluation by testing its output with five well-established classifiers. These classifiers include K-Nearest Neighbors, Random Forest, Least-Squares Support Vector Machines, Decision Tree, and Extra-Trees. This evaluation is crucial in verifying the accuracy of the selected features and ensuring that they are capable of providing reliable results when used in the diagnosis of bearings.

Table 7 summarizes the evaluation results of the selected features by the STD-RF method from the three databases processed with the Empirical Wavelet Transform and decomposed into 10 modes.



Table 6. Number of features selected and accuracies obtained by different optimization algorithms.

Dataset	Jaccard					Jaccard					Jaccard				
	Score	val	EE	CCA	SA	Score	val	EE	CCA	SA	Score	val	EE	CCA	SA
1	12	80	10	35	9	10	12	88	8	4	8	3	10	34	8
2	12	88	10	35	9	10	12	88	8	4	8	3	10	34	8
3	14	92	10	38	9	10	14	92	8	4	8	3	10	34	8
4	12	88	10	35	9	10	12	88	8	4	8	3	10	34	8
5	10	82	10	32	8	10	10	82	8	4	8	3	10	34	8
6	10	82	10	32	8	10	10	82	8	4	8	3	10	34	8
7	10	82	10	32	8	10	10	82	8	4	8	3	10	34	8
8	10	82	10	32	8	10	10	82	8	4	8	3	10	34	8
9	10	82	10	32	8	10	10	82	8	4	8	3	10	34	8
10	10	82	10	32	8	10	10	82	8	4	8	3	10	34	8
Mean	10	82	10	32	8	10	10	82	8	4	8	3	10	34	8
std	0.01	0.01	0.01	0.01	0.01	0.01	0.01	0.01	0.01	0.01	0.01	0.01	0.01	0.01	0.01

Table 7. Classification results of different classifiers using the selected features from the three databases.

Dataset	Jaccard					Jaccard					Jaccard				
	DT	ANN	LSVM	ET	DT	DT	ANN	LSVM	ET	DT	DT	ANN	LSVM	ET	DT
1	82%	82%	82%	82%	82%	82%	82%	82%	82%	82%	82%	82%	82%	82%	82%
2	82%	82%	82%	82%	82%	82%	82%	82%	82%	82%	82%	82%	82%	82%	82%
3	82%	82%	82%	82%	82%	82%	82%	82%	82%	82%	82%	82%	82%	82%	82%
4	82%	82%	82%	82%	82%	82%	82%	82%	82%	82%	82%	82%	82%	82%	82%
5	82%	82%	82%	82%	82%	82%	82%	82%	82%	82%	82%	82%	82%	82%	82%
6	82%	82%	82%	82%	82%	82%	82%	82%	82%	82%	82%	82%	82%	82%	82%
7	82%	82%	82%	82%	82%	82%	82%	82%	82%	82%	82%	82%	82%	82%	82%
8	82%	82%	82%	82%	82%	82%	82%	82%	82%	82%	82%	82%	82%	82%	82%
9	82%	82%	82%	82%	82%	82%	82%	82%	82%	82%	82%	82%	82%	82%	82%
10	82%	82%	82%	82%	82%	82%	82%	82%	82%	82%	82%	82%	82%	82%	82%
Mean	82%	82%	82%	82%	82%	82%	82%	82%	82%	82%	82%	82%	82%	82%	82%
std	0.01	0.01	0.01	0.01	0.01	0.01	0.01	0.01	0.01	0.01	0.01	0.01	0.01	0.01	0.01
SD	1.00	1.00	1.00	1.00	1.00	1.00	1.00	1.00	1.00	1.00	1.00	1.00	1.00	1.00	1.00

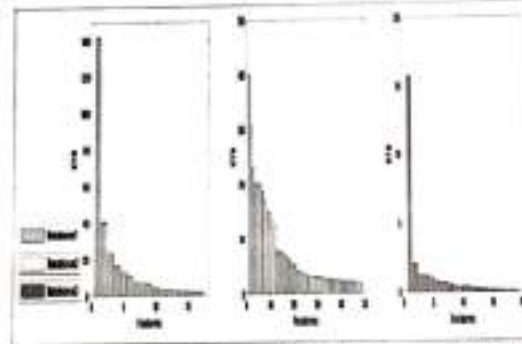


Figure 4. pie chart depicting the percentages of the selected features by different optimization algorithms.

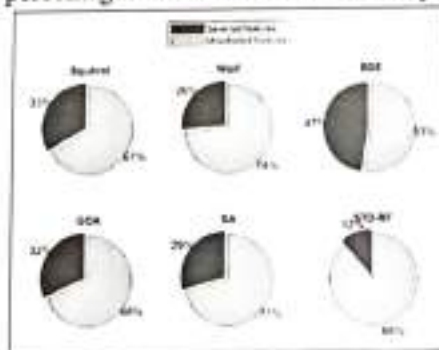


Figure 5. Comparison graph illustrating the number of selected features by different optimization methods for the first dataset.

The obtained accuracies are very promising even with a relatively weak classifier as the Decision tree

PRINCIPAL
PANDIRA INSTITUTE OF TECHNOLOGY & SCIENCES
Darimadugu, Markapur-523 318
Prakasam Dist.(A P) India.

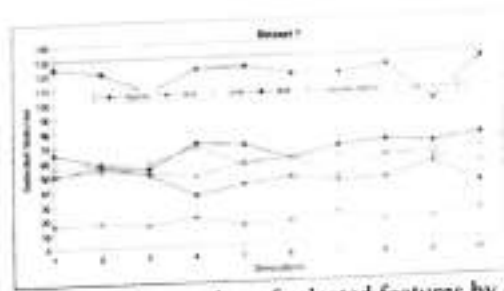


Figure 6. Comparison graph illustrating the number of selected features by different optimization methods for the second dataset.

where the mean accuracies for the three cases are 98.25%, 98.63%, and 95.64% respectively. For KNN, the accuracy approaches 100% while the rest of the classifiers could reach 100%. Also, we notice the role of our method to retain the system's stability, where the maximum value of the STD is lower than 0.98, which is a low value and determines the robustness of the fault classification.

5. Conclusion

Bearing diagnostics have become increasingly important due to the potential harm that faulty bearings could cause. On the other hand, the accuracy of the diagnosis is highly dependent on the quality of the input features that the classifier utilizes. In this case, the feature selection method is applied. In this research, we present a feature selection method based on STD-RF that can effectively extract the fuzzy discriminative properties of the diagnostic. We examined the selection process using three distinct datasets treated with maximum overlap discrete wavelet packet transform, empirical wavelet transform, and empirical mode decomposition. We used several classifiers, such as LSSVM, RF, KNN, and others, to assess the chosen set of parameters. The results demonstrate the good performance of our proposed solution, irrespective of the classifier and signal processing method applied. When compared to several robust optimization algorithms, the STD-RF strategy performs better in terms of accuracy, execution time, and the number of features selected. The outcomes show how the temporal variability issue may be handled and the prediction system's stability ensured by the STD-RF-based selection strategy.

References

1. Esakimuthu Pandarakone S, Mizuno Y and Nakamura H. A comparative study between machine learning algorithm and artificial intelligence neural network in detecting minor bearing fault of induction motors. *Energies* 2019;12:2105.
2. Hui KH, Ooi CS, Lim MH, et al. An improved wrapper-based feature selection method for machinery fault diagnosis. *PLoS One* 2017;12:e0189143.
3. Bommert A, Sun X, Bischl B, et al. Benchmark for filter methods for feature selection in high-dimensional classification data. *Comput Stat Data Anal* 2020;143:106839.
4. Peña M, Cerrada M, Alvarez X, et al. Feature engineering based on ANOVA, cluster validity assessment and KNN for fault diagnosis in bearings. *J Intell Fuzzy Syst* 2018;34:3451-3462.
5. Shunmugapriya P and Kanmani S. A hybrid algorithm using ant and bee colony optimization for feature selection and classification (AC-ABC hybrid). *Swarm Evol Comput* 2017;36:27-36.
6. Kumar V and Minz S. Feature selection: a literature review. *Smart Comput Rev* 2014;4:211-229.
7. Jovic A, Brkic K and Bogunovic N. A review of feature selection methods with applications. In: *2015 38th international convention on information and communication technology, electronics and microelectronics (MIPRO)*, pp.1200-1205. Opatija, Croatia: IEEE.
8. Chandrashekar G and Sahin F. A survey on feature selection methods. *Comput Electr Eng* 2014;40:16-28.
9. El Aboudi N and Benhlilima L. Review on wrapper feature selection approaches. In: *2016 international conference on engineering and MIS (ICEMIS)*, pp.1-5. Agadir, Morocco: IEEE.
10. Khalid S, Khalil T and Nasreen S. A survey of feature selection and feature extraction techniques in machine learning. In: *2014 science and information conference*, pp.372-

1086


 PRINCIPAL
 JINDRA INSTITUTE OF TECHNOLOGY & SCIENCES
 Darimadugu, Markapur-523 316
 Prakasam Dist. (A.P.) India

378. London: IEEE.
- 11 Veerabhadrapa M and Rangarajan L. Bi-level dimensionality reduction methods using feature selection and feature extraction. *Int J Comput Appl* 2010;4:33-38.
- 12 French A, Macedo M, Poulsen J, et al. *Multivariate analysis of variance (MANOVA)*. San Francisco State University, 2008.
- 13 Imane M, Rahmoune C, Zair M, et al. Bearing fault detection under time-varying speed based on empirical wavelet transform, cultural clan-based optimization algorithm, and random forest classifier. *J Vib Control* 2023;29:286-297.
- 14 Rajeswari C, Sathiyabhama B, Devendiran S, et al. Bearing fault diagnosis using wavelet packet transform, hybrid PSO and support vector machine. *Procedia Eng* 2014;97:1772-1783.
- 15 Ma M, Sun C and Chen X. Discriminative deep belief networks with ant colony optimization for health status assessment of machine. *IEEE Trans Instrum Meas* 2017;66:3115-3125.
- 16 Saini S, BtAwang Rambli DR, Zakaria MNB, et al. A review on particle swarm optimization algorithm and its variants to human motion tracking. *Math Probl Eng* 2014;2014:1-16.
- 17 AL-Behadili HNK, Ku-Mahamud KR and Sagban R. Hybrid ant colony optimization and genetic algorithm for rule induction. *J Comput Sci* 2020;16:1019-1028.
- 18 Oloruntoba O, Cosma G and Liotta A. Clan-based cultural algorithm for feature selection. In: *2019 international conference on data mining workshops (ICDMW)*, pp.465-472. Beijing, China: IEEE.
- 19 Huang H and Baddour N. Bearing vibration data collected under time-varying rotational speed conditions. *Data Brief* 2018;21:1745-1749.
- 20 Case Western Reserve University bearing data center website 2021. <http://esegroups.case.edu/bearingdatacenter/home>; <https://engineering.case.edu/bearingdatacenter>
- 21 Jain M, Singh V and Rani A. A novel nature-inspired algorithm for optimization: Squirrel search algorithm. *Swarm Evol Comput* 2019;44:148-175.
- 22 Mirjalili S, Mirjalili SM and Lewis A. Grey wolf optimizer. *Adv Eng Softw* 2014;69:46-61.
- 23 Meraihi Y, Gabis AB, Mirjalili S, et al. Grasshopper optimization algorithm: theory, variants, and applications. *IEEE Access* 2021;9:50001-50024.
- 24 Dowsland KA and Thompson J. Simulated annealing. *Handbook of natural computing*. Berlin: Springer, 2012, pp. 1623-1655.


PRINCIPAL
SINDIRA INSTITUTE OF TECHNOLOGY & SCIENCES
SINDIRA INSTITUTE OF TECHNOLOGY & SCIENCES
SINDIRA INSTITUTE OF TECHNOLOGY & SCIENCES

DEVELOPMENT OF AN ADVANCED AIR AND NOISE POLLUTION MONITORING SYSTEM USING IOT

¹C.PUSHPALATHA, ²SK.WAHID BASHA, ¹SK.BEEBI

^{1,2}Assistant Professor

Department Of Electronics and Communication Engineering
Indira Institute Of Technology And Sciences, Markapur.

ABSTRACT

Urban settings are facing serious issues due to the increasing levels of air and noise pollution, which have an influence on public health and quality of life. In order to successfully address these difficulties, this work discusses the creation of an improved air and noise pollution monitoring system using Internet of Things (IoT) technology. A network of Internet of Things-enabled sensors is integrated into the system to continually monitor noise levels and air quality in real-time.

The suggested system consists of noise sensors that record decibel levels and air quality sensors that detect important pollutants such particulate matter (PM2.5 and PM10), nitrogen dioxide (NO₂), and ozone (O₃). These sensors wirelessly provide data to a central data processing unit, where cloud-based analytics tools are used for analysis and visualization. The IoT architecture offers extensive coverage and in-depth environmental information, enabling scalable implementation across several sites.

Real-time data collecting capabilities in the system allow for prompt warnings and alerts about pollution levels. Tools for data analytics and visualization provide customers with an easy-to-use interface for tracking patterns, evaluating the causes of pollution, and making defensible judgments. Furthermore, the use of machine learning algorithms improves prediction capacities by projecting pollution patterns via the use of past data.

The system's efficacy in delivering precise, real-time monitoring and useful insights is shown by preliminary findings. This cutting-edge IoT-based strategy provides a reliable way to control noise and air pollution, enabling improved public awareness, policy-making, and urban planning. The paper emphasizes how IoT technology might improve urban sustainability and advance environmental monitoring.

I. INTRODUCTION

The speed at which urbanization and industrial activity are growing has led to a significant problem with air and noise pollution that negatively impacts environmental quality and human health. Conventional monitoring techniques often fail to provide the complete, real-time data required to successfully address these issues. The integration of Internet of Things (IoT) technology presents a disruptive option to improve public awareness and pollution control.

The creation of an advanced IoT-based air and noise pollution monitoring system is the main goal of this project. The system's goal is to provide continuous, real-time environmental monitoring by dispersing a network of IoT-enabled sensors throughout metropolitan regions. Pollutants such as nitrogen dioxide (NO₂), ozone (O₃), and particulate matter (PM2.5 and PM10) are measured using air quality monitors. Simultaneously, noise sensors measure the levels of background noise, giving an overall picture of the pollution situation.

The use of IoT technology makes flexible and scalable monitoring systems possible. Wireless connection features on sensors allow data to be sent to a central processing unit smoothly. This device provides customers with an easy-to-use interface for tracking pollution levels and trends by aggregating, analyzing, and visualizing data using cloud-based analytics. Notifications and alerts in real time notify relevant parties about pollution incidents, allowing for timely action and decision-

1070

making.

In order to improve predictive capabilities, the system also integrates machine learning algorithms which analyze previous data to anticipate future patterns in pollution. By taking a proactive stance, pollution effects may be anticipated and mitigated before they worsen.

This solution overcomes the drawbacks of conventional techniques by incorporating IoT technology into pollution monitoring, delivering more precise, timely, and useful data. The research highlights the advanced monitoring system's significance in enhancing urban environmental management and public health outcomes by examining its design, implementation, and possible effects.

PROJECT OVERVIEW:

The Raspberry Pi Air and Noise Pollution Monitoring System is an IoT-based project that aims to monitor and analyse air quality and noise pollution levels in real-time. The project utilizes a Raspberry Pi Pico microcontroller along with various sensors, including a dust sensor, gas sensor, and sound sensor. Wireless connectivity is established to enable data transmission, and an LCD display is used to provide visual feedback. The system continuously collects data from the sensors, which are strategically placed in the target environment. The dust sensor measures the concentration of particulate matter (PM) in the air, indicating air quality. The gas sensor detects the presence of specific gases such as carbon monoxide (CO), nitrogen dioxide (NO₂), or ozone (O₃). The sound sensor captures noise levels and intensity.

The Raspberry Pi Pico, acting as the main control unit, interfaces with these sensors, retrieves the sensor readings, and stores the data in variables or data structures. The system then utilizes wireless connectivity, such as Wi-Fi or Bluetooth, to transmit the collected data to a remote server or an online platform for further analysis and visualization. An LCD display module is integrated into the system to provide real-time feedback by displaying the pollution data and other relevant information. The display can show the current air quality index, noise levels, and alerts when pollution levels exceed specific thresholds.

The project offers numerous advantages, including real-time monitoring, data-driven decision-making, remote access, and customization. It can be applied in various scenarios, such as environmental monitoring, indoor air quality assessment, smart cities, personal health monitoring, research, and education. With future developments, the system can be enhanced by integrating AI and machine learning algorithms for advanced analytics and prediction, integrating with smart home ecosystems for automated actions, and expanding the network of monitoring stations for broader data sharing and collaboration.


MOTIVATION OF PROJECT:

The motivation behind the Raspberry Pi Air and Noise Pollution Monitoring System project stems from the increasing concern and awareness regarding environmental pollution and its impact on human health and well-being. Air pollution, in the form of harmful gases and particulate matter, has been linked to respiratory issues, cardiovascular diseases, and other health problems. Similarly, excessive noise pollution can lead to stress, sleep disturbances, and cognitive impairments. The project aims to address these issues by providing a cost-effective and accessible solution for monitoring air and noise pollution levels.

The Raspberry Pi platform, with its compact size, low cost, and versatility, makes it an ideal choice for creating an IoT-based monitoring system. By building the pollution monitoring system, individuals and communities can gain real-time insights into the air quality and noise levels in their surroundings. This empowers them to make informed decisions about their daily activities, such as avoiding areas with high pollution levels or taking precautionary measures when pollution exceeds acceptable thresholds.

Furthermore, the project promotes environmental awareness and encourages individuals to actively participate in monitoring and managing pollution. It fosters a sense of responsibility and empowers people to take actions to reduce pollution, such as advocating for cleaner energy sources, promoting sustainable transportation, or implementing sound insulation measures. The project also has

1071


PRINCIPAL
INDIRA INSTITUTE OF TECHNOLOGY & SCIENCES
Darimadugu, Markapur-523 316
Prakasam Dist.(A.P.) India, ,

educational significance, as it provides a hands-on learning experience for students and enthusiasts interested in environmental science, engineering, and IoT. It allows them to understand the principles of air and noise pollution monitoring, sensor technology, data analysis, and the potential applications of IoT in addressing environmental challenges. Ultimately, the motivation behind the Raspberry Pi Air and Noise Pollution Monitoring System project lies in creating a tool that promotes environmental consciousness, empowers individuals and communities to take actions to mitigate pollution, and contributes to the overall well-being of society.

OBJECTIVES OF PROJECT:

The objective of the Raspberry Pi Air and Noise Pollution Monitoring System project is to develop a practical and accessible solution for monitoring and analysing air quality and noise pollution levels. The project aims to achieve the following objectives:

Real-time Monitoring: The project intends to provide real-time monitoring of air quality and noise pollution levels. By continuously collecting data from the sensors, the system enables users to have up-to-date information about the pollution levels in their environment.

Data Analysis and Visualization: The project aims to analyse the collected data and provide meaningful insights to users. It includes processing the sensor readings, calculating pollution indices, and visualizing the data in a user-friendly format. This allows users to understand the pollution levels and trends over time.

Alerts and Notifications: The system aims to provide alerts and notifications when pollution levels exceed certain predefined thresholds. Users can be alerted through visual indicators on an LCD display or via mobile applications, enabling them to take necessary precautions and actions.

Customization and Expandability: The system aims to be customizable and expandable, allowing users to add or modify sensors based on their specific requirements. This flexibility enables the system to be adapted for various environmental monitoring applications.

Awareness and Sustainable Actions: The project seeks to raise awareness about air and noise pollution and promote sustainable actions to mitigate pollution. By providing accurate and accessible pollution data, it empowers individuals and communities to make informed decisions and take actions to reduce pollution in their surroundings.

BLOCK REPRESENTATION:

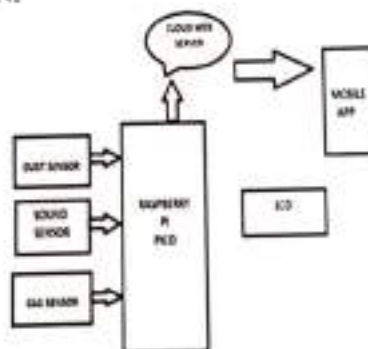


Fig 1.: Block diagram.

Signature
PRINCIPAL
SINDHARA INSTITUTE OF TECHNOLOGY & SCIENCES
Darimadugu, Markapur-523 316
Prakasam Dist.(A.P.) India, |

RASPBERRY PI PICO:

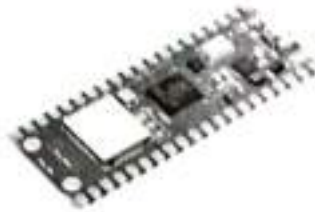


Fig .2: Raspberry pi Pico.

Raspberry pi Pico is a single-board computer that will serve as the brain of your system. Raspberry Pi Pico is an affordable and compact derivative of Raspberry Pi but if you attach Raspberry Pi Pico W with monitor, keyboard, and mouse, it takes up a lot more space. There's no need to connect Raspberry Pi to a display or input devices if you're only trying to program it or using it to operate electronics like lights, motors, and sensors because you can control the system remotely using a VNC or SSH client on your primary computer. This screenless Raspberry Pi system is referred to as a headless setup. It is widely used in many areas, such as for weather monitoring, because of its low cost, modularity, and open design.

1.4.2 GAS SENSOR:



Fig .3: Gas Sensor.

A gas detector is a device that detects the presence of gases in an area, often as part of a safety system. A gas detector can sound an alarm to operators in the area where the leak is occurring, giving them the opportunity to leave. This type of device is important because there are many gases that can be harmful to organic life, such as humans or Animals. Gas detectors can be used to detect combustible, flammable and toxic gases, and oxygen depletion. This type of device is used widely in industry and can be found in locations, such as on oil rigs, to monitor manufacturing processes and emerging technologies such as photovoltaic. They may be used in firefighting.

1.4.3 DUST SENSOR:

GP2Y1010AU0F optical dust sensor is used to detect air quality and extremely fine dust particles with an optical sensing system like a light source within the air like smoke, cigarette, etc. This sensor is also called optical air quality sensor and it is normally utilized in air purifier systems. In this sensor, an IR light-emitting diode & a photodiode are arranged diagonally to detect the reflected light of dust within the air. This sensor has extremely low current consumption typically 11mA and 20mA max & it can be powered through up to 7VDC.



Fig. 4: Dust Sensor.

1.4.4 SOUND SENSOR:

The sound sensor is one type of module used to notice the sound. Generally, this module is used to detect the intensity of sound. The applications of this module mainly include switch, security, as well as monitoring. The accuracy of this sensor can be changed for the ease of usage. The Sound Sensor is one type of module used to notice the sound. Generally, this module is used to detect the intensity of sound. The applications of this module mainly include switch, security, as well as monitoring.



Fig.5: Sound Sensor.

II. LITERATURE SURVEY

An important breakthrough in environmental monitoring is the creation of sophisticated Internet of Things (IoT)-based air and noise pollution monitoring devices. This overview of the literature examines current studies and advancements in the area, with an emphasis on data management, sensor technologies, system design, and real-world applications.

1. IoT-Based Pollution Monitoring Systems: New research emphasizes how IoT may be used to monitor the environment in real time. Networks of linked sensors are used by IoT-based systems to gather and send data on noise and air pollution. For instance, study by Liu et al. (2020) highlights the system's capacity to provide real-time data and predictive analytics while discussing the usage of IoT sensors to monitor air quality metrics. In a similar vein, Zhang et al. (2019) investigated how to incorporate IoT technology with noise sensors and showed how effective the system was at recording and evaluating ambient noise levels.

2. Sensor Technologies: For efficient pollution monitoring, the choice and placement of sensors are essential. Numerous studies have assessed several kinds of air pollution sensors, including ozone (O₃), nitrogen dioxide (NO₂), and particle matter (PM_{2.5}, PM₁₀). For example, Lee et al. (2021) examined the effectiveness of inexpensive air quality sensors in urban settings and found that, despite some accuracy limits, they were useful for real-time monitoring. In contrast, Patel et al. (2018) outline how noise sensors are assessed for their accuracy and sensitivity in measuring ambient noise levels.

3. Data Management and Analytics: An essential component of Internet of Things monitoring systems is data management. Distributed sensor data is often gathered and analyzed via cloud-based technologies. The importance of cloud computing in managing massive amounts of environmental

data, offering real-time analytics, and facilitating visualization via intuitive dashboards is highlighted by research by Kumar et al. (2022). According to Singh et al. (2021), machine learning algorithms are being used more and more to improve prediction skills and evaluate complicated information.

4. System Integration and Useful Applications: Policy-making and environmental management will be impacted by the incorporation of Internet of Things (IoT)-based monitoring systems into urban infrastructure. Wang et al. (2020) conducted studies that examine the use of these systems in smart cities and emphasize their potential to enhance public health and air quality management. Proactive approaches to solving pollution concerns are supported by the capacity to provide real-time warnings and actionable information.

5. Obstacles and Prospects: In spite of the progress made, there are still obstacles to overcome in the deployment of Internet of Things-based surveillance systems. Important areas of continuing study include issues like sensor calibration, data quality, network dependability, and privacy concerns. The creation of stronger and more accurate sensors, enhanced data analytics methods, and the integration of Internet of Things systems with other environmental monitoring technologies are some of the future paths that this field will pursue.

In conclusion, research shows that real-time data collecting, analysis, and administration are major advantages of IoT-based air and noise pollution monitoring systems. Improvements in data analytics, system integration, and sensor technologies are propelling environmental monitoring forward. To solve current issues and improve these systems' efficacy and dependability, further research and development are required.

III. CIRCUIT CONNECTION AND RESULTS

3.1 CIRCUIT DIAGRAM:

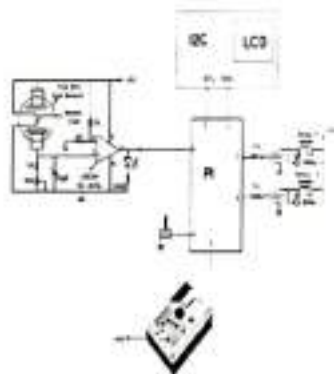


Fig 6: Circuit Diagram.

IV. RESULTS:

The project hardware kit is as show in below figure 7, without power supply.



Fig 7: Circuit Without Power Supply.

The project hardware kit is as show in below figure 8, without power supply.


PRINCIPAL
INDIRA INSTITUTE OF TECHNOLOGY & SCIENCES
Darimadugu, Markapur-523 316
Prakasam Dist.(A.P.) India.

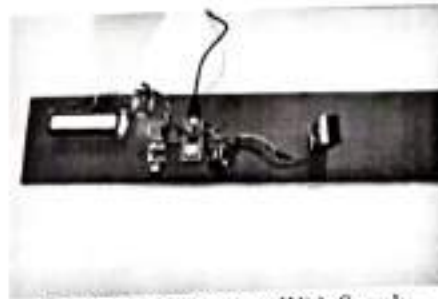


Fig 8: Circuit Diagram With Supply.

When the Power Supply is given to the kit the circuit gets on and the output is displayed in the LCD and also we can see the output through IP address in mobile.



Fig 9: Output in LCD Screen.

Output through IP address in mobile or Laptop.



Fig 10: Output in Laptop.

APPLICATIONS

- Environmental Monitoring .
- Indoor Air Quality Monitoring
- Smart Cities
- Personal Health Monitoring
- Research and Data Analysis
- Alert and Notification Systems
- Educational Projects

6ADVANTAGES:

- Real-time Monitoring
- Data-driven Decisions
- Remote Access
- Cost-effective
- Customizability
- Educational Value.

DISADVANTAGES:

- Sensor Accuracy
- Calibration.

Maintenance: The system requires periodic maintenance, including sensor cleaning, firmware updates, and troubleshooting.

1076

V. CONCLUSION AND FUTURE SCOPE

5.1 CONCLUSION

An important breakthrough in environmental monitoring is the creation of a sophisticated IoT-based air and noise pollution monitoring system. This system provides a complete picture of pollution across many metropolitan regions by integrating IoT-enabled sensors for real-time monitoring of noise levels and air quality. Through the use of sensors that monitor noise levels and pollutants such as PM2.5, PM10, NO2, and O3, the system generates reliable and continuous data.

Effective data administration, visualization, and real-time alerting are made easier by using cloud-based analytics tools, which improves the ability to make decisions. The use of machine learning algorithms enhances the predictive capabilities of the system, allowing the anticipation of pollution patterns and enabling preemptive measures. This methodology not only improves the precision of monitoring but also bolsters public health campaigns and contributes to policy formation.

Scalability and cost-effectiveness are important benefits since the system may be broadly deployed using inexpensive IoT sensors and an infrastructure built around a Raspberry Pi. Notwithstanding these advantages, the system's full potential cannot be realized unless issues like sensor calibration, data privacy, and network dependability are resolved.

All things considered, this cutting-edge monitoring system is an essential first step toward better environmental management, offering insightful information that helps create healthier urban living environments. To enhance its impact and efficacy, future advancements should concentrate on improving data analytics, extending system integration, and refining sensor technology.

FUTURE SCOPE:

IoT-based enhanced air and noise pollution monitoring will continue to evolve in the areas of improving sensor accuracy, incorporating machine learning for better data analytics, and scalability expansion for broader deployment. Real-time data processing and more thorough pollution insights will be made possible by advancements in edge computing and sensor technologies. Comprehensive monitoring and the enforcement of policies will be facilitated by the system's integration with other environmental technology and regulatory systems. Improvements in data security, energy efficiency, and cost reduction will also increase the system's sustainability and accessibility. Community participation in pollution control would be further enhanced via public interaction through user-friendly apps.

REFERENCES

- <https://howtomechatronics.com/projects/air-quality-monitoring-with-raspberry-pi-and-mq-sensor/>
- <https://www.hackster.io/lukebennett/raspberry-pi-air-quality-monitor-2b4522>
- <https://www.instructables.com/Make-a-DIY-Air-Quality-Monitor/>
- <https://diymachines.co.in/air-quality-monitoring-system-using-raspberry-pi-pico/>
- <https://circuitdigest.com/microcontroller-projects/raspberry-pi-iot-air-quality-monitor>


PRINCIPAL
SRI SUDARSHANA INSTITUTE OF TECHNOLOGY & SCI
Darimadugu, Markapur-523 -
Prakasam Dist.(A.P.) India

INVESTIGATING THE COUNTING FUNCTION OF SEMIPRIMES: ANALYSIS AND APPLICATIONS

¹P.PARABRAHMAM, ²B.VIJAYA BHARATHI

¹Associate Professor, ²Assistant Professor

Department Of H&S

Indira Institute Of Technology And Sciences, Markapur

Abstract

A natural number that may be expressed as the sum of two prime numbers is called a semiprime. Examined is the asymptotic behavior of the function $\pi_2(x)$, which returns the number of semiprimes that are equal to or less than x . The asymptotic series of $\pi_2(x)$ is found using a combinatorial argument, where each term is explicitly presented. The constants involved in the asymptotic series are calculated to 20 significant digits and a technique for doing so is described. We look at the partial sum mistakes of the asymptotic series. For $k \geq 3$, an extension of this method to products of k primes is also suggested.

1. Introduction

For a positive integer k and a positive integer (or real number) x , let $\pi_k(x)$ be the number of integers less than or equal to x which can be written as the product of k prime factors. The behaviour of $\pi_k(x)$ has been extensively studied during last two centuries, with the main focus on the case $k = 1$, where $\pi_1(x)$ is the prime counting function, denoted $\pi(x)$ in the rest of this paper. The prime number theorem states that $\pi(x) \sim \text{li}(x)$, where the logarithmic integral function $\text{li}(x) = \int_0^x \frac{1}{\log t} dt$ can be written as an asymptotic expansion $\text{li}(x) \sim x \log x + \gamma_0 x + \frac{\gamma_1 x}{\log x} + \frac{\gamma_2 x}{(\log x)^2} + \dots$. Bounds on the error term have been established in the literature, including the recent work of Trudgian [22], who proved that, for sufficiently large x ,

$$|\pi(x) - \text{li}(x)| \leq 0.2795 \frac{x}{(\log x)^{3/2}} \exp\left(-\sqrt{\frac{\log x}{6.455}}\right).$$

This implies the existence of constants d_1 and d_2 such that

$$-d_1 \frac{x}{(\log x)^{3/2}} \exp(-d_2 \sqrt{\log x}) \leq \pi(x) - \text{li}(x) \leq d_1 \frac{x}{(\log x)^{3/2}} \exp(-d_2 \sqrt{\log x}) \quad (1.1)$$

Assuming the Riemann hypothesis, Rosser and Schoenfeld [19, 20] established even sharper bounds on the error term, including

$$|\pi(x) - \text{li}(x)| < \frac{\sqrt{x} \log x}{8\pi}$$

for large enough x . Other explicit estimates of $\pi(x)$, in terms of x and $\log x$ are achievable, as proved by Axler [1].

In this paper, we focus on the case $k = 2$, where the numbers written as products of two (not necessarily distinct) primes are called semiprimes. In this case, Ishmukhametov and Sharifullina [14] recently used probabilistic arguments to approximate the behaviour of $\pi_2(x)$ as

$$\pi_2(x) \sim \frac{x \log \log x}{\log x} + 0.200 \frac{x}{\log x} - 1.549 \frac{x}{(\log x)^2} \quad (1.2)$$

The first term of (1.2) has already been known to Landau [15, §56], with his result stated, for general $k \in \mathbb{N}$, as

$$\pi_k(x) \sim \frac{1}{(k-1)!} \frac{x (\log \log x)^{k-1}}{\log x} \quad (1.3)$$

Delange [6, Theorem 1] obtained the asymptotic expansion of $\pi_k(x)$ in the form

$$\pi_k(x) \sim \frac{x}{\log x} \sum_{n=0}^{\infty} \frac{P_{n,k}(\log \log x)}{(\log x)^n} \quad (1.4)$$

where $P_{n,k}$ are polynomials of degree $k-1$, with the leading coefficient equal to $n!/(k-1)!$. Tenenbaum [21] proved a similar result, giving an expression for the coefficients in the polynomial $P_{0,k}$ in terms of the derivatives of $1/\Gamma(z+1)$ at $z=0$. Considering $k=2$ in (1.4), we can write an asymptotic expansion for $\pi_2(x)$ as



$$\pi_2(x) \sim \sum_{p \leq x} \left(1 - \frac{1}{p}\right) \frac{x}{\log(x/p)} - \sum_{p < q \leq x} \frac{x}{pq} + \dots \quad (1.6)$$

In Theorem 2.3, we prove that $C0 = M$, where $M = 0.261497\dots$ is the Meissel–Mertens constant defined

$$M = \lim_{x \rightarrow \infty} \left(\sum_{p \leq x} \frac{1}{p} - \log(\log(x)) \right) \quad (1.8)$$

where we sum over all primes such that $p \leq x$. In Section 3, we calculate the rest of constants Cn appearing in equation (1.5). They are given in Table 1 and obtained by the formula

$$C_n = x^n \left(\sum_{p \leq x} \frac{1}{p^n} - \sum_{i=1}^{n-1} \frac{1}{i} \right) - n! \left(\sum_{p \leq x} \frac{1}{p^n} - B_n \right) \quad (1.7)$$

where H_i is the i -th harmonic number, $B0 = M$ and constants B_i are defined using the asymptotic behaviour of sums [15, §56]

$$\sum_{p \leq x} \frac{1}{p^i} = \frac{1}{i-1} \log \log(x) + B_i + o\left(x^{-1/(i-1)}\right) \quad \text{for } i \in \mathbb{N} \quad (1.8)$$

Constants B_i are given as limits (3.1) in Section 3, where we present an algorithm to efficiently calculate them to a desired accuracy. They are computed in Table 1 to 20 significant digits. Rosser and Schoenfeld [18] prove that the error term in (1.8) can be given explicitly in terms of an integral, which contains the error terms in the prime number theorem. For the case $i = 1$ in equation (1.8), explicit estimates of this sum and, in particular, of the constant $B1$ involved, were recently obtained by Dusart [8].

A related arithmetic function, $\Omega(m)$, is defined to be the number of prime divisors of $m \in \mathbb{N}$, where prime divisors are counted with their multiplicity. Considering fixed x in equation (1.3), we can view this approximation of $\pi_k(x)/x$ as the probability mass function of the Poisson distribution with mean $\log(\log(x))$. Erdős and Kac [9] showed that the distribution of $\Omega(x)$ is Gaussian with mean $\log(\log(x))$ (see also Rényi and Turán [17] and Harper [13] for generalizations and better bounds). Diaconis [7] obtained the asymptotic expansions for the average number of prime divisors as (see also Finch [11, Section 1.4.3].

$$\frac{1}{x} \sum_{m \leq x} \Omega(m) = \log \log(x) + \sum_{i=1}^{\infty} \gamma_i \frac{1}{i} \frac{1}{\log(x)^{i+1}} \quad (1.9)$$

where the constants γ_i are the Stieltjes constants, numerically computed in [3] to 20 significant digits. An asymptotic series for the variance of Ω have also been obtained [11, Section 1.4.3].

The Stieltjes constants γ_i are used in Section 3 during our calculation of the values of constants Bn and Cn , for $n \in \mathbb{N}$. This paper is organized as follows. Section 2 begins with a counting lemma for expressing the semiprime counting function π_2 in terms of the prime counting function π . Using this lemma, the main results on the asymptotic behaviour of π_2 are stated and proved in Section 2 as Theorem 2.3 and Theorem 2.5. While Theorem 2.3 only gives the first two terms, its proof is more coincide than the proof of Theorem 2.5, which gives the full asymptotic series of π_2 . The constants Cn which appear in this asymptotic series are computed in Section 3, where we present an efficient approach to calculate both constants Bn and Cn , based on the differentiation of the prime zeta function. In Section 4, we investigate the behaviour of the error terms given by the partial sums of the asymptotic series of π_2 . We conclude with a generalization of the counting argument in Section 5, discussing the extensions of the presented results to the general case of counting functions π_k for $k \geq 3$.

2. Asymptotic behaviour of the counting function of semiprimes

As in equation (1.6), we denote primes by p and the sums over p shall be understood as sums over all primes satisfying the given condition. In the case of summing over primes twice, we denote the corresponding prime summation indices by $p1$ and $p2$. We begin with a simple counting formula [14], that gives a way of computing $\pi_2(x)$.

Lemma 2.1. For a positive integer x , the following holds

$$\pi_2(x) = \frac{\pi(\sqrt{x})^2}{2} + \sum_{p \leq \sqrt{x}} \pi\left(\frac{x}{p}\right) \quad (2.1)$$

Proof. By the definition of counting functions π_2 and π , we have

$$\pi_2(x) = \sum_{p_1 < p_2} 1 = \sum_{p_1 < \sqrt{x}} \sum_{p_2 < \frac{x}{p_1}} 1 = \sum_{p_1 < \sqrt{x}} \left(\pi\left(\frac{x}{p_1}\right) + \pi(p_1) - 1 \right)$$


PRINCIPAL
 VICTORIA INSTITUTE OF TECHNOLOGY & SCIENCES
 Darimadugu, Markapur-523 316
 Prakasam Dist.(A.P.) India.

and formula (2.1) follows by renaming p_1 to p in the first term and observing that the rest of the right hand side is the sum of all natural numbers from 1 up to $\pi(\sqrt{x}) - 1$.
 Formula (2.1) gives an expression of $\pi_2(x)$ in terms of the prime counting function $\pi(x)$, which can be approximated using the prime number theorem [21] as

$$\pi_2(x) \sim \pi_2(x) + O\left(\frac{x}{(\log x)^{n+1}}\right) \quad (2.2)$$

where $n \in \mathbb{N}$ and

$$\pi_2(x) \sim \frac{x}{\log x} \left(\sum_{i=1}^{n-1} \frac{1}{(\log x)^i} \right) \quad (2.3)$$

Using Landau [15, §56], we can rewrite equation (1.6) for any integer $n \in \mathbb{N}$ as

$$\sum_{p \leq \sqrt{x}} \frac{1}{p} \sim \log(\log x) - \log 2 + M + o\left(\frac{1}{(\log x)^2}\right) \quad (2.4)$$

where we use the little o asymptotic notation [5], as opposed to the big O asymptotic notation used in the prime number theorem (2.2). First we use this result to approximate the sum on the right hand side of equation (2.1).

Lemma 2.2. Let $n \in \mathbb{N}$ and $a_n(x)$ be defined by (2.3). Then we have

$$\sum_{p \leq \sqrt{x}} \pi\left(\frac{x}{p}\right) \sim \sum_{p \leq \sqrt{x}} a_n\left(\frac{x}{p}\right) + o\left(\frac{x \log(\log x)}{(\log x)^{n+1}}\right) \quad (2.5)$$

Proof. Using equation (2.2), we have

$$\sum_{p \leq \sqrt{x}} \pi\left(\frac{x}{p}\right) \sim \sum_{p \leq \sqrt{x}} a_n\left(\frac{x}{p}\right) + o\left(\frac{x}{(\log x)^{n+1}}\right) + \dots + \sum_{p \leq \sqrt{x}} \frac{1}{\log p}$$

where $c > 0$ is a constant. Equation (2.5) then follows by estimating the right hand side by

$$\frac{x \cdot 2^{n+1}}{(\log x)^{n+1}} \sum_{p \leq \sqrt{x}} \frac{1}{p} = O\left(\frac{x \log(\log x)}{(\log x)^{n+1}}\right),$$

where the last equality follows from equation (2.4)

2.1 The first two terms of the asymptotic series for $\pi_2(x)$

Using (2.5) for $n = 1$, we obtain

$$\sum_{p \leq \sqrt{x}} \pi\left(\frac{x}{p}\right) \sim \sum_{p \leq \sqrt{x}} \frac{x}{p \log x} + o\left(\frac{x \log(\log x)}{(\log x)^2}\right) \quad (2.6)$$

Using Landau [15, §56], we can rewrite equation (1.8) for any integers $i \in \mathbb{N}$ and $n \in \mathbb{N}$ as

$$\sum_{p \leq \sqrt{x}} \frac{(\log x)^i}{p} = \frac{(\log x)^i}{i+1} + B_i + o\left(\frac{1}{(\log x)^n}\right) \quad (2.7)$$

We will use this to prove the first theorem of this section.

Theorem 2.3. Let M be the Meissel–Mertens constant defined by (1.6). Then

$$\pi_2(x) \sim \frac{x \log(\log x)}{\log x} + M \frac{x}{\log x} + o\left(\frac{x}{\log x}\right) \quad (2.8)$$

Proof. Using equations (2.1), (2.2) for $n = 1$, and (2.6), we obtain

$$\pi_2(x) \sim \sum_{p \leq \sqrt{x}} \pi\left(\frac{x}{p}\right) - \frac{x}{\log x} + \frac{x}{\log x} \sum_{p \leq \sqrt{x}} \frac{1}{p} + o\left(\frac{x}{\log x}\right) \quad (2.9)$$

We have the following identity

$$\frac{\log x}{p(\log x - \log p)} = \frac{1}{p} + \frac{\log p}{\log x} \left(\frac{\log x}{p(\log x - \log p)} \right)$$

Substituting the left hand side into the right hand side, we obtain, for any natural number $n \in \mathbb{N}$, that

$$\frac{\log x}{p(\log x - \log p)} = \frac{1}{p} \sum_{i=0}^{n-1} \left(\frac{\log p}{\log x}\right)^i + \left(\frac{\log p}{\log x}\right)^n \left(\frac{\log x}{p(\log x - \log p)}\right)$$

Summing over all primes $p \leq \sqrt{x}$, we get

$$\sum_{p \leq \sqrt{x}} \frac{\log x}{p(\log x - \log p)} = \sum_{p \leq \sqrt{x}} \left(\frac{1}{p} \sum_{i=0}^{n-1} \left(\frac{\log p}{\log x}\right)^i \right) + \frac{1}{(\log x)^n} \sum_{p \leq \sqrt{x}} \frac{(\log p)^n}{p(\log x - \log p)}$$

Each term on the right hand side can be evaluated using equations (2.4) and (2.7), with $o(1)$ accuracy, as

$$\sum_{p \leq \sqrt{x}} \frac{\log x}{p(\log x - \log p)} = \log 2 + M + \sum_{i=1}^{n-1} \frac{1}{i+1} + f(n) + o(1) \quad (2.10)$$

where $f(n)$ is a decreasing function of n satisfying $f(n) \rightarrow 0$ as $n \rightarrow \infty$. This can be deduced by applying equation (2.7) to the error term



$$\frac{1}{\log 2} \sum_{p \leq x} \frac{\log p^{n+1}}{p(\log x - \log p)} = \frac{2}{(\log 2)^2} \sum_{p \leq x} \frac{\log p^{n+1}}{p} - \frac{1}{(\log 2)^2} + o(1)$$

Since we have

$$\log 2 + \sum_{i=1}^n \frac{1}{2^i} + f(n) \rightarrow 0, \quad \text{as } n \rightarrow \infty.$$

equation (2.10) implies that

$$\sum_{p \leq x} \frac{\log x}{p(\log x - \log p)} = \log(\log x) + M + o(1).$$

Substituting into equation (2.9), we obtain formula (2.8).

2.2. Asymptotic series for the counting function of semiprimes

To derive formulas for all terms in the asymptotic series of π_2 , we first define an auxiliary sequence of numbers q_n for $n \in \mathbb{N}$ by

$$q_n = \sum_{i=1}^n \frac{1}{2^i} \quad \text{for } n \geq 2 \quad \text{and} \quad q_0 = 0 \quad (2.11)$$

Then q_n is an increasing sequence of rational numbers with the first few terms given as $q_1 = 0$, $q_2 = 1$, $q_3 = 5/2$, $q_4 = 29/6$, $q_5 = 103/12$ and $q_6 = 887/60$, which satisfies the following identity.

Lemma 2.4. Let $n \in \mathbb{N}$ and let q_n be given by equation (2.11). Then we have

$$\sum_{i=1}^n \binom{n+i-1}{n-1} \frac{1}{2^i} = q_n + \log 2 \quad (2.12)$$

Proof. Considering the binomial series

$$(1-t)^{-n} = 1 + t \sum_{i=0}^{\infty} \binom{n+i}{n-1} t^i, \quad \text{for } t \in (-1, 1),$$

we can rewrite it as

$$\sum_{i=0}^{\infty} \binom{n+i}{n-1} t^i = \frac{(1-t)^{-n} - 1}{t} = \sum_{i=1}^{\infty} (1-t)^{-i-1}.$$

Integrating, we get

$$\sum_{i=0}^{\infty} \binom{n+i}{n-1} \frac{t^{i+1}}{i+1} = -\log(1-t) + \sum_{i=1}^n \frac{(1-t)^{-i+1} - 1}{i-1},$$

which holds for $t \in (-1, 1)$. Substituting $t = 1/2$, we obtain (2.12).

We will use Lemma 2.4 in the proof of the following theorem, giving the asymptotic series for the semiprime counting function $\pi_2(x)$.

Theorem 2.5. The constants C_n appearing in the asymptotic expansion (1.5) are given by equation (1.7) for $n \in \mathbb{N}$ and as $C_0 = B_0 = M$ for $n = 0$.

Proof. The case $n = 0$ is studied in Theorem 2.3, which states that $C_0 = M$. To derive equation (1.7), we again use formula (2.1) from Lemma 2.1 and approximate each term using the prime number theorem (2.2). We need to analyze sums of the form

$$S_n(x) = \sum_{p \leq x} \frac{(\log p)^n}{p(\log x - \log p)} = \sum_{p \leq x} \frac{1}{p} \left(1 - \frac{\log p}{\log x}\right)^n \quad (2.13)$$

Using the binomial series on the right hand side, we get

$$S_n(x) = \sum_{i=0}^n \binom{n+i-1}{n-1} \left(\frac{\log p}{\log x}\right)^i - \sum_{i=0}^n \binom{n+i-1}{n-1} \frac{1}{p \log x^i} \quad (2.14)$$

Substituting $x/2$ for x , we obtain

$$S_n(x/2) = \sum_{i=0}^n \binom{n+i-1}{n-1} \frac{1}{2^i} \sum_{p \leq x/2} \frac{(\log p)^i}{p} \quad (2.15)$$

To estimate the sums over primes on the right hand side, we apply the result of Rosser and Schoenfeld [18, equation (2.26)], which can be formulated as

$$\sum_{p \leq x} \frac{1}{p} = \log(\log x) + \mathcal{L}_0(x), \quad \sum_{p \leq x} \frac{(\log p)^i}{p} = \frac{(\log x)^i}{i} + \mathcal{L}_i(x),$$

where the error terms $\mathcal{L}_i(x)$ are defined by



$$L(x) = -\log(\log x) + \frac{b(2)}{2} + \frac{v(x) - b(x)}{x} + \int_0^x \frac{v(y) - b(y)}{y^2} dy$$

$$L(x) = -\frac{(\log 2)^2}{2} + \frac{(\log 2^2) b(2)}{2} + \frac{(\log x)^2}{2} (v(x) - b(x))$$

$$= \int_0^x \frac{(\log y)^2 (v(y) - b(y))}{y^2} dy + \log(x) - \log(2) \quad \text{for } x > 2$$

Using this notation and identity (2.12) in Lemma 2.4, we rewrite equation (2.15)

$$s_n(x) - \log(x) = \log(2) - \sum_{k=1}^n \binom{-1}{k} \frac{L(x)^k}{k!} \quad (2.16)$$

Using the inequality (1.1), there exist constants d_1 and d_2 such that

$$\frac{L(x)^k}{k!} \leq \frac{1}{k!} \left(\frac{d_1}{\log x} \right)^k \leq \frac{d_2}{k!} \left(\frac{1}{\log x} \right)^k$$

where we define (note that we allow the second argument to be ∞ in this definition)

$$I(x, z) = d_2 \int_2^x (\log y)^{z-1} \frac{\exp(-d_2 \sqrt{\log y})}{y} dy$$

Choose $\ell \in \mathbb{N}$. Our goal is to use (2.17) to estimate the rate of convergence of the sum on the right hand of equation (2.16). To do this we first observe that, for $i \geq \ell$, we have

$$\frac{L(x)^i}{i!} \leq \frac{1}{i!} \left(\frac{d_1}{\log x} \right)^i \leq \frac{I(x, i)}{i!} \quad (2.17)$$

Using inequalities (2.17) and (2.18) and assuming $\log(x) \geq 1$, we can estimate the remainder of the series on the right hand of equation (2.16) as

$$\sum_{k=1}^{\infty} \binom{-1}{k} \frac{L(x)^k}{k!} \leq \left(\frac{d_1}{\log x} + \frac{d_2}{\log x} \right) \sum_{k=1}^{\ell} \binom{-1}{k} \frac{L(x)^k}{k!}$$

$$+ \frac{d_2}{\log x} \sum_{k=\ell+1}^{\infty} \binom{-1}{k} \frac{L(x)^k}{k!} \leq \frac{d_2}{\log x} \sum_{k=\ell+1}^{\infty} \binom{-1}{k} \frac{L(x)^k}{k!}$$

Since all three sums on the right hand side converge independently of x , we deduce that the remainder is of the order $O(\log x)^{-(\ell+1)}$. Therefore, equation (2.16) becomes

$$s_n(x) - \log(x) = \log(2) - \sum_{k=1}^n \binom{-1}{k} \frac{L(x)^k}{k!} + O(\log x)^{-(\ell+1)}$$

This means that an asymptotic expansion of $S_n(x)$ in terms of negative powers of $\log x$ is given by the sum of the asymptotic series of terms in equation (2.15). The same is true for $S_n(x)$ in equation (2.14). Thus, using equations (2.4), (2.7), (2.12) and (2.14), we obtain

$$s_n(x) = \sum_{k=1}^n \binom{-1}{k} \frac{L(x)^k}{k!} + \sum_{k=1}^n \frac{B_k}{k!} + O(\log x)^{-(\ell+1)}$$

$$= \log(x) + \log(2) - \sum_{k=1}^n \binom{-1}{k} \frac{L(x)^k}{k!} + O(\log x)^{-(\ell+1)} \quad (2.18)$$

Using equations (2.3) and (2.5), we have

$$\sum_{k=1}^n \binom{-1}{k} \frac{L(x)^k}{k!} = \sum_{k=1}^n \sum_{j=0}^k \binom{-1}{k} \frac{L(x)^j}{j!} = \sum_{j=0}^n \left(\sum_{k=j}^n \binom{-1}{k} \right) \frac{L(x)^j}{j!}$$

where we used the definition (2.13) of $S_n(x)$ to get the second equality. Using equation (2.19) and notation $B_0 = M$, we obtain

$$\sum_{k=1}^n \binom{-1}{k} \frac{L(x)^k}{k!} = \sum_{j=0}^n \left(\sum_{k=j}^n \binom{-1}{k} \right) \frac{L(x)^j}{j!} = \sum_{j=0}^n \left(\sum_{k=j}^n \binom{-1}{k} \right) \frac{L(x)^j}{j!}$$

Thus, using formula (2.1) and the prime number theorem (2.2), we obtain the asymptotic expansion (1.5), where we have

$$C_n = n^{\ell} \left(\log n + \sum_{j=1}^{\ell} \frac{B_j}{j!} \right) - 2^{\ell} \sum_{i=1}^{\ell} (i-1)^{\ell} (n-i)^{\ell}$$

This can be further simplified by using definition (2.11) of q_n . We get

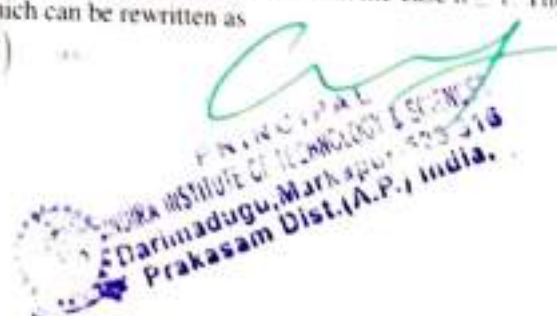
$$C_n = \left(\sum_{j=0}^{\ell} \binom{-1}{j} \frac{L(x)^j}{j!} \right) - \left(\sum_{j=0}^{\ell} \binom{-1}{j} \frac{L(x)^j}{j!} \right)$$

Subtracting the first and the third sum, we obtain (1.7).

3. Computing the constants

In this section, we use a fast converging series to determine the values of the constants B_n and, as a result, of the constants C_n given by equation (1.7). The first constant, $B_0 = C_0 = M$, is the well-studied Meissel–Mertens constant, so we will focus on constants B_n in the case $n \geq 1$. They have been defined by equations (1.8) or (2.7), which can be rewritten as

$$B_n = \left(\sum_{k=1}^{\infty} \frac{(-1)^k}{k!} \right) - \left(\sum_{k=1}^{\infty} \frac{(-1)^k}{k!} \right)$$



To derive a formula for evaluating B_n on a computer, we use the prime zeta function [12] defined by

$$P(s) = \sum_{p \text{ prime}} \frac{1}{p^s} \quad \text{for } s > 1, (\infty) \quad (3.2)$$

Differentiating equation (3.2), we get the formula for the n -th derivative of the prime zeta function as

$$P^{(n)}(s) = -\sum_{p \text{ prime}} \frac{(\log p)^n}{p^{s+n}} + n \sum_{p \text{ prime}} \frac{(\log p)^{n-1}}{p^{s+n}} + \dots + \sum_{p \text{ prime}} \frac{(\log p)^n}{p^{s+n}} \quad (3.3)$$

The prime zeta function $P(s)$ can also be related to the Riemann zeta function $\zeta(s)$ through the formula [12]

$$P(s) = \sum_{n=1}^{\infty} \mu(n) \frac{\log \zeta(ns)}{n}, \quad \text{for } s > 1, (\infty)$$

where $\mu(n)$ is the M obius function. Taking the derivative of order n of this expression, we obtain

$$P^{(n)}(s) = \sum_{n=1}^{\infty} \mu(n) s^{n-1} \left(\frac{\zeta'}{\zeta} \right)^{(n-1)}(ns)$$

Substituting into (3.3), we obtain

$$\sum_{p \text{ prime}} \frac{(\log p)^n}{p^{s+n}} + \dots + \sum_{p \text{ prime}} \frac{(\log p)^n}{p^{s+n}} = \sum_{n=1}^{\infty} \mu(n) s^{n-1} \left(\frac{\zeta'}{\zeta} \right)^{(n-1)}(ns) \quad (3.4)$$

Using integration by parts, we obtain

$$\int_1^{\infty} \frac{(\log u)^{n-1}}{u^n} du = \frac{(\log u)^{n-1}}{(n-1)u^n} + \dots + \left(\frac{\log u}{n-1} \right)^{(n-1)}$$

Thus, the second sum on the right hand side of equation (3.4) can be approximated by

$$\sum_{p \text{ prime}} \frac{(\log p)^n}{p^{s+n}} = \left[\frac{(\log p)^{n-1}}{p^{s+n}} + \dots + \left(\frac{\log p}{n-1} \right)^{(n-1)} \right] \left[\frac{(\log p)^n}{p^{s+n}} + \dots \right]$$

Substituting into equation (3.4), we get

$$\sum_{p \text{ prime}} \frac{(\log p)^n}{p^{s+n}} = \left[\frac{(\log p)^{n-1}}{p^{s+n}} + \dots + \left(\frac{\log p}{n-1} \right)^{(n-1)} \right] \left[\frac{(\log p)^n}{p^{s+n}} + \dots \right]$$

Taking the limit as $s \rightarrow 1$ and substituting into equation (3.1), we obtain

$$B_n = \sum_{p \text{ prime}} \left(\frac{\log p}{p} \right)^n + \dots + \left(\frac{\log p}{n-1} \right)^{(n-1)} \left[\frac{(\log p)^n}{p} + \dots \right] \quad (3.5)$$

n	B _n	C _n
0	0.00000000000000000000	0.00000000000000000000
1	1.11571775116439898792	1.11571775116439898792
2	2.97895864568544755911	2.97895864568544755911
3	64.1249120000111010042	64.1249120000111010042
4	10.1473361100000000000	10.1473361100000000000
5	0.11111111111111111111	0.11111111111111111111
6	0.00000000000000000000	0.00000000000000000000
7	0.00000000000000000000	0.00000000000000000000
8	0.00000000000000000000	0.00000000000000000000
9	0.00000000000000000000	0.00000000000000000000
10	0.00000000000000000000	0.00000000000000000000

Table 1. Table of constants B_n and C_n , for $n = 0, 1, 2, \dots, 10$, defined by equations (2.7) and (1.7), which appear in the asymptotic expansion of $\pi_2(x)$. The values of constants B_n are computed by formula (3.5) using the Laurent series (3.6). The values of constants C_n are computed by equation (1.7).

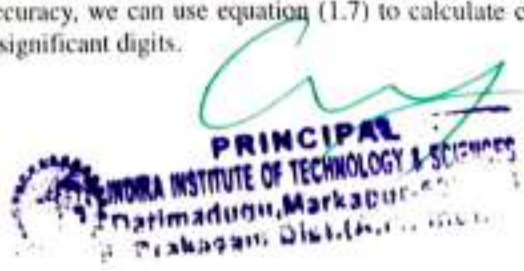
where the first term on the right hand side is a quickly converging series and the limit in the second term can be evaluated using the Laurent expansion of $\zeta(s)$ around $s = 1$. This is given by

$$\zeta(s) = \frac{1}{s-1} + \sum_{n=0}^{\infty} \frac{(-1)^n}{n!} \gamma_n (s-1)^n,$$

where the Stieltjes constants γ_n are computed to 20 significant digits in [3]. Then, the Laurent expansion of the logarithmic derivative [4] of the Riemann zeta function is

$$\frac{\zeta'(s)}{\zeta(s)} = -\frac{1}{s-1} + \sum_{n=0}^{\infty} \left(\frac{\gamma_n}{n!} + \dots \right) (s-1)^n + \dots$$

Constants B_n computed by formula (3.5) using the Laurent series (3.6) are presented in Table 1. Once we know constants B_n to the desired accuracy, we can use equation (1.7) to calculate constants C_n . They are also presented in Table 1 to 20 significant digits.



4. Discussion

In this paper, we have studied the behaviour of the semiprime counting function $\pi_2(x)$, which is a special case ($k = 2$) of the k -almost prime counting function $\pi_k(x)$. To generalize the presented results to the case $k \geq 3$, we need to first generalize the counting Lemma 2.1. Using the inclusion-exclusion principle, it is possible to deduce the following counting formula

$$\pi_k(x) = \sum_{i=1}^k (-1)^{i+1} \sum_{p_1 < \dots < p_i} \pi_k\left(\frac{x}{p_1 p_2 \dots p_i}\right) \quad (5.1)$$

where we define function $\pi_0(x)$ to be identically equal to 1, i.e. $\pi_0(x) = 1$, and the sum over $p_1 < p_2 < \dots < p_i \leq \sqrt[k]{x}$ means that we are summing i -times over all primes satisfying the given condition. Substituting $k = 2$ into equation (5.1), we obtain

$$\pi_2(x) = \sum_{p_1 \leq \sqrt{x}} \pi_1\left(\frac{x}{p_1}\right) - \sum_{p_1 < p_2 \leq \sqrt{x}} \pi_0\left(\frac{x}{p_1 p_2}\right)$$

Using $\pi_0(x) = 1$, we deduce equation (2.1). Thus, equation (5.1) provides a generalization of equation (2.1), which expresses the k -almost prime counting function $\pi_k(x)$ in terms of the counting functions $\pi_1(x), \pi_2(x), \dots, \pi_{k-1}(x)$. It can be inductively used to derive forms of coefficients of polynomials $P_{n,k}$ in the asymptotic series (1.4). In addition to constants B_n and C_n , certain new constants will appear in such calculations, including the (converging) sums of the form $P \sum_p (\log p)^{i-p-1}$ with $i \geq 2$ and $i \in \mathbb{N}$. For a detailed discussion of the asymptotic behaviour of these sums for $i = 1$, see Axler [2]. Substituting $n = \pi(x)$ in [2, Theorem 5] gives a different expansion for the sums in (1.8), which may be further examined using the prime number theorem. There are, also, other possible approximations for $\pi_k(x)$. For example, Erdős and Sárközy [10] prove that

$$\pi_k(x) \sim \begin{cases} c(k) \frac{x}{\log x} \frac{(\log \log x)^{k-1}}{(k-1)!} & \text{for } 1 \leq k \leq (2-\delta) \log(\log x) \\ c k^2 2^{-k} x \log x & \text{for } k \geq 1 \end{cases}$$

for some constants $c(\delta)$ and c . Other approximations, relating the function π_k to some other products over primes are possible to obtain, as explained in [21]. Functions $\pi_k(x)$ and $\Omega(x)$, used in expansion (1.9), count the prime divisors with their multiplicity. Another possible generalization is to investigate the related functions $N_k(x)$ and $\omega(x)$, counting prime divisors without multiplicity. That is, functions $N_k(x)$ and $\omega(x)$ are defined to be the number of natural numbers $n \leq x$ which have exactly k distinct prime divisors and the number of distinct prime divisors of x , respectively. Finch [11, page 26] shows that

$$\sum_{n \leq x} \omega(n) \sim \log \log x + 0.2614972129 \dots + \sum_{p=1}^{\infty} \left(1 - \sum_{q=1}^p \frac{1}{q}\right) \frac{x^{-p}}{\log x^p}$$

which has the higher order terms in the same form as in the expansion (1.9). Using the prime number theorem, we also observe that $N_1(x) = \pi(x) + \pi(\sqrt{x}) + \pi(\sqrt[3]{x}) + \dots \sim \text{li}(x)$ admits an identical asymptotic expansion as $\pi(x)$. Delange [6, Theorem 1] and Tenenbaum [21] obtained the asymptotic expansion of $N_k(x)$ in the form

$$N_k(x) = C \frac{x \log x}{2^k} \left(1 + O\left((\log x)^{-k^2/6}\right)\right)$$

where $Q_{n,k}$ are polynomials of degree $k-1$. Here, the expansion is similar to the expansion (1.4) for $\pi_k(x)$, but the polynomials $P_{n,k}$ and $Q_{n,k}$ are different. Results about the leading terms of polynomials $Q_{n,k}$ and about $Q_{0,k}$ have also been obtained, as in the case of π_k . Several different approximations for $N_k(x)$ are also possible to derive, as shown in Tenenbaum [21], who points out that the function N_k is easier to analyse than π_k , for larger values of k , relative to $\log(\log x)$. For example, the following holds uniformly for $x \geq 3$ and $(2 + \delta) \log(\log x) \leq k \leq A \log(\log x)$:

$$N_k(x) = C \frac{x \log x}{2^k} \left(1 + O\left((\log x)^{-k^2/6}\right)\right)$$

where $A > 0$, $0 < \delta < 1$ and $C \approx 0.378694$. Similar results, but for larger values of k , can be obtained for functions π_k as well [16].

Acknowledgements. Authors would like to thank Julia Stadlmann for helpful comments during the preparation of this manuscript.


PRINCIPAL
 VIDYARAJA INSTITUTE OF TECHNOLOGY & SCIENCES
 Darimadugu, Markapur-523 316
 Prakasam Dist.(A.P.) India.

5. CONCLUSION

Studying the counting function of semiprimes offers important new perspectives on number theory and its uses. Semiprimes, which are prime number products, are important in many areas of mathematics and cryptography. The behavior and characteristics of the counting function, which counts the semiprimes up to a certain value, have been examined in this work.

According to our investigation, there is a growth trend in the counting function that is closely related to the prime number distribution. We learn more about the distribution and frequency of semiprimes across a wider range by analyzing this function. Applications in cryptography, where semiprimes are utilized for safe key generation and encryption techniques, need a grasp of this concept.

The study draws attention to the asymptotic behavior of the counting function and its link to prime number theory, as well as the mathematical principles that underpin it. The findings have ramifications for strengthening security protocols in cryptographic systems and optimizing semiprime-based algorithms.

Issues like the need for effective techniques to compute the counting function and computational complexity are also discussed. Subsequent research need to concentrate on improving these algorithms and investigating other uses in number theory and cryptography.

In conclusion, learning about the counting function of semiprimes improves our understanding of both their mathematical characteristics and real-world applications. It emphasizes how crucial semiprimes are to contemporary cryptography techniques and opens up new avenues for theoretical exploration and computational method optimization in the future.

References

1. C. Axler. New bounds for the prime counting function. *Integers*, 16:A22, 2006.
2. C. Axler. On a family of functions defined over sums of primes. *Journal of Integer Sequences*, 22(5):Article 19.5.7, 2019.
3. J. Bohman and C. Fröberg. The Stieltjes function – definition and properties. *Mathematics of Computation*, 51(163):281–289, 1988.
4. K. Broughan. Extension of the Riemann ζ -functions logarithmic derivative positivity region to near the critical strip. *Canadian Mathematical Bulletin*, 52(2):186–194, 2009.
5. N. de Bruijn. *Asymptotic Methods in Analysis*. North-Holland Publishing Co., Amsterdam, 1958.
6. H. Delange. Sur des formules de Atle Selberg. *Acta Arithmetica*, 19:105–146, 1971.
7. P. Diaconis. Asymptotic expansion for the mean and variance of the number of prime factors of a number n . Technical Report 96, Department of Statistics, Stanford University, Stanford, California, December 1976.
8. P. Dusart. Explicit estimates of some functions over primes. *Ramanujan Journal*, 45:227–251, 2018.
9. P. Erdős and M. Kac. The Gaussian law of errors in the theory of additive number theoretic functions. *American Journal of Mathematics*, 62(1):738–742, 1940.
10. P. Erdős and A. Sárközy. On the number of prime factors of integers. *Acta Scientiarum Mathematicarum*, 42:237–246, 1980.
11. S. Finch. *Mathematical Constants II*. Cambridge University Press, Cambridge, 2018.
12. C. Fröberg. On the prime zeta function. *BIT*, 8:187–202, 1968.
12. A. Harper. Two new proofs of the Erdős-Kac theorem, with bound on the rate of convergence, by Stein's method for distributional approximations. *Mathematical Proceedings of the Cambridge Philosophical Society*, 147(1):95114, 2009.
13. S. Ishmukhametov and F. Sharifullina. On distribution of semiprime numbers. *Izvestiya Vysshikh Uchebnykh Zavedenii. Matematika*, 8:53–59, 2014.
14. E. Landau. *Handbuch der Lehre von der Verteilung der Primzahlen*. Druck und Verlag von B.G. Teubner, Leipzig und Berlin, 1909.

15. J. Nicolas. Sur la distribution des nombres entiers ayant une quantité fixe de facteurs premiers.
Acta Arithmetica, 44(3):191-200, 1984.

